2009

Specific Levels of Therapeutic Ultrasound Stimulate the Release of Inflammatory and Angiogenic Mediators From Macrophages In Culture

Thomas Turner
Virginia Commonwealth University

School of Medicine, Department of Anatomy and Neurobiology
Virginia Commonwealth University

This is to certify that the dissertation prepared by Thomas Todd Turner entitled "Specific Levels of Therapeutic Ultrasound Stimulate the Release of Inflammatory and Angiogenic Mediators From Macrophages In Culture" has been approved by his or her committee as satisfactory completion of the dissertation requirement for the degree of Doctor of Philosophy

Sheryl D. Finucane, P.T., Ph.D., School of Allied Health Professions

David G. Simpson, Ph.D., School of Medicine

Lori Michener, P.T., Ph.D., ATC, SCS, School of Allied Health Professions

John Bigbee, Ph.D., School of Medicine.

Robert F. Diegelmann, Ph.D., School of Medicine

John T. Povlishock, Ph.D., Department Chair, Department of Anatomy and Neurobiology

Jerome F. Strauss III, M.D., Ph.D., School of Medicine

Dr. F. Douglas Boudinot, Dean of the Graduate School

[Click here and type the Month, Day and Year this page was signed.]

SPECIFIC LEVELS OF THERAPEUTIC ULTRASOUND STIMULATE THE RELEASE OF INFLAMMATORY AND ANGIOGENIC MEDIATORS FROM MACROPHAGES IN CULTURE

A Dissertation submitted in partial fulfillment of the requirements for the degree of Doctor of Philosophy at Virginia Commonwealth University.

by

THOMAS TODD TURNER
B.S. Old Dominion University, 1988
M.S.,P.T. Virginia Commonwealth University, 1997

Director: SHERYL D. FINUCANE
ASSISTANT PROFESSOR, DEPARTMENT OF PHYSICAL THERAPY

Virginia Commonwealth University
Richmond, Virginia
August 2009

Acknowledgements

"I knew I should have taken a left in Albuquerque" – Bugs Bunny, so succinctly describing my experiences as a doctoral student.

This document and the work entailed within would not have been possible without the love, care and nurturing of Rich, Sandy and Rick. To them, I've been "Tom Doc" since I was a little boy; it's now obvious that they knew something special even then.

Special shout out to my brother-from-another-mother, Rusty. His great friendship, and unequaled generosity kept me afloat on many rough seas.

Thank you to my committee, Bob, David, John, Lori and Sheryl for providing guidance, advice and expectations that propelled me to completion of this project. Special thanks to my advisor, Dr. Sheryl Finucane, for her mentoring, assistance, and critique. More particularly, thanks for her patience, and the willingness to support me throughout many difficult times. Also special thanks to John Bigbee and David Simpson for their help in formulating many of the experimental designs of this project.

An additional special thank you to David Simpson for essentially taking me into his lab, giving me some space, a computer, lab supplies, assisted in getting me an NIH fellowship and whatever else a student typically gets when part of a lab, all while not being my advisor and generally not having any reason to do all those things to help me. Thanks Dave, you're truly special.

Thank you to all my friends and family for their prayers, support and continued love.

In addition to the support described above, this work was completed with the support of NIH Predoctoral Fellowship, Grant Number: 1F31AR052278-01A1.

Table of Contents

List of Tables

Page

List of Figures

Page

LIST OF ABBREVIATIONS

ALP	Alkaline phosphatase
BMP-7	Bone morphogenetic protein -7
BSA	Bovine serum albumin
°C	Degrees Celsius
Ca^{2+}	Calcium ion
Calcein-AM	Calcein acetoxymethylester
CO_2	Carbon dioxide
Con A	Concavalin A
COX-2	Cyclooxygenase-2
CW	Continuous-wave
DMEM	Dulbecco's Modified Eagle Medium
DMSO	Dimethyl sulfoxide
ECM	Extracellular matrix
ELISA	Enzyme-linked immunosorbent assay
ERK	Extracellular signal-regulated kinase
EthD-1	Ethidium homodimer-1
HCl	Hydrochloric acid
HEPES	4-(2-hydroxyethyl)-piperazineethanesulfonic acid
HIFCS	Heat-inactivated fetal calf serum
hr	Hour
IVD	Intervertebral disc

IFN-γ	Interferon-γ (gamma)
IGF-1	Insulin growth factor-1
IL-1β	Interleukin-1β (beta)
IL-2	Interleukin-2
IL-4	Interleukin-6
IL-6	Interleukin-6
IL-8	Interleukin-8
K^+	Potassium ion
LDH	Lactate dehydrogenase
LTB4	Leukotriene B_4
MCL	Medial collateral ligament
MCM	Macrophage conditioned media
mg	Milligrams
MHz	Megahertz
ml	Milliliter
mM	Millimolar
mRNA	Messenger ribonucleic acid
mW/cm^2	Milliwatts per square centimeter
NADH	Nicotinamide adenine dinucleotide
ng	Nanograms
NO	Nitric oxide
OA	Osteoarthritis

OD	Optical density
PBS	Phosphate buffered saline
pg	Picograms
PGE_2	Prostaglandin E2
PMA	Phorbol-12-myristate-13-acetate
PMNL	Polymorphonuclear leukocyte
PKC	Protein Kinase C
PW	Pulsed-wave
rhPDGF-bb	Recombinant, human platelet derived growth factor-bb
RPMI	Rose Park Memorial Institute (culture media)
SAFHS	Sonic accelerated fracture healing system
SATA	Spatial average temporal average
SDS	Sodium docecyl sulfate
SEM	Standard error of the mean
TGF-β	Transforming growth factor-β (beta)
TNF-α	Tumor necrosis factor-α (alpha)
Tukey's HSD	Tukey's honestly significant differences
TUS	Therapeutic ultrasound
µg	microgram
VEGF	Vascular endothelial growth factor
W/cm^2	Watts per square centimeter
WST-1	Tetrazolium salt

Abstract

SPECIFIC LEVELS OF THERAPEUTIC ULTRASOUND STIMULATE THE RELEASE OF INFLAMMATORY AND ANGIOGENIC MEDIATORS FROM MACROPHAGES IN CULTURE

By Thomas Todd Turner, P.T, Ph.D

A Dissertation submitted in partial fulfillment of the requirements for the degree of Doctor of Philosophy at Virginia Commonwealth University.

Virginia Commonwealth University, 2009

Major Director: Sheryl D. Finucane
Assistant Professor, Department of Physical Therapy

Therapeutic ultrasound (TUS) is a treatment modality that is used to accelerate tissue healing. TUS is thought to affect cellular processes of tissue healing, especially those that occur in the inflammatory and early proliferative phases. TUS can be applied using various parameter selections including intensity, wavelength, duty cycle and treatment duration and no clear consensus exists on optimal parameters for healing enhancement. Macrophages are important mediators of inflammation and their actions are critical to normal progression into the proliferative phase of healing. They complete many functions during these periods of tissue healing, among those being release of cytokines and growth factors. These paracrine factors affect other inflammatory cells, resident cells

of the healing tissue, including fibroblasts and endothelial cells that are necessary for restoration of damaged tissue. The hypothesis of this investigation is that TUS enhances early healing, in part, through stimulation of macrophage release of paracrine factors involved in coordination of the cellular aspects of tissue healing and that specific levels of TUS are most stimulatory for macrophages. This study examined macrophage release of interleukin-1β (IL-1β), vascular endothelial growth factor (VEGF), transforming growth factor-β1 (TGF-β1) and fibroblast mitogens, in response to varied levels of TUS. Fibroblasts incubated up to 48-hours in media conditioned by TUS-stimulated macrophages were not induced to proliferate regardless of the parameters sets of TUS applied. TUS (1 MHz, 400mW/cm^2 SATA, 20% duty cycle, 10-minute exposure) induced macrophage release of VEGF and IL-1β within 10-minutes post-TUS, without any additional release being stimulated at 1-hour post-insonation. No other combination of TUS parameters studied induced release of IL-1β and VEGF. TUS did not induce release of TGF-β1 at either time point post-TUS. VEGF and IL-1β release occurred in conjunction with lactate dehydrogenase (LDH) release from treated macrophages, indicating non-specific cell membrane permeabilization was involved in the cellular response. For IL-1β, TUS-stimulated release was inhibited at lower exposure temperatures. Inhibition of TUS-induced release at lower temperatures indicates that a cellular metabolic process, most likely exocytosis, was also stimulated by TUS. Based on these results, it appears that TUS exposure at 1 MHz, 400mW/cm^2 SATA, 20% duty cycle induces non-specific and cell-mediated release of secretory proteins. Thus, enhanced

release of cytokines and growth factors from macrophages is a possible mechanism by which TUS enhances tissue healing.

This document was created in Microsoft Word 2007.

Chapter 1

Therapeutic Ultrasound and Tissue Healing: Review of Literature

Introduction

Therapeutic ultrasound (TUS) has been utilized for over sixty years in the clinical setting and continues to be widely used to treat a variety of conditions. Typical clinical rationale for its use include; reduction of edema and pain, acceleration of tissue repair, and modification of scar formation [1,2]. Despite frequent clinical use, there is a deficiency in the understanding of the mechanism of action of TUS on various tissues, and also a dearth of scientifically generated treatment parameters for achieving the optimal effect of TUS.

As will be discussed in the following review, TUS has been studied using various experimental methods: 1) in vitro cell culture experiments, 2) in vivo animal experiments, and 3) clinical trials. Many in vivo and in vitro studies have noted beneficial effects of TUS on healing of injured tissues namely, integument, ligaments, tendons and bone [3-12]. This enhanced tissue healing, appears to be greatest when TUS is applied during the inflammatory phase of healing [13-16].

Much of the research on TUS effects on fracture healing has utilized a common set TUS treatment parameters: 1.5 MHz, 30 mW/cm^2, 20% pulsed wave (PW), 20-minute treatments. Experimental investigations using these TUS exposure parameters have generated data that demonstrate the benefit of TUS on fracture healing in various research models [17-22]. Use of a standardized parameter set allows direct comparison of findings among a variety of studies. In addition, identification of a consistently effective TUS dose creates a comparison point for other TUS parameter sets for clinical effectiveness and cellular effects.

Among the body of investigations on soft tissue healing, many variant TUS application parameters have been reported to generate beneficial effects [4,23-27]. However, definition of optimal TUS application parameters has not been accomplished. The following will examine the molecular, biochemical and mechanical effects of TUS on cells and tissues and how those effects relate to enhanced healing.

Ultrasound Parameters

Ultrasound consists of high frequency sound waves generated by conversion of electrical energy into mechanical energy, utilizing a piezoelectric crystal [28]. Piezoelectricity is a material property of natural and synthetic crystals and it defines the process by which a crystal produces an electrical voltage when compressed and produces an electrical voltage of opposite polarity when expanded [29]. Using a reverse piezoelectric effect TUS transducers create an alternating voltage across a crystal, which causes the crystal to expand and contract and results in the establishment of high frequency waves of

pressure within the ultrasound spectrum. These ultrasound waves are propagated through a medium at the same frequency as the alternating current, and this propagating pressure wave can produce a mechanical force when applied to biological tissues [30-32]. Wave propagation through tissues occurs via molecular collision and vibration, and the induced molecular vibration results in energy absorption and heating of tissue [31]. As the sound wave propagates through tissue, a progressive loss of energy occurs due to absorption and scattering of the wave. This process, known as attenuation, results in a decrease in the intensity of the sound wave as it penetrates deeper into tissue [33]. Different tissues absorb ultrasound energy to varying degrees, based mainly on protein content [34]. Bone, followed by ligaments and tendons, absorb energy most readily. By comparison, skin and muscle absorb intermediate amounts, with adipose tissue absorbing the least [31].

Ultrasound is typically applied therapeutically in the frequency wavelength range of 0.75 to 3.0 MHz [35]. Higher frequency (3 MHz) sound waves are thought to cause more rapid movement of molecules resulting in greater attenuation of ultrasound energy at more superficial levels and a reduced depth of penetration into tissue when compared to lower frequency sound waves (1 MHz) [31]. TUS exposure at 1 MHz has been shown to produce tissue heating to a depth of 5 cm while 3 MHz is attenuated at more superficial levels with heating confined to < 2 cm below the treated surface in human lower extremities [36].

Energy emitted from the transducer is not uniform across the crystalline surface of the TUS transducer; rather, hot spots of intense energy can develop along portions of the transducer during sonication [28,32]. Two methods are used to reduce the heating effect of TUS. Constant slow, gentle movement of the transducer over the target site eliminates

heat buildup generated by the hot spots that would otherwise remain over one site for the full duration of treatment. This moving applicator method is most often employed when treating tissues with a continuous wave (CW) application, which has a greater propensity to result in heating. The second method to reduce the heating effect is to apply TUS in a pulsed-wave (PW) mode in which "off" periods interrupt the sound waves. The percentage of total treatment time during which US energy is being emitted is referred to as the duty cycle. A 20% duty cycle is used most often clinically and in research reports, however, duty cycles of 10%, 25%, 33%, and 50% are available on most TUS generators [1,33,37]. Beyond reduced tissue heating, the effect of different duty cycles on the overall efficacy of TUS is unknown.

The intensity of applied ultrasound is defined as the rate of energy delivery per unit area of the transducer (watts/cm^2), with typical therapeutic values of 30-2000 mW/cm^2 [2]. The total amount of energy delivered to a specific site by TUS varies as a function of the tissue location, the types and numbers of tissue interfaces, the TUS intensity and duty cycle utilized, and the total duration of treatment. TUS exposure dosage is often reported as the "spatial average, temporal average" (SATA). Multiplying the duty cycle by the intensity of exposure generates the SATA value. The resultant SATA value can then be used to compare more directly, the overall TUS dosage between different investigations. For example, the different treatment parameters below result in an identical SATA value of 400 mW/cm^2 (with treatment duration remaining the same for each set):

2000 mW/cm^2 at 20% duty cycle is: 2000 mW/cm^2 x 20% = 400 mW/cm^2 SATA

800 mW/cm^2 at 50% duty cycle is: 800 mW/cm^2 x 50% = 400 mW/cm^2 SATA

400 mW/cm^2 at 100% duty cycle is: 400 mW/cm^2 x 100% = 400 mW/cm^2 SATA

Given the variance in available TUS intensities and wavelength frequencies (0.75 to 3 MHz), the disparity between the depth and amount of energy absorption among tissue types, measurement of the TUS energy that is imparted to tissues is inexact. In addition, many of the studies discussed in this review utilized different intensities, frequencies, durations, and repetitions of TUS exposure. Therefore conclusions and generalizations about TUS effects in relation to dosage are often limited and additional study is needed to identify optimal TUS parameters for specific effects. The next section of the review will focus on cellular and tissue processes affected by TUS, with emphasis on the biological effects on healing tissues.

Proposed Biophysical Mechanism of TUS: Thermal

The physical mechanism(s) of TUS that generate cellular responses are typically divided into two classifications, thermal and nonthermal. Thermal effects are believed to create increased metabolic activity due to elevated temperature as TUS propagates through tissues. Propagation of the ultrasound wave results in absorption of energy by tissues, via molecular vibration and friction in sonicated tissue, with the extent of energy absorbed being dependent on the physical characteristics of the intervening tissues [31,38]. In general, increased temperature (> 1ºC) is believed to increase metabolic activity in cells and

tissue [39]. According to Lehman, temperature increases of 2-3°C and > 4°C produce increased blood flow and increased collagen extensibility, respectively [40].

The ability of TUS to increase tissue temperature has been demonstrated experimentally. Using hogs, TUS applied to knee joints at 1 MHz, 1500 mW/cm^2 SATA, CW for 5 minutes has been reported to result in a temperature increase of 4-8°C at 5 cm below the sonication surface [41]. Measuring at fixed tissue depths (2.5 and 5.0 cm for 1 MHz) and (0.8 and 1.6 cm for 3 MHz) Draper et al investigated tissue heating in humans following TUS and reported average temperature elevation of 3-4°C in calf musculature of subjects measured at a depth of 5 cm when treated with TUS (1 MHz, 1500 mW/cm^2 SATA, CW, 10 minutes) [36,42]. Sonication at lower intensities (500 mW/cm^2 or 1000 mW/cm^2 SATA) resulted in heating of 0.4°C and 1.6°C, respectively at a depth of 5 cm. TUS application at 3 MHz, CW at intensities between 500-2000 mW/cm^2 SATA resulted in temperature increases of 3-6°C at 1.6 cm tissue depth [36]. These results appear to confirm the correlation between TUS frequency and depth of tissue heating. However, by measuring at fixed depths for each frequency, the depth limit of heating was not completely investigated. Using cadaveric specimens, Cambier et al reported increased temperature of nearly 5°C at a depth of 3 cm, following 10-minute sonication (1MHz, 1000-2000 mW/cm^2 SATA) of the legs of human cadavers while Demmink et al reported tissue heating of 4 - 8°C in pig hind limbs treated with varying CW TUS frequencies (0.86, 2.0 and 3.0 MHz) for 5 minutes at 2000 mW/cm^2 SATA [43,44].

In rats, CW TUS was reported to accelerate restoration of joint motion following experimentally induced knee-joint contractures. The authors attributed the increased motion to increased extensibility of peri-articular structures due to TUS-induced heating [45]. The effect of TUS on tissue extensibility in humans has been reported for healthy subjects only and with conflicting results. In separate studies using healthy female subjects, triceps surae extensibility was increased due to TUS application, however, medial collateral ligament extensibility was not influenced by TUS [46,47]. The importance of these findings in humans is questionable given that the increasing extensibility of healthy connective tissue is not a rationale for TUS application. Furthermore, increased extensibility of healthy tissues may create laxity of supporting structures (i.e. ligaments) and be detrimental to the supportive role of connective tissues.

The overall evidence supports the ability of TUS to heat tissues to therapeutic levels (temperature rise of at least 1° and up to 5°C) given a high enough intensity and long enough treatment duration. Thus, it is reasonable to conclude that TUS can have a thermal affect on tissues. However, TUS dose necessary to heat tissues to therapeutic levels, and the effect of TUS-induced tissue heating on healing, tissue mechanics or metabolic properties remains undefined.

Proposed Biophysical Mechanism of TUS: Nonthermal

Beyond the effects generated through heating, TUS also affects treated tissue via nonthermal actions. These non-thermal mechanisms are typically divided into acoustic cavitation and acoustic streaming. Both mechanisms are theorized to create shearing

forces along membranes of cells and organelles, subsequently altering membrane permeability [31,32,48]. Furthermore, alterations in ion flux, especially calcium (Ca^{2+}) are thought to result in extracellular matrix molecule (ECM) production, secretion of growth factors and cytokines, cell proliferation and changes in cell motility [7,49-54]. All of these TUS-stimulated cellular functions occur during normal tissue healing processes and provide a theoretical framework for investigation of TUS and tissue healing.

Acoustic Cavitation.

Cavitation describes the formation and activity of gas or vapor filled cavities when a medium (fluid) is exposed to an ultrasonic field [29]. These phenomena are separated into inertial and stable cavitation. Inertial cavitation describes gas bubbles that grow in size then collapse violently, generating locally high temperatures and pressures and this form of cavitation has been shown to induce cellular damage in mammalian cells and in general its effects are believed to be detrimental to cells [55,56]. Inertial cavitation has been shown to occur as a result from exposure of fluid media to ultrasound, particularly in response to high intensity, pulsed ultrasound (> 3 W/cm^2) [29]. These high intensity ultrasound exposures have been investigated as a method for gene delivery and are not typical of TUS parameters. The effectiveness of these treatments are reported to be directly associated with acoustic cavitation, but the high intensities are greater than what is considered to be TUS (< 2000 mW/cm^2) [57,58].

Stable cavitation differs from inertial cavitation in that the gas bubbles oscillate in size as a result of ultrasonically induced pressure changes without any collapse occurring.

Ultrasound-induced pressure waves enable production of high velocity gradients of oscillating bubbles at membrane-medium interfaces, and these gradients are hypothesized to generate shear forces on cell membranes and subsequently change membrane characteristics, most notably, permeability [29,31]. Stable cavitation induced by TUS has been reported in a number of in vitro models, but its relationship to cellular response has not been clarified. Cavitation during TUS exposures has been associated with membrane permeability changes in epithelial cells, and increased collagen synthesis by fibroblasts treated with TUS [59,60].

Evidence of cavitation following in vivo TUS is limited and contradictory. Stable bubble formation has been measured in guinea pig hind limbs treated with a single, 5-minute TUS exposure (0.75 MHz, 80-680 mW/cm^2 SATA, 25% PW) [61,62]. The authors reported that development of cavitation bubbles was directly proportional to increasing TUS intensity. However, the authors admitted difficulty in interpretation of their images due to artifact when using a pulse-echo ultrasound imaging to detect cavitation. In contrast, Gross et al applied TUS to canine left ventricles for 2 to 5 minutes (0.51 MHz - 1.61 MHz, 125 - 16,000 mW/cm^2 SATA) and reported no bubble formation at any frequency, intensity or duration tested [63]. Given the unique composition of the fluid-filled heart and unique characteristics of the moving fluid compared to tissues typically treated with TUS (i.e., ligaments, tendons, integument, bone), it is difficult to generalize their findings to other tissues.

Based on the available evidence it appears that cavitation can occur during in vitro TUS exposures. However, the link between cellular responses and TUS-induced cavitation

has not been identified. Regarding in vivo exposures, additional evidence to support TUS-induced cavitation in the hind limbs of guinea pigs has not been reported. Given this limited evidence for in vivo cavitation and the unclear relationship between in vitro cavitation and cellular response, it is premature to conclude that TUS effects are mediated by cavitation.

Acoustic Streaming

Acoustic streaming is referred to as movement of fluid in a propagating ultrasonic wave and is classified as either bulk streaming or microstreaming [31]. Microstreaming is the result of eddies of fluid flow around TUS-induced vibrating gas bubbles. By definition, the occurrence of microstreaming is dependent on cavitation, since movement of gas bubbles in the media is necessary to create fluid flow. Bulk streaming describes propagation of unidirectional fluid flow by an ultrasound pressure wave.

Microstreaming due to TUS exposure has not been reported, but bulk streaming has been measured during in vitro sonication of human bone cells [64]. The authors found measurable bulk streaming at intensities of 130, 480 and 1770 mW/cm^2 SATA when TUS was applied at 3 MHz, CW for 10 minutes. In addition, gene expression of transforming growth factor-β (TGF-β) was up-regulated at all three TUS intensities, which suggests a possible role of bulk streaming in generating a cellular response. No other evidence has been reported to support the role of either type of acoustic streaming as a mechanism of action of TUS. This may be due to the difficulty in measuring these phenomena given the available experimental models and monitoring equipment.

Free Radicals

Formation and activity of free radicals following TUS exposure is another proposed mechanism to explain the action of TUS. Because free radicals are capable of disrupting cell membranes, via peroxidation of lipid components, their formation has been hypothesized to be responsible for permeability changes and subsequent alterations in cellular activity following TUS application [65]. Free radical formation has also been reported in cultured frog skin exposed to TUS [66]. The sonicated tissue (1 MHz, 300 mW/cm^2 SATA, CW, 4 minutes) exhibited increased ionic conductance that was eliminated by adding free radical scavengers to the bathing media. Ultrasound exposure at various intensities 500-3000 mW/cm^2 SATA and variable duty cycles (15% to 100%) has also been reported to induce free radical production in sonicated tap water [67]. To date however, no evidence of TUS-induced free radical production has been reported in vivo.

Free radicals do exist in tissues, but free radical scavengers often limit their actions [66]. Proponents of a free radical mechanism of action of TUS suggest that scavengers protect membranes from damage, but do allow some reactions to occur that would account for increased permeability [32]. On the other hand, an increase in free radicals could exceed the ability of tissue to control oxidizing reactions, thereby resulting in cell membrane damage rather than enhancement of cellular activities.

Conclusion: Nonthermal Mechanisms of Action

It is unclear which, if any, of the proposed non-thermal mechanisms have a role in the actions of TUS. The preponderance of evidence does not indicate the most likely

candidate mechanism, and it may be that the final response to TUS exposure occurs due to components of each mechanism. The findings of Harle et al, in which the authors reported measurement of cavitation and bulk fluid streaming during in vitro TUS treatment of human osteoblasts appear to support the hypothesis of multiple mechanisms being responsible for TUS effects[64].

TUS and Tissue Healing

TUS enhancement of healing is supported for many injured tissues, but the nature and extent of its effect on healing, much like the mechanism of action, is not fully understood. The effects of TUS on tissue healing have been described in numerous models and tissue types including dermal wounds, ligaments, tendons, and bone as well as for a variety of cell types involved in the healing process. The overall body of evidence provides a strong basis for enhancement of healing following exposure to TUS.

A variety of TUS treatment parameters have shown an ability to improve numerous aspects of tissue healing, with the greatest support for the benefits of TUS being reported for acceleration of fracture healing. Fibroblasts, chondrocytes, osteoblasts, muscle satellite cells, Schwann cells, endothelial cells, monocytes, macrophages, spleenocytes, and thymocytes have demonstrated responsiveness to TUS exposure with in vitro and in vivo models. The following sections will describe the relevant findings regarding TUS effects on tissues and cells. Where appropriate, differential responses based on the exposure parameters will be discussed. Lastly, evidence describing TUS affects on the early phases of healing, especially the inflammatory phase, will be presented in an effort to clarify the

hypothesis that the most beneficial aspects of TUS occur when exposures are given during early stages of the healing process.

Fracture Healing

The ability of TUS to enhance fracture healing is strongly supported by various investigations. Clinical trials, as well as numerous in vivo and in vitro models, have consistently generated results indicating that TUS positively alters processes that occur during fracture healing. Unlike studies of TUS effects on soft tissue healing discussed later, a majority of reports investigating TUS effects on fracture healing have utilized the same set of TUS parameters (1.5 MHz, 30 mW/cm^2 SATA, 20% PW, 20 minutes). An ultrasound generator designed to transmit TUS energy at these specific settings for acceleration of fracture healing is available clinically and is referred to as the "Sonic Accelerated Fracture Healing System" (SAFHS) [68]. Development and use of this TUS device permits more liberal inter-study comparison and generalization of results.

In vivo studies utilizing rabbits, rats, dogs and sheep have demonstrated TUS-enhanced healing of experimentally induced fractures. At 21 days post-injury, healing femoral fractures in rats had increased maximum torque to failure and torsional stiffness compared to untreated fractures after daily TUS exposures (0.5 MHz, 50 and 100 mW/cm^2 SATA, 20% PW, 15 minute treatments) [69]. The increased callus strength coincided with increased expression of aggrecan mRNA, up to two weeks post-injury. Azuma et al reported increased strength of healing femoral fractures in rodents following sonication at SAFHS parameters [22]. TUS exposures were given in varied interval schedules post-injury:

days 1-8, 9-16, 17-24, and 1-24. Overall the effect of repeated TUS exposures appeared to be additive such that 24 consecutive treatments post-injury resulted in the greatest improvement in fracture strength compared to controls and the other treatment intervals. TUS exposures during the post-injury interval days 1-8, 9-16 and 17-24 enhanced fracture strength significantly more than controls, but significantly less than fractures treated from days 1-24. No difference in fracture strength was reported among any of the eight-day treatment intervals. Based on this study, it appears that the additive effects of TUS, rather than early treatment initiation, is the most important factor for improving fracture healing. This finding is inconsistent with the theory of greatest effect on the inflammatory phase of healing.

Daily application of SAFHS improved tibial osteotomy healing in sheep, noted by reduction in healing time from 103 days to 79 days, compared to untreated controls [70]. In this study, the authors used a transosseous application of TUS, utilizing a stainless steel pin to transmit ultrasound energy directly on the bone surface. Given the ability of non-invasive, transcutaneous ultrasound application to improve fracture healing, there seems to be no clear indication at this time for use an invasive, possibly infection-generating TUS application protocol.

In addition to the osteotomy fracture models noted above, TUS enhancement of healing of nonunion fractures and fractures in diabetic rodents has been demonstrated. Nonunion tibial fractures in rats exposed to SAFHS daily for 6 weeks demonstrated a 50% healing rate compared to 0% healing in untreated tibial fractures [17]. Femoral fractures in diabetic rats had improved torque to failure and stiffness after only 1 week of SAFHS

exposures [20]. TUS exposures 6 days per week for 5 months (1 MHz, 50 mW/cm^2 SATA, 20% PW, 15 minutes) to canine ulnas accelerated healing and reduced non-unions from 60% to 0% compared to controls [6].

TUS has also been effective for enhancing healing in spinal fusion models. Six weeks of daily SAFHS exposures improved the rate of healing and the histological quality of bone following lumbar spinal fusion in rabbits, compared to untreated controls [71]. In addition, sonication reduced pseudoarthroses, a common complication of spinal fusion, from 35% to 7%, increased stiffness and load to failure of healing bone compared to sham treatment [72]. Lumbar spinal fusion in canines exposed to SAFHS 6 days a week for 12 weeks exhibited increased mechanical stiffness and accelerated rate of bony fusion when compared to untreated controls [73].

In an investigation of rabbit mandibular fracture, daily SAFHS exposures for 3 weeks accelerated endochondral ossification and increased failure load and stiffness of healing mandibles, compared to sham [74]. Sakurakichi et al reported accelerated bone formation using a distraction osteogenesis model in rabbit tibiae treated with SAFHS [75]. TUS exposures resulted in increased bone mineral density, maximal torque at failure and stiffness 4 weeks post-injury.

Randomized, placebo-controlled clinical trials have reported enhanced fracture healing in the tibia, distal radius, scaphoid and metatarsals after SAFHS exposures. Radiographically assessed healing of fresh fractures of the tibia treated with SAFHS was accelerated by 28 days, with cast discontinuation improved by 26 days and complete cortical bridging improved by nearly 70 days over placebo [76]. For distal radius fractures,

SAFHS accelerated healing by 37 days, as assessed by radiographic evidence of complete bridging of the cortex of the fracture site [18]. Leung et al reported on complex tibial fractures, classified as open shaft or comminuted fracture, treated with SAFHS for 90 consecutive days [77]. SAFHS improved bone mineral content, alkaline phosphatase activity and reduced time to removal of external fixator and the time to full weight bearing compared to sham treatment. Alkaline phosphatase, an enzyme that contributes to processes involved with bone formation, is considered a marker of fracture healing [78].

Enhanced fracture healing in patients with compromised healing has also been reported. Nonunion fractures, defined as fracture gaps bridged with soft tissue and exhibiting lack of healing for 6-8 months post-injury, represent a major problem for some patients [78]. Non-union fractures generally require some type of intervention, often invasive surgery, to promote healing and allow patients to return to premorbid function [68]. Based on clinical and radiographic assessment, SAFHS induced full healing of nonunions in 86% (25 of 29 cases) and 85% (57 of 67 cases) of subjects, with average time to healing of 22 - 24 weeks [79,80]. Both studies included a variety of fracture sites including tibia, femur, radius, ulna, scaphoid, humerus, metatarsal, and clavicle, with all sites being responsive to TUS.

In addition to nonunions, TUS has been shown to improve delayed fracture healing associated with cigarette smoking. Cigarette smoking is directly related to poor healing generally and delayed fracture healing specifically. Cook et al reported that healing time was reduced for fractures of the tibia by 72 days (41% reduction in healing time) and the radius by 50 days (51% reduction) in smokers receiving SAFHS compared to sham [19].

Given the evidence of TUS benefits on compromised fracture healing, the question of TUS effects on intact osteoporotic bone has been investigated [81]. Rat hind limbs made osteoporotic through bilateral ovariectomy were exposed to 12 weeks of daily SAFHS. In a similar investigation, rat hind limbs made osteoporotic by sciatic neurectomy, were exposed to 4 weeks of daily TUS (1 MHz, 125 mW/cm^2 SATA, CW, 15-minutes) [82]. TUS had no effect on restoration of bone mineral content or bone mineral density. Taken together, these reports do not support improvement of osteoporotic bone loss following SAFHS exposures. Beneficial effects of TUS on tissues generally involve injured, healing tissue and it might be expected that no benefit would occur for intact, non-injured tissues, such as osteoporotic bone.

Accelerated fracture healing following TUS exposure has been verified using a variety of in vivo markers of bone healing as discussed above. The cellular mechanisms that are affected by TUS have been investigated utilizing in vitro assays. Much of this area of research has focused on chondrocyte and osteoblast response to TUS, with bone marrow stromal cells and in vitro bone tissue culture models also being employed.

Tissue culture models of isolated bone tissue from fetal mice metatarsals have been used to analyze cellular responsiveness to TUS [83,84]. Metatarsal rudiments from fetal mice exposed to daily TUS for 1 week (1 MHz, 154 mW/cm^2 SATA, 20% PW, 5 minutes) increased total longitudinal growth and length of the proliferative zone of cartilage as compared to untreated controls, suggesting that TUS enhanced chondrocyte proliferation [83]. Sonication at lower intensities (20, 66 and 98 mW/cm^2 SATA, 20% PW,

and 100 and 500 mW/cm^2 CW, 5 minutes) was reported to have no effect on length of the proliferative zone or total bone rudiment length [84].

In contrast, SAFHS has been reported to increase the length of the calcified diaphysis of metatarsal bone rudiments from fetal mice following 7 consecutive days of exposures, without any changes in the length of the proliferative zone of cartilage or in total bone rudiment length [84]. The authors suggested that the lower intensity (30 vs. 154 mW/cm^2), in comparison to Wiltink et al[84] affected the hypertrophic zone, specifically chondrocyte hypertrophy and matrix calcification, rather than chondrocyte proliferation in the proliferative zone. However, Wiltink et al included sonication at intensities comparable to SAFHS intensities (20 and 66 mW/cm^2 SATA) and did not report alterations in the hypertrophic zone. The variance in treatment duration (5 vs. 20 minutes) may provide a better explanation for the difference in findings between these two studies, since TUS dose may influence the overall tissue response to sonication [12]. These reports indicate chondrocytes in regions of endochondral ossification are stimulated by TUS. Also, it appears that different TUS intensities may differentially affect processes in the bone-healing continuum. Findings from these similar experimental models of developing bone treated with different TUS exposure parameters illuminate the difficulty in identifying optimal TUS doses. However, the ability of non-SAFHS exposure parameters to alter bone formation indicates that a range of TUS exposure parameters may affect bone healing and regeneration.

Concomitant with studies examining the effect of TUS on chondrocytes of fetal bone, osteoblast response to TUS has been investigated using in vitro models [9,85]. Sun et al

treated bone defects in isolated rat femora with daily TUS (1.5 MHz, 320 or 770 mW/cm^2 SATA, 20% PW, 15-minutes) for 2 weeks and found accelerated healing and enhanced trabecular regeneration compared to sham [85]. In a follow-up study, Sun et al co-cultured mouse osteoblasts and osteoclasts and exposed them to 2 weeks of daily TUS (1 MHz, 68 mW/cm^2 SATA, 20% PW, 20-minutes) [9]. Osteoblasts were induced to proliferate, while osteoclast numbers declined. Increased levels of tumor necrosis factor-α (TNF-α), alkaline phosphatase and prostaglandin E2 (PGE_2) were also measured in the culture media following sonication. TNF-α is an inflammatory cytokine that is believed to have a role in regulation of bone repair via stimulation of endochondral ossification and osteoclast function [86,87]. PGE_2 is a lipid compound considered to be a potent inflammatory regulator of bone repair [78,88,89]. These combined findings indicate that TUS stimulated aspects of the inflammatory phase (i.e. TNF-α and PGE_2) and the reparative phase (i.e. osteoblast proliferation and alkaline phosphatase production).

Release of other cytokines related to bone healing has also been related to TUS exposure. Rat osteoblasts treated with TUS (1 MHz, 120 mW/cm^2, 20% PW, 15-minutes) had altered cytokine release following sonication [90]. The authors found increased release of transforming growth factor-β1 (TGF-β1) after two exposures, while release of TNF-α and interleukin-6 (IL-6) was reduced after two and three exposures, respectively. IL-6 acts to enhance osteoclast function in bone as well as promoting angiogenesis and extracellular matrix (ECM) synthesis [78,87], while TGF-β1 is a signaling peptide involved in recruitment and stimulation of ECM producing cells, including osteoblasts [86,87,91].

In addition to TUS induction of cytokine, protein and inflammatory mediator release, in vitro models have been used to identify the effects of TUS on gene expression in osteoblasts. Using osteoblastic cells exposed to a single SAFHS treatment, investigators have reported induction of mRNA expression of cyclooxygenase-2 (COX-2), c-fos, alkaline phosphatase, osteocalcin, bone sialoprotein and insulin growth factor-1 (IGF-1) [92,93,94]. Bone sialoprotein and osteocalcin are non-collagenous matrix bone proteins, and IGF-1 promotes cellular activity associated with bone growth [86,,87]. c-fos is a proto-oncogene that is thought to influence osteoblast proliferation and differentiation and to regulate constituents of the bony matrix [91]. COX-2 is an enzyme that appears to be involved in regulating bone formation and remodeling through stimulation of prostaglandin synthesis by osteoblasts [92,95].

Utilizing SAFHS, Sena et al showed induction of immediate early response genes (c-jun, c-myc, COX-2, Egr-1, TSC-22) and bone differentiation marker genes (osteonectin, osteopontin) 3 hours after a single sonication of bone marrow stromal cells [96]. These results suggest that in addition to effects on osteoblasts, osteoclasts and chondrocytes, TUS enhances differentiation and maturation of progenitor cells involved in fracture healing.

In two separate studies of single TUS exposures, Harle et al exposed osteoblastic cells to continuous TUS at 3 MHz for 5 or 10 minutes at varying intensities (140-1770 mW/cm^2 SATA) [64,97,98]. Sonication altered ECM protein production in a dose-dependent manner [97]. Specifically, TUS intensities of 140 and 990 mW/cm^2 SATA reduced levels of osteonectin, while intermediate intensities 230 and 540 mW/cm^2 had no effect on this ECM protein. Osteopontin levels were reduced following 990 mW/cm^2 exposures but not

at lower intensities. TGF-β gene expression was also reported to have a dose-dependent relationship to TUS [64]. A single TUS application at varying intensities (3 MHz, 130-1770 mW/cm^2 SATA, CW, 10-minutes) induced TGF-β gene expression that was dose-dependent, with the highest intensity (1770 mW/cm^2) inducing the greatest expression. According to the overall results by Harle et al, it is apparent that TUS intensities can affect cellular activities differentially. These investigations indicate a transcriptional response to TUS exposure in addition to a secretory or more general release response. In addition, this trio of investigations utilized TUS exposure parameters different from SAFHS parameters, strengthening the hypothesis that many different TUS exposure parameters can be effective in altering cellular function.

Similar to the findings of Harle et al, dose-response relationships between TUS and cell function have been reported utilizing SAFHS. Osteoblastic cells exposed to SAFHS have been reported to generate differential expression of genes associated with osteogenesis (alkaline phosphatase, osteopontin, and bone morphogenic protein-7 (BMP-7), based on the number of daily TUS exposures (1, 3, 5 or 7 exposures), with 3 exposures inducing the greatest up-regulation [99]. Production of alkaline phosphatase, osteocalcin and vascular endothelial growth factor (VEGF) were dependent on the number of TUS treatments in human periosteal cells exposed to SAFHS parameters [10]. VEGF is a cytokine that has a critical role in angiogenesis during tissue repair [86,100,101]. The response of periosteal cells suggests that they may also have a role in TUS-enhanced fracture healing.

The evidence that supports enhancement of fracture healing by TUS is extensive. Based on the overall findings on fracture healing with in vivo and in vitro models, it appears that TUS enhances bone healing by: alterations in ECM protein production (by chondrocytes, osteoblasts, and periosteal cells), release of inflammatory mediators and cytokines, and through the enhancement of cell proliferation and differentiation. TUS-induced alteration of gene expression appears to be the mechanism for some of these effects. Therefore, it is plausible to suggest that TUS-enhanced fracture healing occurs through stimulation of some, if not all, of these processes. However, given that nearly all in vivo and clinical reports of TUS-enhanced fracture healing have utilized the 30 mW/cm^2 intensity, it is difficult to determine which of the reported in vitro responses noted at intensities above 30 mW/cm^2 actually contribute to the fracture healing process.

Hyaline Cartilage

Articular cartilage is an avascular tissue and resident chondrocytes have a minimal capacity for tissue repair, especially in comparison to resident cells of other connective tissues (bone, ligament, tendon and dermis). Among the postulates generated to explain the poor healing of articular cartilage is the hypothesis that the avascular nature results in the inability to recruit stem cells to aid healing [12,102]. Many surgical techniques and medical treatments have been employed by orthopedic surgeons in efforts to improve articular cartilage healing, but none have generated consistent success [102]. In an effort to discover other treatment options, several authors have undertaken studies to determine whether TUS can enhance healing of cartilage [12,103,104].

In a pair of investigations, Huang et al treated chemically induced osteoarthritis (OA) in rat knee joints with TUS (1 MHz, 500 or 625 mW/cm^2 SATA, 20% or 25% PW, 7 minutes, 3x/wk for 4 weeks)[104]. They found TUS exposures improved repair of arthritic cartilage with superficial damage and prevented further arthritic deterioration in more severely damaged cartilage at 2-months post-injury (one month after cessation of TUS treatment) [103]. In addition, articular cartilage healing was correlated with increased chondrocyte proliferation and with increased production of stress proteins in treated joints [104]. Stress proteins, also known as heat shock proteins, can be produced by and then protect cells exposed to trauma as a result of arthritis, autoimmune disease, heat and ischemia [105,106]. Huang et al theorized that the stress proteins protected chondrocytes and allowed them to proliferate and modulate cartilage repair via increased ECM production. Stress protein production following TUS exposure and their relation to enhanced healing has not been confirmed by other investigations.

Full-thickness osteochondral defects in rabbit knee joints treated with SAFHS have been induced toward earlier and better morphological and histological repair [12]. SAFHS treatment for 12 weeks (6 days per week) resulted in fewer degenerative changes up to 52 weeks post-injury compared to untreated controls. Additional TUS treatments beyond 12 weeks (18, 24, and 52 weeks of TUS) did not result in any additional benefit in the quality of healing defects. The authors also reported that daily 40-minute treatments improved the histological appearance of healing deficits compared to 20-minute treatments up to 18 weeks post-injury. When TUS exposure time was reduced to 5 or 10 minutes, there was

no difference in healing compared to the 20-minute exposures. This duration-dependent improvement in healing cartilage indicates a dose-dependent response to TUS.

In vitro studies have also been utilized to demonstrate the ability of TUS to affect chondrocyte function, supporting in vivo findings and indicating these cells can be stimulated to improve healing of articular cartilage [11,107,108]. Parvizi et al exposed isolated rat chondrocytes to five daily TUS treatments (1 MHz, 50 and 120 mW/cm^2 SATA, 20% PW, 10 minutes) and reported increased aggrecan gene expression at both intensities and increased proteoglycan synthesis at the higher intensity [11]. Isolated rabbit chondrocytes embedded in three-dimensional collagen gel matrices treated with SAFHS twice weekly for 3 weeks increased chondroitin-6-sulfate production [107]. Chondroitin-6-sulfate is an important matrix protein in articular cartilage.

Chondrocyte response to TUS has been related to the state of cellular differentiation. Chondrocytes within sternal cartilage explants from chick embryos exhibited variable responsiveness following exposure to 1 week of daily SAFHS [109]. Sonication of explants from the proximal sternum, cartilage that is destined for terminal differentiation and endochondral ossification, resulted in stimulation of hypertrophic chondrocytes and subsequent maturation of bony tissue. Chondrocytes in the explants from the distal sternum, cartilage that retains its hyaline cartilage characteristics in the adult, were stimulated to increase production of ECM molecules aggrecan and type II collagen without further cellular differentiation.

In a subsequent investigation, Zhang et al applied a single TUS treatment (1.5 MHz, 2 or 30 mW/cm^2 SATA, 20% PW, 20 minutes) to chicken chondrocytes isolated

from hyaline cartilage and reported alterations in cell proliferation, and gene expression of ECM proteins [108]. Compared to untreated controls, TUS at 2 mW/cm^2 SATA increased cell proliferation, but TUS at 30 mW/cm^2 SATA did not. Both TUS intensities induced elevated gene expression of type II collagen and reduced aggrecan gene expression. The differences between 2 and 30 mW/cm^2 SATA further illustrates an apparent dose-dependent response to TUS.

TUS enhancement of chondrocyte ECM production has been reported to involve growth factor production [110]. Epiphyseal chondrocytes isolated from distal femora of neonatal rats were sonicated with SAFHS for 5 or 10 consecutive days and responded by increased gene expression for type II collagen, aggrecan and TGF-β1, as well as increased cell proliferation, when compared to sham exposures. Addition of human recombinant TGF-β1 to control cells resulted in increased type II collagen and aggrecan mRNA expression comparable to TUS treatment effects. Pretreatment with anti-human TGF-β1 antibody prior to TUS application cancelled the increases in cell proliferation, type II collagen and aggrecan mRNA expression, indicating that chondrocyte response to TUS was likely mediated through TGF-β1 production and its ensuing effect on cellular metabolism.

The reported benefits of TUS on articular cartilage healing and chondrocyte function have led some investigators to explore the ability of TUS to enhance healing of intervertebral disc (IVD) injury, which includes nucleus pulposus (NP) and annulus fibrosus (AF) cell types. Nucleus pulposus cells are considered to have chondrocyte-like function, while those of the annulus fibrosus are believed to have a phenotype more closely

related to fibroblasts [111]. Both cell types isolated from bovine and rabbit annulus fibrosus and nucleus pulposus have been shown to be responsive to TUS [52,112]. SAFHS for 20 consecutive days increased collagen and proteoglycan synthesis by bovine cells, without any effect on cellular proliferation [52]. Daily TUS treatment for 5 or 12 days at variable intensities (7.5, 15, 30, 60 or 120 mW/cm^2 SATA) increased proliferation and proteoglycan synthesis in a dose-dependent manner in rabbit cells [112]. Compared to untreated controls, TUS intensities 7.5 and 15 mW/cm^2 increased chondrocyte proliferation and TUS intensities $\geq$ 30 mW/cm^2 increased proteoglycan content. The proliferative response at intensity levels below SAFHS (< 30 mW/cm^2) substantiates findings by Zhang et al [108] of enhanced proliferation of chondrocytes following treatment at sub-SAFHS intensities.

Cartilage and isolated chondrocytes have repeatedly demonstrated responsiveness to TUS in research investigations. TUS exposure is related to enhancements of articular cartilage healing, hyaline cartilage growth, and endochondral ossification. Strong evidence exists to signifying that these responses are related to enhancement of chondrocyte function, including matrix production, cellular proliferation and cytokine release. Analyses of hyaline cartilage and fibrocartilage models suggest that chondrocyte proliferation and protein synthesis are regulated by different TUS treatment intensities, indicating differential response to varied doses of TUS energy. Chondrocytes from a variety of species and tissue origins are responsive to TUS; therefore TUS may be a plausible modality for enhancement of articular cartilage healing and chondrocyte function.

Tendons

Several investigators have examined the efficacy of TUS on tendon and ligament healing in vivo, and have demonstrated benefits of TUS on numerous characteristics of these tissues including collagen deposition, collagen fiber alignment, cell number, ultimate tensile strength, ultimate load, stiffness, and energy absorption capacity. A variety of TUS treatment parameters have been reported to improve the healing processes in surgically transected tendons, up to 30 days post-injury. However, SAFHS parameters have not been studied in relation to TUS enhancement of tendon healing.

TUS has been reported to enhance aspects of healing in partially ruptured rat Achilles tendons. Frieder et al reported that TUS exposures for 3 weeks (1500 mW/cm^2 SATA, CW, 3-minutes, 3x/wk, no reported TUS frequency) improved collagen fiber density and alignment, and decreased overall cellular content at 3 weeks post-injury [113]. Similar TUS exposure parameters (1500 mW/cm^2 SATA, CW, 4 minutes, daily, no reported TUS frequency) resulted in increased collagen content and tendon breaking strength by 5 days post-injury that remained elevated at 9, 15 and 21 days post-injury when compared to sham treatments [114]. TUS delivered at < 1000 mW/cm^2 SATA has also been reported to improve healing in partially ruptured rat Achilles tendons as 9 consecutive daily TUS exposures (1 MHz, 500 mW/cm^2 SATA, CW, 5-minutes) increased collagen content and breaking strength of treated tendons up to 21 days post-injury [115].

Completely ruptured rat Achilles tendons treated with TUS (1 MHz, 1000 mW/cm^2 SATA, CW, 5 minutes, 9 consecutive days) had greater ultimate tensile strength compared to sham-sonicated controls at 9 days post-injury [116]. In a follow-up study, Enwemeka et al

utilized an identical protocol with the exception of reducing the TUS intensity from 1000 mW/cm^2 to 500 mW/cm^2 SATA and reported enhanced healing, as indicated by increased tensile strength, tensile stress and energy absorption capacity [23]. In comparing the data between studies, Enwemeka et al noted that all three variables of tendon function (tensile strength, tensile stress and energy absorption capacity) were greater in tendons sonicated at 500 than 1000 mW/cm^2 SATA.

Other investigators using variable TUS intensities (1 MHz, 1000 and 2000 mW/cm^2 SATA, CW, 4 minutes, 22 consecutive daily exposures) have reported conflicting results between the two intensities in relation to the healing response [5,117]. Ng et al reported improved ultimate tensile strength in hemi-transected rat Achilles tendon at both treatment intensities, compared to untreated injury controls [5]. However, in an identical tendon injury and TUS exposure model, Ng et al reported that 2000 mW/cm^2, but not 1000 mW/cm^2, improved ultimate tensile when each was compared to untreated controls [117]. The only reported difference among the biomechanical testing protocol was the performance of load-relaxation testing prior to tendon strength testing [5] which was not performed in the subsequent study [117]. Otherwise, no explanation of the variable findings is readily apparent.

In addition to a possible intensity-dependent effect, duty cycle has also been reported to alter the healing benefit of TUS [118]. Using a complete tendon rupture model, TUS exposures (1 MHz, 500 mW/cm^2 SATA, 5 minutes, 12 treatments) delivered in CW or 20% PW were compared. Analysis of collagen fiber alignment revealed improved fiber alignment in PW treated tendons compared to mock-sonicated tendons, while fiber

alignment following CW exposures was significantly worse (more random fiber alignment) than the controls and tendons treated with PW.

Since collagen fiber alignment is a factor in imparting strength to tendons, this finding contrasts the reports of CW TUS enhancing tendon healing. However, the enhanced tendon strength noted with CW TUS is likely related to the reported overall increase in collagen deposition rather than orientation of collagen fibers, suggesting varied treatment duty cycles affect different aspects of the healing response. Other researchers have corroborated the finding of improved collagen fiber alignment in tendons treated with PW TUS [119]. Utilizing methods identical to Da Cunha et al [118], complete tendon transection and TUS treatment regimen (1 MHz, 500 mW/cm^2 SATA, 20% PW, 5-minutes, 12 treatments), the authors reported improved collagen fiber alignment compared to sham treatments [119].

While Da Cunha et al [118] reported that PW TUS, but not CW TUS, improved collagen alignment, Frieder et al [113] reported that CW TUS does improve collagen fiber alignment in healing tendons. The contradictory findings here are likely due to experimental differences. Frieder et al utilized TUS treatment parameters that were quite different than those of Da Cunha et al: treatment intensity (1500 vs. 500 mW/cm^2 SATA), treatment durations (3 minutes vs. 5 minutes), treatment frequency (3 treatments per week vs. daily treatments), and overall treatments (9 vs. 12), respectively. Additionally, Frieder et al employed a partial tendon rupture model compared to the full tendon rupture model of Da Cunha et al.

Despite the evidence discussed above, reports of limited or no benefit of TUS on tendon healing have been published [120,121,122]. These investigations of healing of tenotomized chicken flexor tendons exposed to TUS have provided less promising results in comparison to tendon healing studies in rat Achilles tendon. Chicken flexor tendons treated with TUS (3 MHz, 750 mW/cm^2 SATA, CW, 5 minutes, 20 daily treatments) exhibited no enhancement of either collagen production or breaking strength at 10 weeks post-injury, when treatments were initiated 28 days post-injury [121]. Additionally, sonication provided no improvement in breaking strength 6 weeks post-injury in TUS-treated chicken flexor tendons, when treatments were initiated 7 days post-injury (3 MHz, 200 mW/cm^2 SATA, 20% PW, 4 minutes, 3x/wk for 5 wks) [122]. In a comparison study, Gan et al applied TUS (3 MHz, 200 mW/cm^2 SATA, 25% duty cycle, 3-minutes, 10 daily treatments) to chicken flexor tendons, with TUS initiated 7 days or 42 days post-injury [120]. In agreement with the other investigations using chicken flexor tendons[122], the authors found no improvement in strength of the healing tendons, regardless of the timing of TUS treatments.

The data regarding TUS enhancement of chicken flexor tendon healing appears to conflict with reports involving rat Achilles tendon. Most notable in comparing investigations among chicken and rat models, researchers utilizing rats initiated TUS treatments on the day of surgery or on post-operative day one, rather than 7, 28 or 42 days after injury. Following the hypothesis that TUS affects the early stages of healing (inflammatory and early reparative phases), the lack of effect of TUS on chicken flexor tendon healing compared to rat tendon healing are likely due to the inability of TUS to

affect early healing when initiated 7 days or later post-injury. Yet for bone TUS enhances healing of delayed and non-union fractures, tissues that are not progressing through the normal healing phases. This apparent discrepancy may indicate that the healing benefit provided by TUS is tissue specific. Additionally, given the responsiveness of bone cells to mechanical forces, including ultrasound [123,124,125], it may be that bone cells are better able to transduce ultrasound energy into cellular activity compared to fibroblasts.

Although variable methodologies inhibit direct inter-study comparison, the overall body of investigations into TUS effects on tendon healing indicates that CW and PW TUS can enhance tendon healing in animals. These benefits appear to be related to improvements in quantitative and qualitative deposition of collagen into the ECM. Further research is needed to clarify the differential effect of TUS duty cycle on collagen deposition and collagen fiber alignment, as well as clarifying the effect of the timing of initiation of TUS-exposures on healing of tendons.

Ligaments

TUS effect on ligament healing has not been studied to the same extent as tendon healing, but sonication of transected ligaments has demonstrated improved healing up to 6 weeks post-injury [4,13,126,127]. Takakura et al reported enhanced healing of transected rat medial collateral ligaments (MCL) after exposure to SAFHS [127]. Specifically, ultimate load, stiffness, energy absorption, and collagen fibril diameter were all increased in the TUS treated MCLs at 12 days post-injury. No differences were noted at 21 days post-injury. Sparrow et al treated completely transected rabbit MCLs with TUS (1 MHz, 300

mW/cm^2 SATA, CW, 10 minutes, every other day for 6 treatments) and reported increased energy absorption to failure, ultimate load and increased cross sectional area of sonicated ligaments 6 weeks post-injury [4]. Also, the proportion of type I collagen relative to the amount of type III collagen was increased in MCLs at 3 and 6 weeks post-injury. During healing, type I collagen, which provides greater tensile strength to ligaments compared to type III collagen, replaces much of the initially deposited type III collagen [128,129]. The finding of an increased proportion of type I collagen suggests that TUS affects either the normal replacement of type III collagen with type I collagen or that TUS enhances the initial deposition of type I collagen.

TUS-enhanced MCL healing has been associated with the production of TGF-β1 [126]. Transected MCLs treated with TUS (3 MHz, 460 mW/cm^2 SATA, 20% PW, 5 minutes) had increased levels of the cytokine growth factor. TUS exposure (3 MHz, 100 mW/cm^2 SATA, 20% PW, 5-minutes) had no effect on TGF-β1. Furthermore, 10 days of TUS (3 MHz, 460 mW/cm^2 SATA, 20% PW, 5-minutes) induced greater amounts of TGF-β1 compared to 1 and 5 days of treatment. As discussed previously, TGF-β1 activity during healing enhances cellular recruitment, ECM production and angiogenesis [130], but Leung et al [126] did not investigate any of these variables.

TUS (3 MHz, 460 mW/cm^2 SATA, 20% duty cycle, 5 minutes, 10 daily treatments) has also been shown to affect the levels of inflammatory mediators during healing of completely transected rat MCLs [13]. This experimental model was identical to that of Leung et al [126]. The authors reported increased PGE_2 and decreased leukotriene B4 (LTB_4) from 2 to 11 days post-injury. These arachidonic acid derivatives are known mediators of

the inflammatory response to wounding, with PGE_2 being produced by endothelium, monocytes, macrophages and fibroblasts, and LTB_4 being released from neutrophils and mast cells [88,131]. TUS effect on inflammation has been hypothesized to be an acceleration of the process [48]. However, increased PGE_2 and decreased LTB_4 up to 11 days post-injury, coupled with increases in TGF-β1 suggest that TUS effects on inflammation may be more complicated than simply accelerating the cellular processes.

The limited data regarding TUS and healing ligaments indicates that TUS can improve healing up to 6 weeks post-injury most notably through increased mechanical strength of the treated ligaments. This benefit to healing appears to be the result of enhancement of growth factor production, alteration of the inflammatory process and modulation of collagen deposition, presumably via affect on fibroblast protein synthesis. The effect of TUS on fibroblast proliferation has not been explored in these in vivo models, but as will be discussed later, TUS has been reported to increase fibroblast proliferation in vitro.

Integument

Healing integument wounds require connective tissue matrix deposition, angiogenesis and regeneration of epithelium [131,132]. In non-fetal tissues, this healing process results in replacement tissue that is suboptimal (decreased tensile strength and pliability) compared to the uninjured, original tissue. Studying the effect of TUS on full-thickness and incision wounds in animal models including pig, rat, and human, researchers

have reported acceleration of the inflammatory phase and enhancement of the proliferative phase of healing [3,24,133,134,135].

Using a pig model, Byl et al found that 5 daily exposures to TUS (1 MHz, 100-300 mWcm^2 SATA, 20% PW) increased tensile strength and collagen deposition in incision wounds, and accelerated full-thickness wound closure when compared to sham controls assessed 1 week post-injury [3]. Full-thickness wounds were sonicated for 5 minutes and incision wounds were sonicated for 10 minutes. All wounds were treated at 100 mW/cm^2 SATA for the first 2 days, and at 300 mW/cm^2 SATA for the final 3 days of treatment.

In rats, incision wounds treated with 7 or 10 daily TUS exposures (1 MHz, 100 mW/cm^2 SATA, 20% PW, 5 minutes) had increased fibroblast number 4 days post-injury [133], increased collagen deposition 7 days post-injury [133,134] and increased wound breaking strength 25 days post-injury [133,134]. Healing of full-thickness wounds in rats has also been reported to be enhanced by TUS after 5 daily treatments (0.75 or 3 MHz, 100 mW/cm^2 SATA, 20% PW, 5 minutes) when compared to sham [135]. Five days post-injury treated wounds had more extensive granulation tissue, increased fibroblast number, and fewer macrophages and leukocytes, all of which suggest acceleration of the inflammatory phase with earlier initiation of the proliferative phase. There were no differences in healing characteristics between wounds treated with TUS at 0.75 MHz and 3 MHz.

Wound healing studies in humans have generated much less consistent results. TUS-treated chronic human venous stasis ulcers (3 MHz, 200 mW/cm^2 SATA, 20% PW, 5-10 minute treatments, 3x/wk for 4weeks) had decreased wound area after 4 weeks of

sonication [136]. However, Lundeberg et al reported that TUS treatments (1 MHz, 100 mW/cm^2 SATA, 10% PW, 10-minutes, 3x/wk for 4wks) had no effect on the rate of wound healing or wound closure for patients with chronic venous stasis ulceration compared to sham TUS [137]. Eriksson et al also found no improvement in wound closure or wound healing rates following treatment of chronic venous stasis ulcers with TUS (1 MHz, 1000 mW/cm^2 SATA, CW, 10 minutes, 2x/wk for 8wks) [138].

The effect of TUS on pressure ulcer healing has also been described [139,140]. McDiarmid et al [139] utilized TUS (3 MHz, 160 mW/cm^2 SATA, 20% PW, 5-10 minutes, 3x/wk), while Ter Riet et al [140] utilized TUS (3.28 MHz, 100 mW/cm^2 SATA, 20% PW, 4-8 minutes, 5x/wk for 12wks) to investigate enhancement of healing. Both studies reported no effect on pressure ulcer healing compared to sham treated wounds, but McDiarmid et al reported enhanced rate of healing of "infected" wounds treated with TUS. Because infected wounds were classified by visualization and not bacteriological assay, and given the small sample size of the groups, (TUS = 11 and placebo = 8) little can be inferred, regarding the response of infected wounds to TUS exposure.

Based on the overall evidence, it appears that TUS does positively affect early stages of healing of acute integument wounds. This benefit has been demonstrated in animal models, but has not been established in treating wounds in humans. The discrepancy between in vivo and clinical studies is likely due to differences in methodology and types of wounds. In animal studies investigators treated acute wounds daily, while investigators in clinical trials utilized TUS intermittently for treatment of chronic wounds. The effect of consecutive versus non-consecutive TUS exposures has not

been explored in relation to integumentary wound healing, but an additive effect of repeated TUS exposures has been reported in articular cartilage [12]. The clinical investigations have focused on patients with compromised healing (i.e., chronic venous stasis or pressure ulceration), while animal studies utilized acute wounds without healing deficiencies. Chronic ulceration involves dysfunctional healing physiology, and it is possible that TUS cannot influence inadequate or compromised wound healing states such as chronic ulceration [130,141].

However, TUS has shown the ability to improve compromised fracture healing at SAFHS parameters. Clinical studies discussed here have not reported use of SAFHS on chronic ulceration. Based on the ability of SAFHS parameters to enhance inadequate fracture healing, it is possible that specific parameters may be necessary to affect compromised wound healing. Differences in the pathophysiology of chronic venous ulcers and pressure ulcers compared to non-union and delayed union fractures might also be related to the disparate findings of TUS benefit to tissue with compromised healing. Furthermore, differences in the overall treatment regimens (3 to 4 months of treatment for fractures compared to 4 to 8 weeks of treatment for chronic venous ulcers) might explain the discrepancy in TUS effects on healing in these models.

The overall efficacy of TUS in clinical healing remains in question. Despite positive in vivo evidence for enhanced healing of acute wounds in animal models reported, clinical trials with traditional TUS (1-3 MHz, 0.03-2000 mW/cm^2 SATA) have not supported its use for chronic ulceration. Additional investigation using different

parameters, such as SAFHS, are needed to determine if TUS can be beneficial for enhancement of healing in chronic integumentary wounds.

In Vitro Fibroblast Response to TUS

In vitro models have been used to examine cellular response to TUS and to associate the cellular response with demonstrated benefits for tissue healing in vivo [7,8,97]. Ramirez et al investigated fibroblast response to TUS in a matrix injury model using collagenase to partially disrupt a monolayer of neonatal rat fibroblasts [8]. Following a single treatment of TUS (1 MHz, 400 mW/cm^2 SATA, CW, 3 minutes), the fibroblasts had increased collagen synthesis compared to untreated controls. Additionally, three and five TUS exposures increased fibroblast proliferation compared to untreated controls.

Supporting the proposed proliferative and anabolic effect of in vitro TUS on fibroblasts, a single dose of TUS (1 MHz, 20, 80, 140 or 200 mW/cm^2 SATA, 20% PW, 5 minutes) increased proliferation of and collagen production by human gingival fibroblasts [7]. Most TUS intensities (20, 80, and 140 mW/cm^2) resulted in elevated collagen production, but only higher intensities (140 and 200 mW/cm^2) increased cell proliferation. These findings again indicate a dose-dependent relationship between TUS intensity and cellular response.

In contrast to the two previous in vitro studies, a single dose of TUS (3 MHz, 140-990 mW/cm^2 SATA, CW, 5 minutes) did not increase cell proliferation in human ligament fibroblasts, and TUS at several intensities (140, 230, 540 mW/cm^2) decreased collagen

production [97]. However, in agreement with Doan et al [7], cell response to TUS appeared to be dose-dependent.

Comparison of the studies by Doan et al [7] and Harle et al [97] demonstrate that different TUS exposure conditions 1MHz, 20% PW and 3MHz, CW respectively, influence fibroblasts in culture. Both studies utilized TUS doses that are commonly used clinically and that are comparable to doses utilized in the in vivo tendon, ligament and integument wound healing investigations. These contradictory results add to the uncertainty of the effect of TUS parameters on cell proliferation and collagen production. Whether the TUS frequency and duty cycle affected this result is not known and neither study compared the effects of these parameters.

Overall, TUS has many positive effects on tendon, ligament and integument healing. Evidence supports TUS enhancement of healing of these soft tissues, especially when TUS treatments are initiated early in the post-injury phase. This enhancement appears to be related to fibroblast function; specifically, cellular proliferation, as well as collagen deposition and organization, all of which support enhanced in vivo healing following TUS. These responses suggest that TUS can alter processes of the proliferative phase of healing rather than simply affecting the inflammatory phase.

In spite of the convincing body of evidence supporting TUS benefit for soft tissue healing in animal models, the differential effects of the TUS exposure parameters remains unclear. Changes in frequency, intensity, duty cycle, and overall TUS dose (including overall number and duration of TUS exposures) appear to alter TUS effects; however, no consensus exists in the available literature in regard to effects of specific parameters.

Additional comparison studies are critical to elucidate the parameter-response relationships that appear to exist.

Muscle Healing

Unlike the vast number of investigations of TUS enhancement of healing of integument, tendons, and ligaments, minimal experimentation has been undertaken in regard to TUS effects on healing following skeletal muscle injury. Like most tissues, muscle heals following a general, three-step progression of inflammation, repair and remodeling. Unlike other tissues, muscle healing is dependent on activation of normally dormant satellite cells. Satellite cells, and other immature mesenchymal cells differentiate into myoblasts, which fuse together to form myotubes and eventually mature into myofibers as replacement for the original, damaged regions of fibers [142]. Resident fibroblasts in the area of injury proliferate and secrete matrix molecules to replace the connective tissue surrounding the muscle fibers. This fibroblastic activity must be balanced with appropriate myotube formation. Maintaining the balance between satellite cells and fibroblasts represents an additional obstacle to adequate healing of injured muscle [143]. Theoretically, proliferative enhancement of satellite cells would produce improved muscle repair, while proliferative enhancement of fibroblasts would result in increased scar formation. Thus, any modality altering cell number for muscle healing needs specificity in the cells that it affects to provide an appropriate benefit to healing. Given that TUS has been reported to induce proliferation in a number of experimental

models and cell types, application of TUS to injured muscle could be expected to affect cell proliferation and subsequent muscle repair.

Among the investigations of TUS on muscle healing, minimal evidence supports a benefit to healing. Two TUS exposures (3 MHz, 300 mW/cm^2 SATA, 20% PW, 6 minutes) increased satellite cell proliferation at 4 days post-injury and three or four TUS exposures increased fibroblast proliferation at 7 days post-injury, in contusion-injured rat muscle [144]. By 10 days post-injury, neither variable was affected by TUS, nor was there benefit for re-capillarization or myotube formation at any time point. Four consecutive days of TUS exposure (3 MHz, 100 mW/cm^2 SATA, CW, 5 minutes) did not affect muscle mass, contractile protein concentration, fiber cross-sectional area, number and density of myonuclei at 4 days post-injury compared to untreated muscle [145]. However, these variables are not likely to be increased within the 4-day time frame [143].

TUS treatment (1 MHz, 500 mW/cm^2 SATA, CW, 5 minutes) given for 7 consecutive days post-injury has been reported to accelerate muscle repair following contraction-induced muscle injury in rats [26]. At 7 days post-injury, maximum isometric tetanic force of injured muscles was greater following TUS in comparison to untreated, injured controls. Analysis of force production in experimental muscle should be a superior measure of the state of repair compared to cellular and molecular variables assessed by Markert et al [145] and Rantanen et al [144], since force production directly relates to the overall "health" of the muscle.

The evidence of TUS benefit to muscle healing reported by Karnes and Burton [26] may also be related to utilization of a contraction-induced injury; a mode of injury that

typically preserves the basal lamina so as to provide scaffolding for regenerating fibers, unlike a contusion-injury which is more likely to destroy the basal lamina [142]. Furthermore, the reported benefit to healing could be a result of an increased number of TUS exposures, 7 exposures compared to 3-4 days of treatment utilized by Markert et al [145] and Rantanen et al [144], given in vivo evidence of an additive effect of TUS on tissue healing [13,24,126,146].

The data from investigations of muscle healing provide minimal evidence for benefit of TUS, when assessed in the short term (< 2 weeks). However, TUS does appear to have a proliferative effect on skeletal muscle fibroblasts and satellite cells, similar to its mitogenic effect on cells of other healing tissues. Concerning TUS exposure parameters, CW and PW, 1 and 3 MHz and intensities between 100-500 mW/cm^2 have been employed, without the emergence of any trend of effect of those sonication variables on muscle healing. Furthermore, analysis of healing muscle has not been undertaken beyond 10 days post-injury, leaving unanswered the long-term effect of sonication. As such, further experimentation comparing types of muscle injury, TUS parameters, and assessment of increased healing time points should be undertaken to clarify the question of TUS benefit on skeletal muscle healing.

Peripheral Nerve Regeneration

Injury to peripheral nerves occurs as a result of crush, stretch, avulsion or compression, with functional nerve repair often being incomplete [147]. There have been several reports of the effects of TUS on peripheral nerve regeneration. Using rat models of

peripheral nerve injury, investigators have reported that TUS application improves neuronal regeneration and functional outcomes for tissues innervated by the injured nerve.

Following TUS exposure (1.5 MHz, 16 mW/cm^2 SATA, 20% PW, 20 minutes, 12 consecutive days), regenerating neurotomized sciatic nerves in rats had increased numbers of A-type and B-type fibers, myelin sheath thickness and overall axon fiber area when compared to sham treated nerves at 2 weeks post-injury [148]. Functional recovery of crush-injured rat sciatic nerves was enhanced following TUS treatment for 10 consecutive days (1 MHz, 80 mW/cm^2 SATA, 20% PW, 10 minutes) compared to sham [149]. Recovery of hind limb function, recorded at weekly intervals, was accelerated from day 14 to day 21 post-injury, while nerve fiber density was increased in nerve segments distal to the injury site 21 days post-injury. Also employing a crush-injury model of rat sciatic nerve, Mourad et al reported that TUS exposures three times per week for 4 weeks (2.25 MHz, 250 mW/cm^2 SATA, CW, 1 minute) improved functional recovery in hind limbs compared to sham TUS [150]. Over the 30-day time course of healing, recovery of hind limb function was accelerated from day 16 to day 30. Despite the use of the exposure frequency of 2.25 MHz, an unusual treatment frequency not available on many clinical ultrasound generators, and the brief treatment duration (1-minute), a positive influence of TUS on nerve regeneration was demonstrated.

TUS has been reported to increase Schwann cell myelination in regenerating peripheral nerves in rats [27]. After excision of a 10 mm segment of the sciatic nerve, investigators implanted nerve guidance conduits, some seeded with Schwann cells, between the nerve stumps and exposed the nerves/conduits to 12 TUS exposures over 14

days (1 MHz, 40 mW/cm^2 SATA, 20% PW, 5 minutes). At 6 weeks post-injury, sonicated nerve fibers within the seeded conduits had greater mean axonal area and myelination in comparison to sham-treated specimens and when compared to treated conduits that were not seeded. These findings are in concurrence with those of Crisci et al [148] in which neurotomized sciatic nerves had greater axonal area and increased myelination following TUS. Enhanced recovery of limb function noted by Raso et al [149] and Mourad et al [150] also indicates that TUS improves nerve myelination and / or axonal growth.

Together, these investigations suggest that TUS enhances peripheral nerve regeneration, apparently through alteration in Schwann cell activity. Schwann cells are believed to have a predominant role in peripheral nerve regeneration through production of neurotrophic factors, guidance of axonal growth and increased myelination [147]. Thus it is plausible to suggest that TUS directly affects Schwann cell function as well as the regenerating axons. However, the cellular mechanisms involved in the TUS-enhanced nerve regeneration via Schwann cells have not yet been investigated.

Angiogenesis

Angiogenesis is critical for repair of injured tissues, as adequate blood supply must be present for appropriate healing. The process of angiogenesis begins soon after tissue injury, in the inflammatory phase of healing, as endothelial cells proliferate and eventually provide the base for new vasculature [151]. The importance of this process of tissue healing provides a basis for investigating angiogenesis as a potential target for the effects of TUS.

Studies that have examined TUS effects on endothelium and angiogenesis have shown positive results. Capillary density and arteriole blood flow were increased in chronically ischemic rat cremaster muscle following TUS exposure for 3 weeks (1 MHz, 150 mW/cm^2 SATA, 50% PW, 5 minutes, 3x/wk), when compared to sham treatments [152]. Full-thickness wounds in rats treated with TUS up to 7 consecutive days (0.75 MHz, 100mW/cm^2 SATA, 20% PW, 5 minutes) had increased vascularity compared to sham treated wounds after 5 days of treatment [153].

Investigation of TUS effects on angiogenesis following ischemic injury to rat hind-limb has provided additional evidence of the benefit of sonication [154]. TUS exposure (2 MHz, 50 mW/cm^2 SATA, CW, 5 minutes, 3 treatments) was initiated on the day of surgery (injury) and concluded on day 3 post-injury. Histological analysis at 7 days post-injury revealed increases in the number of proliferating endothelial cells, the overall number of blood vessels and the average blood vessel diameter in TUS-treated muscle compared to controls. At 3 weeks post-injury, angiography revealed sustained increase in blood vessel number, while laser Doppler analysis showed increased tissue perfusion for treated limbs compared to controls. The authors also reported a 38-fold increase in vascular endothelial growth factor (VEGF) mRNA in treated limbs at 7 days post-injury compared to controls. VEGF is a potent angiogenic factor and the authors hypothesized that its up-regulation explains the improvement in vascularity, and endothelial proliferation. These results support the findings of Hogan et al [152] and Young and Dyson [153], who reported a beneficial effect of TUS on angiogenesis, and it appears to be the most complete analysis of TUS effect on variables of angiogenesis.

In vitro analysis of the effect of TUS on endothelial cells have been also been reported. Release of nitric oxide (NO) and calcium ions (Ca^{2+}) into culture media was increased by TUS after 6 consecutive days of treatment (1 MHz, 200, 320, and 400 mW/cm^2 SATA, 20% PW, 10 minutes) when compared to untreated controls [155]. Nitric oxide release was increased following TUS at 320 mW/cm^2 SATA, while calcium release was increased following TUS at each intensity. Nitric oxide is an important mediator of vascular function, affecting vascular smooth muscle relaxation, leukocyte adhesion to endothelium and inhibition of platelet aggregation [156,157]. Changes in Ca^{2+} flux in cells have been reported in other cell types treated with TUS, including chondrocytes, fibroblasts, epidermis and this altered ion flux has been implicated by others as a component of the mechanism of TUS effect on cells [49,50,65,158].

This body of research suggests that angiogenesis following injury is enhanced by exposures to TUS, up to 3 weeks post-injury. Improvement in the angiogenic response following tissue injury could accelerate overall tissue healing, although this has not been directly investigated. The mechanism responsible for the enhancement of angiogenesis appears to be related to endothelial cell function. Treatment intensities between 50 and 400 mW/cm^2 SATA appear to be beneficial for an angiogenic effect, which follows the current trend of utilization of intensities below 1000 mW/cm^2 SATA to achieve TUS-enhanced healing [35,37].

Inflammatory Cells

As discussed previously, an appropriate inflammatory response is crucial for proper tissue healing. The inflammatory phase of healing involves functions of a variety of cells including mast cells, monocytes, macrophages, lymphocytes and neutrophils. TUS enhancement of healing is hypothesized to be a function of enhancing the inflammatory and proliferative phases of healing. The ability of TUS to alter the inflammatory phase has been supported by in vivo and in vitro investigations that have directly explored the effect of TUS on various inflammatory cells.

Sonication has been reported to affect mast cell function in vivo and in vitro. Increased mast cell degranulation in rat ankle joints treated with a single TUS exposure (0.75 MHz, 1.5 MHz, or 3.0 MHz, 500 mW/cm^2 SATA, 20% PW, 1 minute) has been demonstrated [159]. No difference in induction of mast cell degranulation was found between the variable frequencies. Byl et al reported increased mast cell degranulation in porcine flank wounds following a single TUS exposure (1 MHz, 500 mW/cm^2 SATA, 20% PW, 5 minutes) [3]. During the inflammatory phase, mast cell degranulation results in release of histamine, serotonin, and heparin, which serve to increase vascular permeability, inflammatory cell recruitment and to enhance angiogenesis [160].

Monocytes and macrophages have been shown to be responsive to TUS in vitro. Human macrophages exposed to TUS (0.75 MHz or 3 MHz, 500 mW/cm^2 SATA, CW, 5 minutes) released a soluble mitogenic factor into culture media, evident by fibroblast proliferation that was induced after fibroblasts were cultured in the macrophage conditioned media [161]. Based on the time of response, the authors hypothesized that TUS

exposure at 0.75 MHz resulted in release of pre-formed products only, while 3 MHz exposures resulted in synthesis and release of the fibroblast mitogenic factor. Doan et al investigated the variable effects of TUS on human monocytes, the blood-borne precursor to macrophages [7]. Single 5-minute exposures at 1 MHz, 20% PW with variable intensities (20, 80, 140, and 200 mW/cm^2 SATA) were compared. The treated monocytes released more vascular endothelial growth factor (VEGF) at each intensity except 140 mW/cm^2 compared to sham. Release of interleukin-8 (IL-8), basic fibroblast growth factor (bFGF), interleukin-6 (IL-6) and tumor necrosis factor-α (TNF-α) was not affected by TUS exposure. The authors did report increased release of IL-1β in response to TUS at 45 Hz, but this very low frequency is not considered traditional TUS and needs to be validated further for clinical usage.

Lymphocytes have also been reported to respond to TUS exposures. Cultured spleenocytes exposed to TUS (1 MHz or 3 MHz, 100 or 500 mW/cm^2 SATA, CW, 10 minutes) exhibited altered production of interleukin-2 (IL-2), interleukin (IL-4) and interferon-γ (IFN-γ) [162]. Following TUS exposure, spleenocytes were cultured with Concanavalin A (Con A), a lectin protein known to stimulate T-cell production of IL-2, IL-4 and IFN-γ. These cytokines are considered inflammatory regulators because they control activities of T and B-lymphocytes, macrophages, natural killer (NK) cells and mast cells [163]. Treatment at both frequencies and intensities, followed by addition of Con A to the culture media, resulted in increased IL-2 production. Con A addition after TUS at 1 MHz also resulted in increased release of IL-4 and IFN-γ, while Con A addition after TUS at 3 MHz resulted in decreased release of IL-4 and IFN-γ. This finding suggests that TUS

can alter cellular response to subsequent stimuli rather than only affecting on-going processes.

In vivo assessment of the effect of TUS on inflammatory cells has also been reported among investigations of wound healing in rats [133,134,135]. Full-thickness flank wounds were exposed to TUS (0.75 MHz or 3 MHz, 100 mW/cm^2 SATA, 20% PW, 5 minutes, 5 or 7 treatments) [135]. At 5 days post-injury, quantitative histological analysis demonstrated a reduced number of neutrophils in wounds treated with TUS at 0.75MHz compared to sham treated wounds. Macrophage number was also reduced in wounds treated at either intensity (0.75 MHz and 3 MHz). No difference in cellular content of healing wounds was noted when assessed at 7 days post-injury. Demir et al treated incision wounds with TUS (1 MHz, 100 mW/cm^2 SATA, 20% PW, 5 minutes, 4 or 10 treatments) and reported reduction in the number of neutrophils at 4 and 10 days post-injury and reduced macrophage and mast cell number 10 days post-injury compared to sham TUS [133]. In addition, fibroblast number and hydroxyproline content were increased at both time points. Taskan et al [134] used an experimental model and TUS exposure parameters identical to Demir et al [133], and reported a decrease in mast cells at 4 and 7 days post-injury. Contrary to the other inflammatory cell studies in rat wounds, Taskan et al reported that macrophage number in the wounds was increased at both post-injury time points.

Most of the changes noted among these rat wound studies are consistent with progression from the acute inflammatory phase to the proliferative phase of healing. The exception being an increase in macrophages reported in one study. Overall, these findings

indicate that the inflammatory phase was affected, and the preponderance of evidence suggests that the change was acceleration rather than exaggeration of the inflammatory phase.

A study examining an indirect effect of TUS on inflammatory cells does provide some evidence for actual enhancement of inflammation [54]. Isolated bovine endothelial cells were exposed to TUS (1 MHz, 1600 mW/cm^2, CW, 15 minutes) and were then incubated with freshly isolated human polymorphonuclear leukocytes (PMNLs). Adhesion of PMNLs to the sonicated endothelial cells was increased from 1 to 240 minutes post-sonication in comparison to sham-treated endothelial cells. Since the initial stages of inflammation include increased migration of leukocytes (PMNLs) from the vasculature into the interstitium, potentiation of this process could result in increased inflammatory activity [163].

Considering evidence from these investigations, numerous cells involved in the inflammatory phase of healing have demonstrated responsiveness to TUS indicating that sonication can affect processes in these cells. Inflammatory cytokine and growth factor release, mast cell degranulation and increased endothelial cell adhesion properties are all activities normally associated with the inflammatory phase of healing. The limited in vivo evidence, suggests that both the inflammatory and early proliferative phases can be accelerated by TUS treatment.

Conclusion

In spite of the vast amount of research on TUS and its effects on healing, many questions about its effects remain, such as the cellular activities that are most responsive to TUS, the long-term benefit for soft tissue healing, the timing of treatment initiation, the optimal TUS exposure parameters for enhanced healing and the biophysical mechanism of TUS effects on various cell types.

The thermal affect of TUS is hypothesized to create some of the reported cellular and tissue responses. Using appropriate TUS parameters, there is little question that tissue heating occurs and this heating effects molecular movement. However, many investigations have demonstrated TUS effects without measurable changes in temperature or using parameters that are not expected to produce temperature increases, thus it is clear that thermal changes need not be present for TUS to be effective.

Regarding nonthermal mechanisms, the current body of investigations has not clearly elucidated the biophysical mechanism of action of TUS on cells and tissues. Research findings suggest that a number of different mechanisms could be responsible for TUS action. However, minimal evidence supports a correlation between any one of the proposed nonthermal mechanisms of action, acoustic cavitation, free radical production and acoustic streaming, to altered cellular functions. The technical difficulty in accurately measuring these phenomena presents a considerable challenge in evaluating the role of these proposed mechanisms. Furthermore, these proposed mechanisms could be occurring in combination rather than exclusively, further complicating understanding of the role each might play in cellular responses.

TUS enhancement of tissue healing is supported in various models and tissue types including bone, tendon, ligament, cartilage and integument. In fractures, the processes responsible for the acceleration of fracture healing appear to be related to enhancement of matrix production, chondrocyte and osteoblast activity, and the ability to enhance vascularity. Accelerated healing of soft tissues (ligaments, tendons, articular cartilage, and dermal wounds) also appears to be enhanced by TUS exposure, although some conflicting results exist. For soft tissue healing, TUS affects cellular activities of inflammatory and reparative phases of healing, with the overall result being enhanced matrix production and deposition through resident cell (fibroblast and chondrocyte) activity.

It is apparent that many different TUS protocols and treatment parameter sets are effective in altering various aspects of cellular function and tissue healing. However, limited research has investigated the exact nature of the effect of different ultrasound parameters, presumably because so many different ones are available. Additional research is needed to assist in identifying the relationships between TUS parameters, possible mechanisms of action and cellular response.

Enhancement of processes of the inflammatory and proliferative phase, many of which are regulated by macrophages, is a likely mechanism by which TUS exposure improves healing of injured tissues. Indeed, TUS exposure has been reported to induce release of growth factors, cytokines and inflammatory mediators, as well as enhance angiogenesis and ECM production and deposition during healing. Macrophages, coordinators of inflammation and the early proliferative phase of healing, play a vital role

in all of these processes during tissue healing and without them, poor healing quality results [142,164-166].

Thus, the following chapters will describe our attempts to characterize the macrophage response to varied TUS parameter sets and how those responses might be related to the acceleration of early healing. In addition, we will explore the possible mechanism of TUS that is associated with the macrophage response.

Chapter 2

Effect of Therapeutic Ultrasound on Macrophage Release of Fibroblast Mitogens

Abstract

Macrophages coordinate the action of many different cells involved in tissue repair following injury. One way macrophages do this is by releasing paracrine factors that can induce proliferation of resident cells that are responsible for rebuilding damaged tissue. Therapeutic ultrasound (TUS) has been associated with enhancing the early stages of tissue repair, when macrophages are likely to be active. The objective of this study was to examine the effect of varied TUS parameter sets on macrophage release of fibroblast mitogens, as evidenced by proliferation of fibroblasts exposed to macrophage conditioned media. Phorbol-12-myristate-13-acetate (PMA) was used to induce differentiation of monocytic U937 cells into activated macrophages. Macrophages were exposed to TUS for 5 or 10 minutes at 0, 40 and 400 mW/cm^2 SATA, using a 20% duty cycle delivered at 1 and 3 MHz wavelength frequency. Macrophage conditioned media was collected at 10-minutes and 1-hour post treatment. Proliferation of human gingival fibroblasts (HGF-1) was assessed after incubation in the macrophage conditioned media. Fibroblasts proliferation was not affected by incubation in macrophage conditioned media for 24 or

48-hours, regardless of the combination of TUS intensity, wavelength and treatment duration utilized for macrophage insonation. Our results indicate that TUS at the parameters studied does not induce release of preformed fibroblast mitogens from activated macrophages. Mitogenic response of fibroblasts to TUS is either mediated directly by fibroblast response to sonication or induced by TUS parameters not included in this study.

Introduction

Following tissue injury, macrophages perform numerous functions including coordination of the inflammatory and reparative phases of healing. Functions of macrophages within the wound environment, include: phagocytosis of cellular and extracellular matrix (ECM) debris, neutrophil removal, cellular recruitment, induction of cell proliferation, and stimulation of cells responsible for ECM deposition and angiogenesis [164-168]. Many of these functions require secretion of chemical mediators (i.e. cytokines, growth factors) by macrophages that act as autocrine and paracrine mediators for cells in the wound healing milieu [163,164]. As such, any altered release of secretory products from macrophages is likely to impact the overall healing process.

Health care practitioners utilize TUS to improve tissue repair. TUS has been reported to enhance healing of many tissues and numerous studies suggest that TUS most likely enhances healing by affecting the early phases of the healing process [3,5,13,114,118,127,134,135,153]. Data from in vitro analyses of osteoblasts, fibroblasts and chondrocytes indicate that TUS can alter many cellular processes including: genetic transcription, granule release, protein secretion, matrix molecule synthesis and deposition, and cell proliferation [8,9,10,96-98,159]. During normal tissue repair, macrophages provide molecular signals that stimulate many of the aforementioned cellular responses. It is possible that TUS-enhanced healing occurs, at least in part, via stimulation of macrophage function. Thus, it is important to understand what role macrophages play in the TUS-induced enhancement of tissue healing. However, only a few investigations have assessed the effects of TUS on macrophage function.

In vitro analysis has demonstrated that macrophages respond to TUS by releasing paracrine factors involved with tissue repair [7,161]. Young and Dyson reported increased fibroblast proliferation following incubation in conditioned-media from sonicated macrophages [161]. The authors surmised that the macrophages released a growth factor into the culture media following sonication, and in this way macrophages contribute to the enhancement of healing induced by TUS. Young and Dyson also reported in vivo findings of an accelerated inflammatory phase, specifically noting increased neutrophil clearance rate, earlier recruitment and proliferation of fibroblasts and increased rate of granulation tissue formation in the first week of healing of full thickness dermal wounds in rats [135].

Following injury to integument, ligaments and tendons, fibroblasts are the primary cell type responsible for restoration of the connective tissue matrix and structural integrity of the healing tissue [116,129,169]. Fibroblasts are recruited to the site of injury via chemotactic agents, are induced to proliferate, and are responsible for deposition of collagen and other ECM proteins necessary for tissue repair [157,170]. These functions of fibroblast are coordinated in part by macrophage-released products such as cytokines and growth factors [129,164,171,172,173,174]. Given the limited data regarding macrophage response to TUS and the possibility that macrophages directly contribute to TUS-enhanced healing, the purpose of this investigation was to explore TUS effects on macrophage release of paracrine mediators that modify fibroblast proliferation and to identify difference in macrophage response to TUS treatment parameters.

The ranges of TUS parameters were selected considering the difference in cellular responses that have been previously reported among in vitro investigations, in order to

identify optimal TUS parameters for macrophage response. The experimental hypothesis was that sonication would result in macrophage release of a stimulatory factor(s) that enhances fibroblast proliferation, a process consistent with progression of the inflammatory phase toward the reparative phase of healing and that these effects on macrophage function will be dose-dependent.

Material and Methods

Materials and Reagents. Phorbol 12-myristate 13-acetate (PMA), dimethyl sulfoxide (DMSO), and lauryl sulfate (SDS) were obtained from Sigma Chemical Co., St. Louis, MO. Tris and the *DC* Protein Assay Kit were obtained from BioRad Laboratories, Hercules, CA. The bovine serum albumin (BSA) protein standard was purchased from Pierce Biotechnology Inc, Rockford, IL. Recombinant human platelet derived growth factor-bb (rhPDGFbb) was purchased from R & D Systems, Minneapolis, MN. Glycerol, sodium hydroxide, hydrochloric acid, and sterile pipets were purchased from Fisher Scientific, Pittsburgh, PA. Other sterile culture equipment: tissue culture plates and centrifuge tubes were purchased from Corning Inc., Corning NY. Microtubes were purchased from ISC Bioexpress, Kaysville, UT. Cell Proliferation Assay Kits were purchased from Chemicon Intl., Temecula, CA. Cell types used in this investigation: human monocytic cells (U937), and human gingival fibroblasts (HGF-1) purchased from American Type Culture Collection, Manassas, VA. Cell culture media reagents including: RPMI-1640 culture media and Dulbecco's Modified Eagle's Medium (DMEM), sodium

pyruvate, sodium bicarbonate, HEPES, L-glutamine, 0.25% trypsin, fetal calf serum and penicillin/streptomycin/amphotericin B were purchased from Invitrogen, Carlsbad, CA.

Cell Culture

U937 cells. All cell manipulations were conducted using sterile technique within a standard biological safety cabinet (Forma Scientific, Waltham, MA). Upon receipt, U937 (human monocytic) cells were thawed, expanded in RPMI growth media (*RPMI-1640 supplemented with 2 mM L-glutamine, 10 mM HEPES, 1 mM sodium pyruvate, 1.5 g/L sodium bicarbonate, 10% heat-inactivated fetal calf serum (HIFCS), penicillin 100 U/ml, streptomycin 100 μg/ml, and amphotericin B 250 ng/ml*), and then stored under liquid nitrogen in cryovials in 1.5 ml aliquots at 1.0 x 10^6 cells/ml in RPMI growth media with 10% DMSO. U937 cells from this stock batch were thawed and cells between passages 3-12 were utilized for all subsequent experimentation.

To begin experiments, U937 cells were thawed at 37°C, suspended in 20 ml of RPMI growth media, and centrifuged for 5 minutes at 200 x g to pellet the cells. Cells were then resuspended in 20 ml of RPMI growth media, placed in 75 cm^2 culture flasks and maintained in a humidified, water-jacketed incubator cabinet at 37°C with 95% air, 5% CO_2 mixture. Cell concentration was maintained between 1 x 10^5 and 2 x 10^6/ml, per manufacturer instruction. Cells were passed every 2-3 days to sustain appropriate concentration and to provide enough cells for each experiment. For cell passages, media containing cells were collected in 50 ml polypropylene tubes and centrifuged for 5 minutes at 200 x g. The supernatant was decanted, and the cells were resuspended in 30 ml of

RPMI growth media. Next, cell concentration was assessed using a standard laboratory hemacytometer (Fisher Scientific, Pittsburgh, PA). Cells were then resuspended in RPMI growth media at a concentration of 1 x 10^5 cells/ml in 20ml aliquots and returned to 75 cm^2 flasks for further propagation.

HGF-1 Cell Propagation. Upon receipt from the vendor, HGF-1 cells were thawed, washed and suspended in 25ml of DMEM growth media (DMEM supplemented with 4mM L-glutamine, 1mM sodium pyruvate, penicillin 100U/ml, streptomycin 100μg/ml, amphotericin B 250ng/ml and 10% fetal calf serum). Cells were placed in a 75cm^2 culture flask and grown in a humidified, water-jacketed incubator with 95% air, 5% CO_2 mixture. DMEM growth media was replaced every 2-3 days until cells reached confluence. At confluence, cells were detached from the culture flask with 0.25% trypsin, collected in sterile 50ml polypropylene tubes and centrifuged at 200 x g for 10 minutes to pellet the cells. The cells were resuspended in DMEM growth media and were split 1:4 into 75cm^2 flasks and returned to the incubator for further propagation. HGF-1 cells were passed another time and grown to confluence. At confluence, cells were trypsinized, collected and suspended in DMEM growth media containing 10% DMSO. Cells at a concentration of 2-4 x 10^5 cells/ml were placed in 1.5ml aliquots in cryovials and stored under liquid nitrogen. Experiments were completed using fibroblasts from the initial stock batch described above. All experiments with fibroblasts were conducted using cells between passages 5-10.

U937 Differentiation and Preparation for TUS Exposure. U937 cells exhibit a monocytic phenotype, but can be induced to differentiate into macrophages through the

addition of phorbol 12-myristate 13-acetate (PMA) [175]. Differentiation of U937 monocytes into macrophages parallels the transformation of circulating monocytes into macrophages upon tissue injury or infection [176]. The newly differentiated macrophages are equipped to fully participate in inflammatory and immune functions. To induce differentiation into macrophages, the following processes were completed. U937 cells were collected in 50 ml tubes, pelleted by centrifugation for 5 minutes at 200 x g, and resuspended in RPMI growth media. Cell concentration was determined and adjusted to a final concentration of 0.5×10^6 cells/ml in 120ml total volume of fresh RPMI growth media. Following this dilution, cell concentration was again verified to insure appropriate final concentration. PMA was added to the cell suspension to a final concentration of 50 ng/ml. U937 cells were plated on 60 x 15 mm polystyrene culture plates in 5ml aliquots and incubated for 24 hrs to allow cellular differentiation and adherence to the plates. Following differentiation, RMPI growth media containing PMA was removed and discarded, and cells were rinsed with serum-free RPMI growth media. Fresh, serum-free RPMI growth media (5ml) was added to each plate, and macrophages were returned to the incubator for an additional 24 hours. After the second incubation period, macrophages were rinsed with 5ml serum-free RPMI growth media, covered with 10ml of serum-free RPMI growth media, placed in the sonication apparatus and exposed to TUS as described below.

TUS Treatment of U937 Macrophages. For all experimental TUS exposures, culture plates (samples) containing cells were treated using a system similar to that described by Reher et al [177](Fig 2.1). A thermostatically controlled, circulation water bath maintained at 37.0° C (Thermo NESLAB Model EX17) was used to maintain temperature

of samples during ultrasound exposure. To allow samples undergoing sonication to maintain contact with the heated water, a custom-designed suspension platform, made of Lexan plastic, was fabricated. Culture plates were set in a centrally placed opening (60mm diameter) and secured to plastic support braces with thumbscrews such that the bottom surface of the dish was submerged in the water bath. A laboratory stand and adjustable clamp were used to hold the ultrasound transducer in place above the sample during sonication. The water bath, platform and transducer stand were placed within the sterile hood for experimentation. Prior to treatment of each sample, the emitting crystal of the transducer was cleaned with de-ionized water and sterilized using 70% ethanol. Once the sample was secured in the platform, the transducer was lowered directly into the media to a set height of 5 mm from the surface of the dish. The sample was then exposed to TUS at the chosen parameters for 5 or 10 minutes using a stationary delivery technique. For sham controls, samples were secured in the platform and the transducer was placed in the sample for 5 or 10 minutes, but the ultrasound generator was not turned on. Immediately following treatment, the media was concentrated by removal of 5ml of media, and the cells were returned to the incubator for 10 minutes or 1 hour. Following post-TUS incubation, conditioned media were collected under sterile conditions, centrifuged for 5 minutes at 200 x g to remove any cellular debris, and dispensed into aliquots in sterile 1.7ml microtubes and stored at -70°C.

TUS was applied at 1 or 3 MHz frequency, with a duty cycle of 20%, resulting in SATA intensity levels of: 0 (sham TUS), 40, or 400 mW/cm^2 SATA. Each intensity/frequency combination was applied for 5 and 10 minutes (Table 2.1). Each

experimental block (set of TUS treatments) included each TUS parameter group for a total of 10 parameter sets per experimental block. The order of application of each TUS parameter set was randomized for each experimental block to reduce the possibility of experimenter bias. Samples for each experimental block were labeled 1-10 following sonication, and recorded in a database along with the corresponding parameter set. All subsequent assays of conditioned media were completed using the 1-10 code from each experimental block. Samples were matched to their particular TUS parameters only after all data collection was completed. Each experimental block was conducted on a single day using cells from the same stock batch to reduce intra-assay variability. A total of n = 5 experimental blocks were completed.

Fibroblast Incubation with Macrophage Conditioned Media. HGF-1 aliquots were thawed, washed in plain DMEM and resuspended in DMEM growth media and propagated under humidified incubation conditions as described above. Once cells neared confluence, they were prepared for exposure to macrophage conditioned media as follows. DMEM growth media was removed and the monolayer of cells was rinsed briefly with 5ml of 0.25% trypsin. The rinse was discarded and 8ml of fresh trypsin was added to each flask. Flasks were returned to the incubator for 3-5 minutes to allow full detachment of cells. The cell suspension was transferred into a sterile 50ml polypropylene tube and cells were pelleted by centrifugation for ten minutes at 200 x g. The pelleted cells were resuspended in fresh DMEM growth media and quantified. Concentration was adjusted to 20,000 cells/ml creating a "batch" of fibroblasts and 100μl of the suspension was added to wells of a 96-well culture plate (Corning, Inc., Corning, NY) for a final concentration of 2,000

cells/well. This concentration was used to insure the monolayer of fibroblasts would be preconfluent and able to expand. From each batch of fibroblasts, two separate 96-well plates were seeded to allow for 24 and 48-hour incubations.

Cells were placed in the humidified incubator for 4 hours to allow adherence to the culture plate. Following cell attachment, the growth media was removed and 100μl of fresh, serum-free DMEM was added to each well and the plate returned to the incubator for 24 hours. The serum-free incubation period served to bring the fibroblasts to a quiescent state of activity prior to experimentation. At the end of the incubation period in serum-free DMEM, media was removed from each well and replaced with 100μl of macrophage conditioned media. Each macrophage conditioned media sample was loaded in duplicate wells on each of the two plates for a total of 4 wells per conditioned media sample.

In addition to experimental macrophage conditioned media, negative and positive control samples were included in the proliferation assay. Negative controls consisted of fibroblasts incubated in non-conditioned (fresh), serum-free RPMI growth media. To insure that the experimental fibroblasts were capable of proliferating, of fibroblasts were incubated in serum-free RPMI growth media supplemented with rhPDGF-bb, a known mitogenic agent for fibroblasts [178,179,180]. Control media were incubated with fibroblasts in the same plates and for the same time periods as the experimental samples.

To reduce intra-assay variability, all conditioned media samples from a single TUS experimental block were added to plates that contained fibroblasts plated from a single batch. Plates with fibroblasts in conditioned media were returned to the incubator for 24 or 48 hours. At the end of each incubation period, fibroblast proliferation was assessed to

determine the effect of varied levels of TUS on macrophage-release of mitogenic factors for fibroblasts.

Fibroblast Proliferation Assay. Fibroblast proliferation following incubation in macrophage conditioned media was analyzed using a Cell Proliferation Assay Kit (Chemicon Intl., Temecula, CA). The assay is based on assessment of mitochondrial dehydrogenase cleavage of tetrazolium salt (WST-1) to formazan dye, a process that increases as cell number increases, due to increased mitochondrial enzymes. At the end of the conditioned media incubation (24 or 48 hours), fibroblasts were removed from the incubator and 10μl of WST-1 reagent was added to each well of the culture plate. The plates were mixed for one-minute using a microplate shaker, and then returned to the incubator for four hours to allow development of the formazan dye. Finally, optical density (OD) of the samples was measured with a microplate reader (SpectraMax Plus, Molecular Devices, Sunnyvale CA) set at 450nm, with 650nm serving as the reference wavelength. For each incubation time point, OD values were obtained from duplicate wells for each conditioned media sample and averaged together prior to data analysis.

Validation of WST-1 Assay for Cell Proliferation. The WST-1 assay measures cellular mitochondrial enzymatic activity. A greater number of cells (e.g. due to proliferation) correlates with an increase in the number of available mitochondrial enzymes [181]. Despite this, it is possible that mitochondrial enzyme activity could change without a change in cell number. To insure that increased OD measurements were consistent with increased cell number, a validation assay was performed.

HGF-1 cells propagated in DMEM growth media as described above were seeded onto 96-well microplates in 100µl volumes for end concentrations of: 0, 1, 2, 4, and 8×10^3cells/well. Each cell concentration was seeded in replicates of five, one set of five for analysis using the WST-1 assay and one set of five for direct cell counting. Cells were incubated 4 hours to allow adhesion, and then media was removed and replaced with 100µl of serum-free DMEM growth media. Cells were incubated 24 hours, after which the serum-free DMEM growth media was removed and replaced with 100µl of RPMI growth media, identical to macrophage RPMI growth media utilized in the TUS exposure experimentation. The cells were returned to the incubator for 24 or 48 hours. At the end of the respective incubation periods, one set of serial dilutions was analyzed by completing the WST-1 assay as described previously, and the other set was analyzed by direct cell counting. For direct counting, cells were released from the microplate using 0.25% trypsin and counted using a standard light microscope and laboratory hemacytometer. OD values that were obtained for 0×10^3 cells/ml were used as background measures of the WST-1 assay and were subtracted from all other values for plated cells at 1, 2, 4, and 8×10^3 cells/well.

Data Analysis/Statistics

For the five TUS experimental blocks, data is reported as the mean± SEM. Overall differences in conditioned-media induced fibroblast proliferation were analyzed by one-way ANOVA (Sigma Stat version 2.03; Systat Software, Inc., Point Richmond, CA). All post hoc analysis of significant differences was performed using Tukey's HSD test using

Sigma Stat version 3.01. All statistical analyses used an a priori p-value < 0.05 to determine significant differences. WST-1 assay validation was completed using a linear regression analysis on the variables of OD and cell counts, and is reported as the coefficient of determination (R^2).

Figure 2.1

A

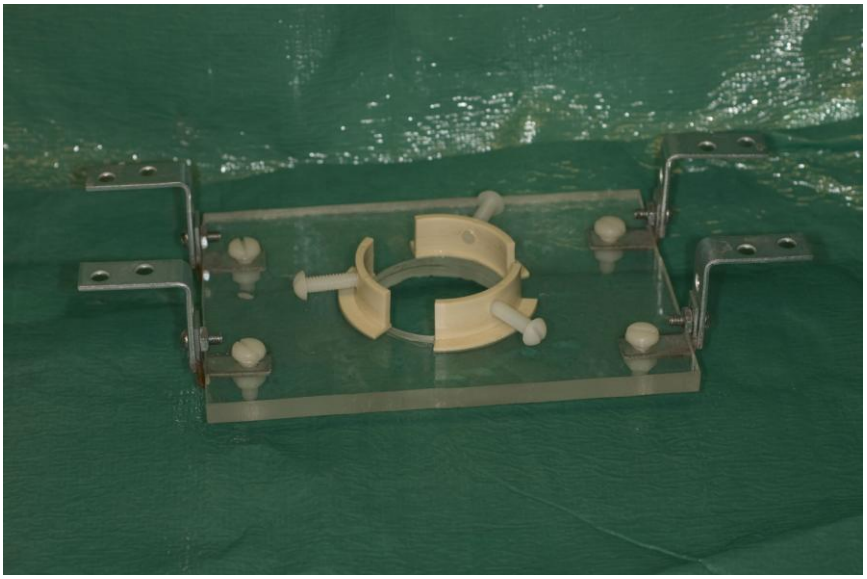

B

Figure 2.1. *Sonication Apparatus***.** *A)* Custom-designed suspension platform for securing culture plates in the water bath and *B)* Sonication apparatus including suspension platform, water bath, laboratory stand and adjustable clamp holding the ultrasound transducer. This apparatus was used for all TUS exposures.

Table 2.1

5 minutes		
	1 MHz	**3 MHz**
0 mW/cm^2 (sham)	40 mW/cm^2	40 mW/cm^2
	400 mW/cm^2	400 mW/cm^2
10 minutes		
	1 MHz	**3 MHz**
0 mW/cm^2 (sham)	40 mW/cm^2	40 mW/cm^2
	400 mW/cm^2	400 mW/cm^2

Table 2.1. *TUS Exposure Parameters*. Listing of the exposure parameter combinations utilized for sonication of macrophages with subsequent 10-minute or 1-hour incubation post-TUS. All intensity values are reported as SATA at 20% duty cycle. Sham treatments were completed for 5 minute and 10 minute exposures.

Results

HGF-1 Fibroblast Proliferation. Differences in fibroblast proliferation following 24-hour or 48-hour incubation in macrophage-conditioned media were assessed using the WST-1 assay and analyzed by one-way ANOVA. Fibroblasts were incubated for each time period in media conditioned by macrophages that were treated with TUS and incubated post-TUS for either 10-minutes or 1-hour. Negative control samples for proliferation consisted of fibroblasts incubated in unconditioned RPMI macrophage growth media and positive control samples for proliferation consisted of fibroblasts incubated in unconditioned RPMI macrophage growth media that was supplemented with 100ng/ml rhPDGF-bb.

After 24-hour incubation in conditioned media, there were no significant differences in fibroblast proliferation among any of the treatment groups for 10-minute conditioned media ($p = 0.783$, $F = 0.608$) or 1-hour conditioned media ($p = 0.747$, $F = 0.641$) compared to sham, negative control unconditioned media or positive control, rhPDGF-bb-supplemented media (Fig. 2.2).

After 48-hour incubation in conditioned media, negative control media or media supplemented with rhPDGF-bb ANOVAs revealed significant differences in fibroblast proliferation for the 10-minute conditioned media plus controls comparison ($p < 0.001$, $F = 7.320$) and for the 1-hour conditioned media plus controls comparison ($p < 0.001$, $F = 17.52$). Post hoc analysis revealed that positive control media supplemented with rhPDGF-bb stimulated significantly increased fibroblast proliferation compared to all other groups ($p < 0.001$), while there were no significant differences in fibroblast proliferation

among any treatment groups (including sham) for 10-minute and 1-hour conditioned media. There were also no differences between any treatment groups and the negative control group. (Fig. 2.3).

WST-1 Proliferation Assay Validation. To validate the ability of the WST-1 assay to measure increasing cell number, WST-1 assay and direct cell counting on known concentrations of HGF-1 fibroblasts was performed. To simulate the media conditions of the experimental fibroblast assay, serum-free, unconditioned, RPMI macrophage growth media was used for fibroblast incubation for 24-hour and 48-hour incubation periods. Fibroblasts were seeded at 0, 1, 2, 4 and 8 x 10^3 cells/well and allowed to incubate for the corresponding time period. For both time points, linear regression analysis revealed a direct correlation between increasing cell number and increasing OD measured via WST-1 assay, (24-hour; $r^2 = 0.907$ and 48-hour; $r^2 = 0.939$) (Fig. 2.4).

FIGURE 2.2

A

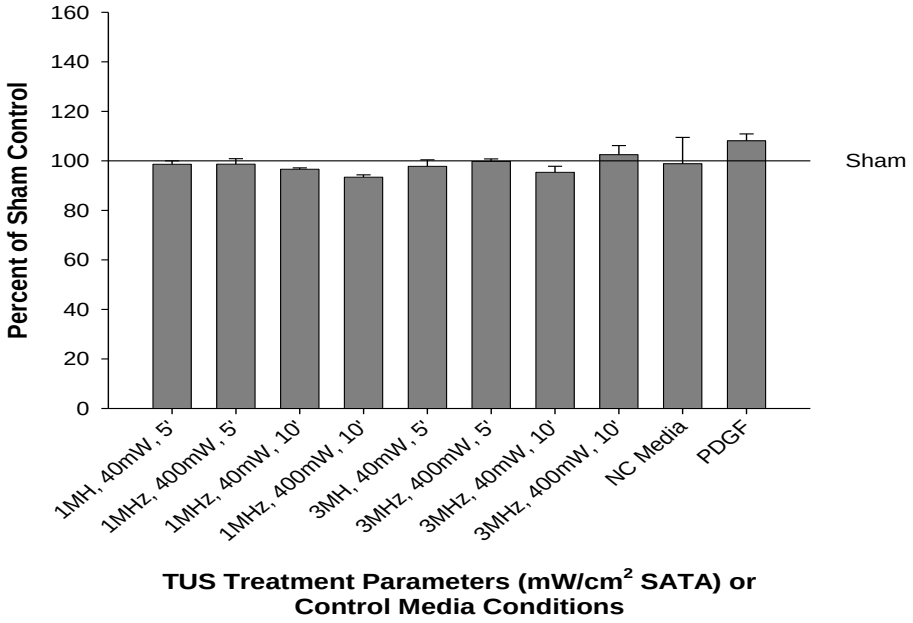
160
140
120
100
80
60
40
20
0
Percent of Sham Control
Sham
1MH, 40mW, 5'
1MHz, 400mW, 5'
1MHz, 40mW, 10'
1MHz, 400mW, 10'
3MH, 40mW, 5'
3MHz, 400mW, 5'
3MHz, 40mW, 10'
3MHz, 400mW, 10'
NC Media
PDGF
TUS Treatment Parameters (mW/cm² SATA) or
Control Media Conditions

B

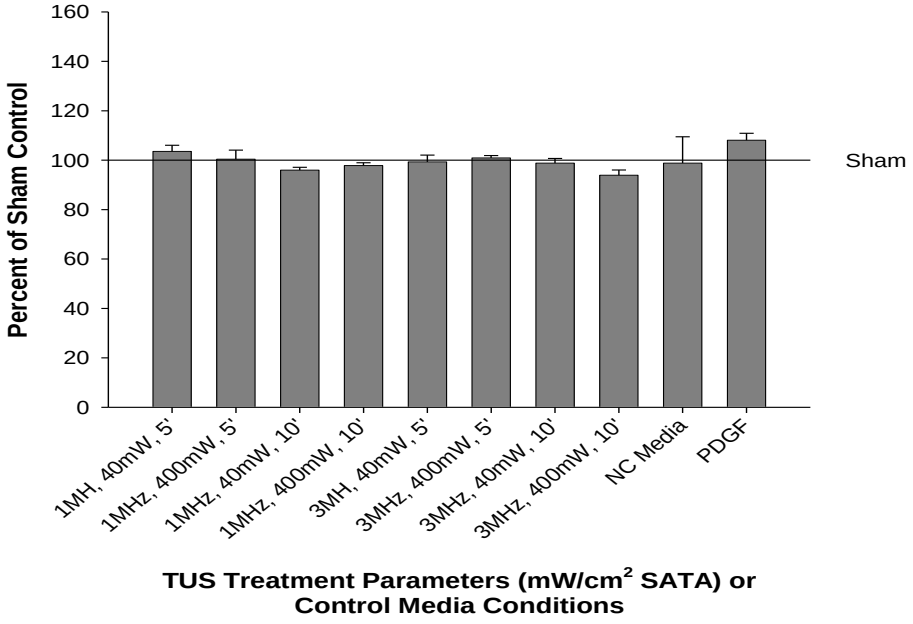
160
140
120
100
80
60
40
20
0
Percent of Sham Control
Sham
1MH, 40mW, 5'
1MHz, 400mW, 5'
1MHz, 40mW, 10'
1MHz, 400mW, 10'
3MH, 40mW, 5'
3MHz, 400mW, 5'
3MHz, 40mW, 10'
3MHz, 400mW, 10'
NC Media
PDGF
TUS Treatment Parameters (mW/cm² SATA) or
Control Media Conditions

Figure 2.2. *HGF-1 Fibroblast Proliferation in Macrophage Conditioned Media – 24 hour incubation.* Fibroblast proliferation was assessed using the WST-1 assay following 24-hour incubation in macrophage-conditioned media. (A) Fibroblast proliferation in c*onditioned media from macrophages incubated for 10 minutes post-TUS, and in negative and positive control media*. Based on one-way ANOVA, there were no significant differences in fibroblast proliferation among any treatment groups including sham, negative control unconditioned media and positive control media supplemented with 100ng/ml rhPDGF-bb ($p = 0.783$, $F = 0.608$). *(B) Fibroblast proliferation in conditioned media from macrophages incubated for 1 hour post-TUS, and in negative and positive control media* . One-way ANOVA revealed no significant differences in fibroblast proliferation among any treatment groups including sham, negative control and positive control media ($p = 0.747$, $F = 0.651$). All data reported as the mean ± SEM of fibroblast proliferation as percent of sham treatment, $n = 5$.

Figure 2.3

A

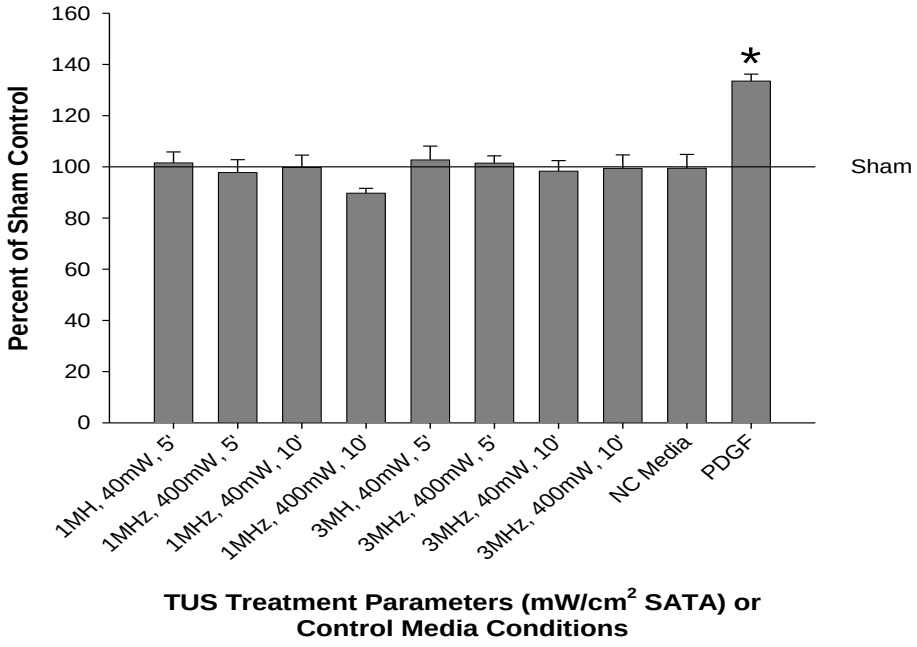
160
140
120
100
80
60
40
20
0
Percent of Sham Control
*
Sham
1MH, 40mW, 5'
1MHz, 400mW, 5'
1MHz, 40mW, 10'
1MHz, 400mW, 10'
3MH, 40mW, 5'
3MHz, 400mW, 5'
3MHz, 40mW, 10'
3MHz, 400mW, 10'
NC Media
PDGF
TUS Treatment Parameters (mW/cm² SATA) or
Control Media Conditions

B

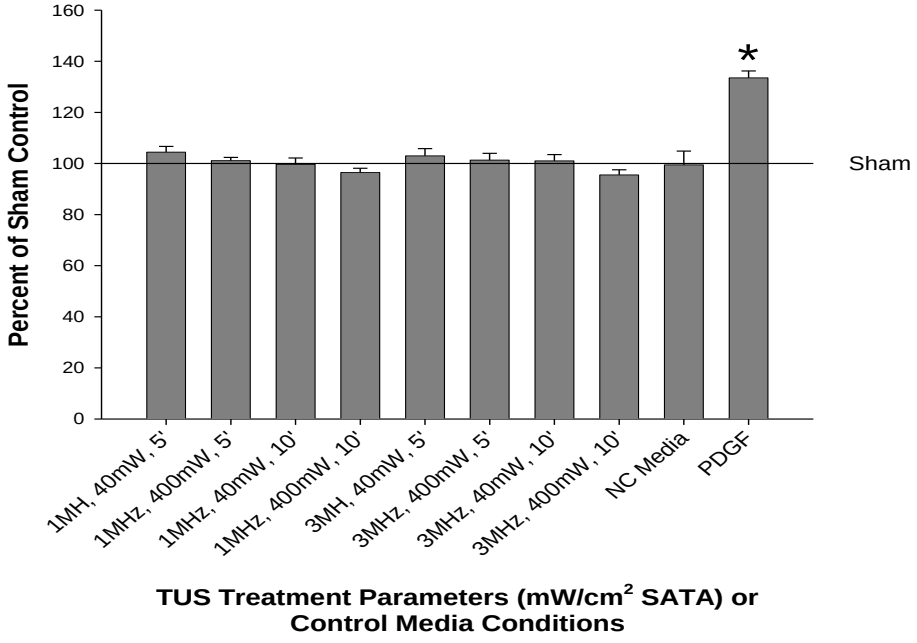
160
140
120
100
80
60
40
20
0
Percent of Sham Control
*
Sham
1MH, 40mW, 5'
1MHz, 400mW, 5'
1MHz, 40mW, 10'
1MHz, 400mW, 10'
3MH, 40mW, 5'
3MHz, 400mW, 5'
3MHz, 40mW, 10'
3MHz, 400mW, 10'
NC Media
PDGF
TUS Treatment Parameters (mW/cm² SATA) or
Control Media Conditions

Figure 2.3. *HGF-1 Fibroblast Proliferation in Macrophage Conditioned Media – 48 Hour Incubation.* Fibroblast proliferation was assessed using the WST-1 assay following 48-hour incubation in macrophage-conditioned media. (A) Fibroblast proliferation in c*onditioned media from macrophages incubated for 10 minutes post-TUS and in negative and positive control media*.. Based on one-way ANOVA there were significant differences in fibroblast proliferation ($p < 0.001$, $F = 7.320$) among the conditions. Post hoc analysis revealed positive control media supplemented with 100ng/ml rhPDGF-bb significantly increased fibroblast proliferation when compared to all groups including sham and negative control samples ($p < 0.001$). (*B) Fibroblast proliferation in conditioned media from macrophages incubated for 1 hour post-TUS and in negative and positive control media*. Significant differences in fibroblast proliferation were found based on one-way ANOVA ($p < 0.001$, $F = 17.52$). Post hoc analysis revealed rhPDGF-bb supplemented media increased proliferation compared to all treatment groups including sham and negative control samples ($p < 0.001$) indicated by *. All data reported as the mean ± SEM of fibroblast proliferation as percent of sham treatment, $n = 5$.

Figure 2.4

A

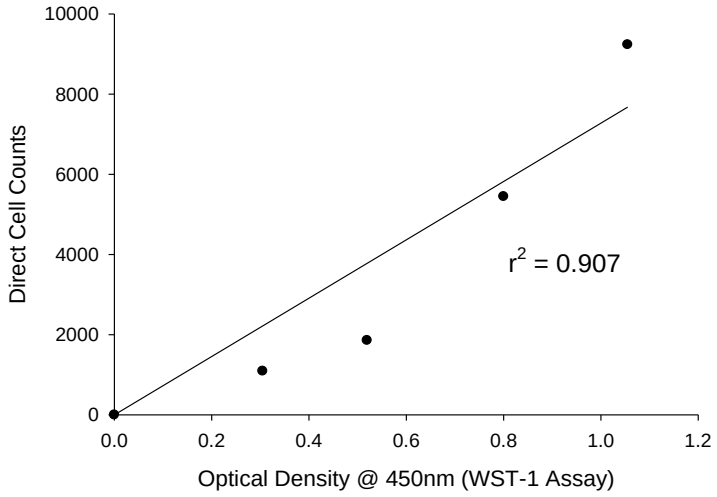
10000
8000
6000
4000
2000
0
Direct Cell Counts
r2 = 0.907
0.0
0.2
0.4
0.6
0.8
1.0
1.2
Optical Density @ 450nm (WST-1 Assay)

B

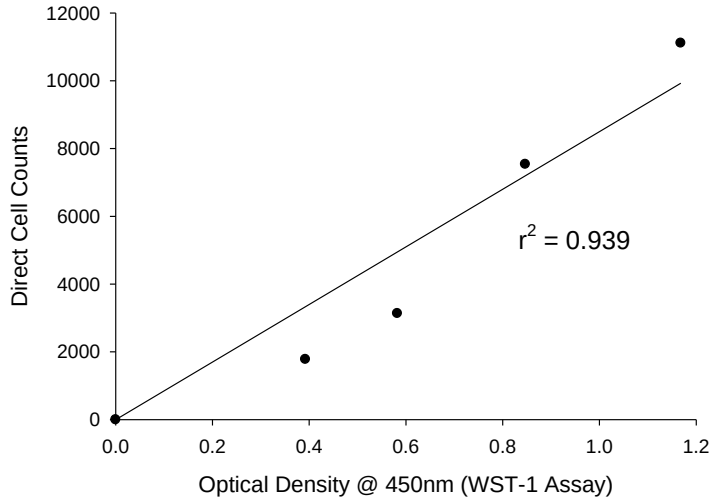
12000
10000
8000
6000
4000
2000
0
Direct Cell Counts
r2 = 0.939
0.0
0.2
0.4
0.6
0.8
1.0
1.2
Optical Density @ 450nm (WST-1 Assay)

Figure 2.4. *WST-1 Proliferation Assay Validation. (A)* Comparison of direct cell counting and WST-1 assay for fibroblasts following 24-hour and, *(B)* 48-hour incubation in unconditioned, macrophage growth media. Cells were seeded at 0, 1, 2, 4 and 8 x 10^3/well and allowed to incubate for the 24 or 48 hours. Optical density values that were obtained for 0 x 10^3 cells/ml were used as background measures of the WST-1 assay and were subtracted from all other values for plated cells at 1, 2, 4, and 8 x 10^3 cells/well. For both time points, linear regression analysis revealed a direct correlation between increasing cell number and increasing optical density measured via WST-1 assay, (24-hour: $R^2 = 0.907$) and (48-hour: $R^2 = 0.939$).

Discussion

Since the WST-1 assay measures mitochondrial enzyme activity, it was imperative to establish validity of the assay for measurement of increased cell number. Similar validation of this colorimetric assay for assessing cellular proliferation has been reported [181]. In the current investigation, identical serial dilutions of fibroblasts were assessed by direct counting and with the WST-1 assay. The regression analysis of these variables showed good correlation ($R^2 = 0.907 – 0.939$) between cell number and optical density, thus verifying the ability of the WST-1 assay to assess cell number using our experimental protocol.

In this study, none of the TUS parameter sets (Table 2.1) utilized for macrophage sonication stimulated the release of fibroblast mitogens into the media that would subsequently induce fibroblast proliferation. Conditioned media from macrophages incubated post-TUS for 10-minutes or 1-hour had no effect on fibroblast proliferation when comparing TUS treatment parameter sets to each other and to sham and negative control samples, regardless of whether fibroblasts were exposed to the conditioned media for 24 or 48 hours. The lack of proliferation of fibroblasts exposed to the conditioned media was not due to the fibroblasts already being at their proliferative maximum, as the ability of the cells to proliferate in response to mitogenic stimuli was demonstrated by the fibroblast response to rhPDGF-bb supplementation of unconditioned RPMI macrophage growth media.

Based on the WST-1 assay, the absence of increased fibroblast proliferation among the conditioned media samples compared to sham, suggests macrophages may not respond

to the selected TUS parameters by release of fibroblast mitogens. The lack of mitogen release is contrary to findings reported by Young and Dyson [161]. They reported increased fibroblast proliferation following incubation in conditioned media from sonicated, undifferentiated U937 macrophages (0.75 or 3 MHz, 500mW/cm^2 SATA, CW, 5-minutes). They also reported different effects on mitogen release from macrophages, as assessed by fibroblast proliferation, based on the TUS wavelength frequency (0.75 and 3 MHz) applied; specifically 0.75 MHz induced release of a fibroblast mitogen within 30 minutes of sonication, while 3 MHz induced release when the media was sampled at 12 hours post-TUS, but not when sampled at 30-minutes post-TUS. The current investigation analyzed media that was conditioned for a maximum of 1-hour post-TUS. Given the comparatively abbreviated incubation period of the current investigation, it was not possible to verify or refute the differential response of macrophage release of fibroblast mitogen at 12 hours post-treatment for 3 MHz TUS.

Methodological differences could be responsible for the variant findings of the current investigation compared to Young and Dyson. U937 cells in the current investigation were induced to differentiate toward terminal macrophages, compared to undifferentiated U937 monocytes. Upon leaving the vasculature, monocytes differentiate into tissue macrophages that will function in the healing process, which results in changes in cellular and secretory activity [164,168]. Effects of sonication on function of some cells, specifically chondroblasts and spleenocytes, have been shown to be dependent on the state of cellular differentiation [83,109,162]. The difference in findings noted here, compared to those of Young and Dyson, may be further evidence of TUS effects being specific to the

state and/or activity of the treated cell. However, this differential cellular response to TUS based on the state of cellular differentiation has not been reported in macrophages. Such a comparison of cellular response to TUS between undifferentiated and differentiated U937 cells would provide insight about this type of response among monocytes and macrophages.

TUS application in the current investigation was conducted using a 20% duty cycle, compared to a CW application used by Young and Dyson. Varied TUS duty cycles have been shown to stimulate different proliferative and secretory responses in sonicated cells including osteoblasts, fibroblasts, and chondrocytes [7,83]. While this effect is a plausible explanation of the differences in findings noted above, the aim of this investigation was not to identify the effect of altered TUS duty cycle and its affect on cellular response. As such, a more detailed, directed experimental protocol designed to address this question would provide better analysis of this question.

Lastly, the current investigation analyzed media that was conditioned for a maximum of 1-hour post-TUS. Given this comparatively abbreviated incubation period, it was not possible to verify or refute the differential response of macrophage release of fibroblast mitogen at 12 hours post-treatment for 3 MHz TUS, as described by Young and Dyson.

Conclusion

Overall, TUS at varied, clinically applicable levels had no effect on macrophage release of fibroblasts mitogens 10 min or 1 hr post TUS. It appears that TUS does not

affect an immediate release of fibroblast mitogens at the TUS parameters used in this model. Differences in the state of cellular differentiation and the TUS duty cycle could explain the lack of effect noted in this study in comparison to the findings of Young and Dyson. The importance of these two variables in relation to macrophage response to TUS deserves additional investigation.

Macrophage release of fibroblast mitogens is only one mechanism by which macrophages could alter tissue healing in response to TUS. Macrophages produce and release other paracrine factors that are capable of improving tissue healing. For example IL-1β, TGF-β and VEGF are released by macrophages and have beneficial effects on tissue healing [182,183,184,185]. These factors induce important aspects of the inflammatory and early proliferative phase such as matrix removal [186,187], matrix deposition [188,189,190,191], and angiogenesis [100,192,193]. The macrophage response to TUS may involve these aspects of tissue healing rather than induction of fibroblast proliferation. Indeed, fibroblasts themselves respond to TUS by increased proliferation [8], and the TUS action on fibroblast proliferation may be through direct action on fibroblasts rather than an indirect mitogenic response mediated via macrophages. Given these other possible mechanisms of healing enhancement by TUS and the lack of fibroblast proliferation in our experimental model, we decided to explore the release of IL-1β, TGF-β and VEGF from TUS-treated macrophages.

Chapter 3

Cytokine and Growth Factor Release From Activated Macrophages Exposed to Various Levels of Therapeutic Ultrasound

Abstract

During tissue healing, macrophages release various paracrine mediators, including cytokines and growth factors. These cytokines and growth factors control various cellular mechanisms of healing. Therapeutic ultrasound (TUS) is a treatment modality that is used to enhance healing of injured tissues. In vitro analyses indicate that various levels of TUS can alter the activity of many different cell types. In vivo investigations suggest that TUS affects the early phases of tissue repair, at a time point which macrophages are likely to be active. As such, we explored the effect of TUS on macrophage release of IL-1β, VEGF and TGFβ1, paracrine factors involved in inflammation, angiogenesis and extracellular matrix production. Activated U937 human macrophages were treated with 5 or 10-minute TUS exposures using 1 and 3MHz frequencies at a 20% duty cycle at the intensities of 40, and 400mW/cm^2 SATA. Conditioned media from treated macrophages was collected at 10 minutes or 1 hour post-treatment and analyzed for the presence of IL-1β, VEGF and TGFβ1 using enzyme-linked immunosorbent assay (ELISA). At 10 minutes post-treatment, TUS exposure for 10-minutes at 1MHz, 400mW/cm^2 SATA, 20% duty cycle

increased the release of IL-1 β and VEGF. However, no levels of TUS exposure affected the release of TGF-β1from treated macrophages. IL-1β and VEGF are important regulators of inflammation and angiogenesis, respectively, and the current findings suggest that TUS may enhance the early phases of tissue healing by stimulating macrophage release of these paracrine mediators.

Introduction

Healing of injured tissues involves a complex array of interactions between cells and cellular processes. When damaged, tissues respond with an orderly sequence of events that leads to repair of the defect. The healing process is typically divided into four overlapping phases; hemostasis, inflammation, repair and remodeling (maturation). Inflammation begins within a few hours after injury and is largely completed by 72 hours [157]. This phase of healing involves a dynamic and complex series of vascular, cellular and biochemical reactions that prepare the wound environment for the reparative phase in which the extracellular matrix and tissue integrity are restored [163,194].

The presence of macrophages in the inflammatory milieu is critical for tissue repair. Absence or malfunction of macrophages during wound healing results in inadequate succession of the reparative and remodeling phases of healing with an outcome of poor tissue repair [195]. In vivo healing models in which macrophage function was prohibited, have demonstrated delayed and incomplete wound healing [165,166,196].

Macrophages develop from blood-borne precursors, monocytes [164,168]. Following tissue injury, products from activated platelets, prostaglandins from neutrophils, leukocyte-derived cytokines, protein products from degraded matrix, and chemical factors from invading microorganisms are capable of inducing monocytes to leave the circulation and differentiate into macrophages [164]. These macrophages are responsible for the coordination of the inflammatory and subsequent reparative phases of healing.

Macrophages coordinate many actions of the inflammatory and reparative phases of healing through the production of a variety of secretory factors, many of which are cytokines and growth factors [132,194]. These paracrine agents stimulate many tissue healing processes such as phagocytosis, cell recruitment and proliferation, matrix molecule degradation and production, and angiogenesis [89,100,166,172,197,198]. Cytokines and growth factors, produced by macrophages, that are believed to enhance healing include insulin-like growth factor-1 (IGF-1), interleukin-1β (IL-1β), transforming growth factor-β1 (TGF-β1), vascular endothelial growth factor (VEGF), basic fibroblast growth factor (bFGF), platelet derived growth factor (PDGF), and epidermal growth factor (EGF) [182,199,200].

TGF-β1 has been shown to increase tendon fibroblast collagen production and result in increased mechanical stiffness of healing ligaments [170]. Experimentally decreased macrophage production of VEGF and bFGF during wound repair resulted in delayed wound healing [195]. PDGF, EGF and bFGF have a mitogenic effect on tendon and ligament fibroblasts in vitro, and exogenous PDGF (20μg) increased the biomechanical strength of rabbit ligaments, when it was added to the ligament after experimental ligament transection [201,202].

Therapeutic ultrasound has been shown to affect the function of cells and tissues during healing. Based on investigations of enhancement of soft tissue healing, TUS appears to exert its primary effect on the inflammatory and repair phases of healing [4,13-16,26,127,135,136,153]. The specific processes of the inflammatory and repair phases that are affected by TUS continue to be identified. Given that macrophage function is crucial for coordinating the inflammatory and early reparative phases of healing, macrophage

response to TUS should be further explored in an effort to better understand the mechanism of TUS effects on healing tissue.

Evidence directly concerning monocyte/macrophage secretory response to TUS is limited to three published investigations [7,161,203]. Young and Dyson treated human monocytes (undifferentiated U937 cells) with TUS (0.75 MHz or 3.0 MHz, 500 mW/cm^2 SATA, CW, 5 minutes) and reported the presence of an unidentified fibroblast mitogenic factor in the culture media at 30 minutes and at 12 hours after TUS exposure [161]. The authors believed that TUS wavelength frequency affected sonicated monocytes differentially based on the findings that 0.75 MHz caused release of the mitogenic factor within 30 minutes of TUS application, while 3.0 MHz induced mitogen release by 12 hours post-TUS only.

Doan et al sonicated primary human monocytes at various intensities (20, 80, 140, and 200 mW/cm^2 SATA, 20% duty cycle, 5 minutes) using a 1.0 MHz frequency, and measured release of cytokines and growth factors thought to be involved in controlling angiogenesis during wound healing (IL-1β, bFGF, VEGF, IL-6, IL-8, and TNF-α) [7]. TUS at 1 MHz had no effect on monocytes release of IL-1β, bFGF, IL-6, IL-8, and TNF-α at 18 hours post-TUS compared to sham-treated monocytes. However, monocytes treated at the intensities 20, 80 and 200 mW/cm^2 released more VEGF compared to sham, when assessed 18-hours post-TUS. The authors also reported monocytes released IL-1β and VEGF in response to ultrasound applied at 45 kHz. While this ultrasound wavelength is much lower than traditional therapeutic ultrasound and continues to be validated for

clinical use, this finding provides further evidence that variable ultrasound frequencies stimulate cytokine/growth factor release.

Iwabuchi et al reported increased release of TNF-α from activated rat peritoneal macrophages within 2 hours of a single TUS exposure at SAFHS, using a macrophage-IVD co-culture model [203]. The difference in TNF-α release post-TUS, compared to Doan et al (1999), is likely due to the difference in experimental protocols, for example single cell type vs. co-culture; primary human macrophages vs. activated rat macrophages; and different TUS treatment parameters.

The within study comparisons of the effect of varied TUS intensity or wavelength frequency on macrophage function demonstrate differential effects on cellular secretion of cytokines and growth factors [7,161]. Furthermore, these three studies indicate that monocytes and macrophages respond to both low-intensity TUS (< 100mW/cm^2 SATA) and higher-intensity TUS (500 mW/cm^2 SATA) by releasing cytokines and growth factors. However, comparison of ultrasound delivered at varied therapeutic levels of intensity, wavelength and duration has not been conducted within one study.

The family of cytokines and growth factors encompasses many different peptides. In order to investigate how TUS might effect the inflammatory and proliferative phases of healing via altered macrophage function, we chose to analyze the release of IL-1β, VEGF, and TGF-β1 from macrophages exposed to TUS. IL-1β is considered to be a pro-inflammatory mediator that stimulates many cellular actions that occur during inflammation [204]. Angiogenesis and ECM repair are major actions occurring during the proliferative phase of healing and the growth factors VEGF and TGF-β1, respectively, are

known mediators of these functions [101,190,192,205,206]. Therefore, the purpose of this investigation is to examine the effects of TUS, applied at varied levels of intensity, wavelength frequency, and treatment duration, on release of IL-1β, VEGF, and TGF-β1 from activated, human macrophages in an effort to identify the TUS parameters that are most stimulatory.

Materials and Methods

Materials and Reagents. Phorbol 12-myristate 13-acetate (PMA), dimethyl sulfoxide (DMSO), and sodium dodecyl sulfate (SDS) were obtained from Sigma Chemical Co., St. Louis, MO. Tris and DC Protein Assay Kit were from BioRad Laboratories, Hercules CA. Glycerol, HEPES, sodium hydroxide, hydrochloric acid, heat-inactivated fetal calf serum (HIFCS) and sterile pipets were from Fisher Scientific, Pittsburgh, PA. Bovine serum albumin (BSA) protein standard was obtained from Pierce Biotechnology Inc., Rockford, IL. Protease inhibitor cocktail was from Roche Applied Science, Mannheim, Germany (Cat # 11 697 498 001). Human monocytic cells (U937) were purchased from American Type Culture Collection, Manassas, VA. Sterile tissue culture plates and centrifuge tubes were from Corning Inc., Corning NY. ELISA antigen detection kits for IL-1β, VEGF, and TGF-β1 were acquired from R & D Systems, Minneapolis MN. All other reagents were obtained from Invitrogen Corp., Carlsbad, CA.

U937 Cell Culture. All U937 cell manipulations were conducted using sterile technique within a standard biological safety cabinet (Forma Scientific, Waltham, MA) and are described in Chapter 2.

U937 Macrophage Differentiation and Preparation for TUS Exposure. Differentiation of U937 cells into macrophages was completed according to the protocol previously described in Chapter 2 of this document.

TUS Treatment of U937 Macrophages. For all experimental TUS exposures, culture plates (samples) containing cells were treated using a system similar to that described by Reher et al, and described in detail in Chapter 2 of this document [177]. Each experimental block was conducted on a single day using cells from the same stock batch to reduce intra-assay variability. A total of n = 3 experimental blocks were completed.

Cell Lysates post-TUS. Following sonication and incubation, macrophage conditioned media was collected, centrifuged, dispensed into four aliquots in sterile 1.7 ml microtubes and stored at -70°C. Cell lysis and total protein extraction was completed for each sample of sonicated macrophages, in order to determine the total cellular protein from each sample. Total cellular protein was used to normalize the data for cytokine release into the media. Immediately after conditioned media collection, macrophages were rinsed three times with 5 ml of sterile phosphate buffered saline (PBS), and covered with 500 ul of sterile-filtered, chilled (4°C) Laemmli buffer, pH 6.8 (60 mM Tris-Cl, 5% SDS, 10% glycerol, and protease inhibitor cocktail including inhibitors of serine, cysteine, metallo and aspartic proteases). Cells were incubated with lysis buffer for 5 minutes on ice and the lysates were collected in 1.7 ml microtubes. Lysates were centrifuged (Eppendorf 5804R, Westbury, NY) at 20,000 g for 20 minutes at 4°C. The supernatant was transferred into a fresh 1.7 ml microtube and stored at -70°C and the pellet was discarded.

Total Protein Determination. Cell lysates from sonicated macrophages were assayed for total protein concentration using the DC Protein Assay System. Protein residues (tyrosine, tryptophan, cystine, cysteine and histidine) react with copper in alkaline medium and then reduce a Folin reagent, which generates a blue color with maximal absorbance at 750 nm. A SpectraMax Plus microplate reader (Molecular Devices, Sunnyvale, CA) set to measure absorbance at 750 nm was used to analyze all samples. Bovine serum albumin (BSA) standards were serially diluted in lysate buffer (0.25 mg/ml to 2.0 mg/ml) to prepare a standard curve of protein concentrations. Total protein concentrations of the cell lysates were interpolated from the standard curves using manufacturer software for the microplate reader (Molecular Devices, Sunnyvale, CA).

ELISA assays for IL-1β, VEGF and TGF-β1. Analysis of conditioned media for these growth factors was completed using commercially available, quantitative, sandwich enzyme-linked immunosorbent assays (ELISA). Initial assays were completed for each cytokine ELISA to determine the need to dilute conditioned media samples. Monoclonal antibodies specific for IL-1β, VEGF and TGF-β1 were pre-coated onto 96-well plates. Serial dilutions of the appropriate recombinant human antigen and macrophage conditioned media samples were pipetted into the wells in duplicate and incubated 2-3 hours (per manufacturer directions) to allow antigen-antibody binding. Wells were washed to remove any unbound material and a secondary polyclonal antibody labeled with horseradish peroxidase was pipetted into each well. Following an incubation period of 1-2 hrs, wells were washed to remove unbound secondary antibody. A substrate solution containing hydrogen peroxide and a stabilized chromogen (tetramethylbenzidine) was

added to each well and incubated in the dark for 20 minutes to allow color development. The degree of color developed in each well is directly proportional to the amount of bound polyclonal antibody-enzyme conjugate. Finally, a stop solution, 2N HCl, was added to each well and the optical densities measured on a SpectraMax Plus microplate reader set at 450 nm with wavelength correction set at 550 nm, per instructions of the ELISA manufacturer. Detection ranges for the various cytokines growth factors are as follows: IL-1β 3.9 - 250 pg/ml, VEGF 15.6 - 1000 pg/ml, and TGF-β1 31.2 - 2000 pg/ml. Cytokine/growth factor content was determined using the standard curve and was recorded as pg/ml of media. The final cytokine growth factor concentrations (pg/ml) were then normalized to total protein concentration (mg/ml) in the cell lysate, generating values reported as pg cytokine/mg total cellular protein.

Data Analysis/Statistics

Each experimental block was repeated for n = 3 replicates for each TUS parameter set tested. All conditioned media assayed for growth factors by ELISA and cell lysates analyzed for total protein concentration were analyzed in duplicate, with the average being reported. Values for statistical analysis are reported as mean ± standard error of the mean (SEM). One-way analysis of variance (ANOVA) was used to evaluate for differences in growth factor release among various TUS parameter sets for 10-minute and 1-hour incubations. Tukey's HSD post hoc analysis was employed to reveal specific differences among treatment parameters. A p-value of $< .05$ was considered significant for all values.

Results

IL-1β Release. One-way ANOVA revealed that IL-1β release was significantly different among macrophages incubated for 10 minutes ($p = 0.012$, $F= 3.584$) and 1 hour ($p = 0.004$, $F= 4.465$) post TUS exposure. Post hoc analysis revealed significant differences in IL-1β release from macrophages among the TUS parameter sets for each incubation period. For both incubation periods, *1 MHz, 400mW/cm^2 SATA, 10-minute treatment* induced greater IL-1β release compared to all other parameter sets except 1 MHz, 400mW/cm^2, 5-minute treatment (Fig. 3.1).

VEGF Release. VEGF release following TUS exposures was significantly different among macrophages treated with various TUS parameters sets incubated for 10-minutes ($p = 0.003$) and 1-hour ($p = 0.036$) post-TUS. Post hoc analysis revealed significant differences in VEGF release among the parameters sets for both time periods (Fig. 3.2). For the 10-minute post-TUS incubation, TUS at *1 MHz, 400mW/cm^2 10-minute treatment* induced greater VEGF release than sham ($p = 0.006$), than 5-minute treatments delivered at 1 MHz, 40mW/cm^2 ($p= 0.004$), 3 MHz, 40 mW/cm^2 ($p = 0.005$), and 3 MHz, 400mW/cm^2 ($p= 0.007$) and than 10-minute treatments delivered at 3MHz, 40mW/cm^2 ($p = 0.013$). For the 1-hour post-TUS incubation, TUS at *1 MHz, 400mW/cm^2 10-minute treatment* induced greater VEGF release compared to sham treatment ($p = 0.044$) and TUS delivered at 3MHz, 40mW/cm^2, 5-minute treatment ($p = 0.028$).

Unlike IL-1β release, VEGF release increased from 10-minutes to 1-hour post-TUS for all samples, including shams. To assess these changes, the mean VEGF levels for each parameter set at 10-minutes and 1-hour were calculated (Fig. 3.3). The difference of the

means between sham samples at 10-minutes and 1-hour was 74.522 pg/mg total cellular protein. In comparison, mean differences between experimental samples ranged from 71.203 to 92.626 pg/mg total cellular protein. One-way ANOVA assessment of means between incubation periods revealed no difference among any of the experimental or sham groups ($p = 0.989$).

TGF-β1 Release. Based on ELISA, TUS exposures had no effect on TGF-β1 release from macrophages. No TGF-β1 was detected in any treated macrophage sample regardless of TUS parameter selection and post-TUS incubation period. A standard curve of serially diluted TGF-β1protein demonstrated that the ELISA was capable of measuring TGF-β1 (Fig. 3.4). To determine whether U937 macrophages were capable of releasing TGF-β1, cells were differentiated in PMA (50ng/ml) for 24 hours as previously described and then incubated for 24-hours in serum-free RPMI growth media. U937 macrophages released TGF-β1 (313.38 ± 16.50 pg/mg total cellular protein, $n = 4$ samples) into the conditioned media, as measured by ELISA.

Total cellular protein. Total cellular protein for each TUS parameter set and for both incubation periods was analyzed by one-way ANOVA (Figs. 3.5 A,B). Cellular protein amounts ranged from 87.5% to 104.9% of sham protein for 10-minute incubation samples, and ranged from 97.4% to 109.9% of sham protein for 1-hour incubation samples. One-way ANOVA revealed that total cellular protein was not significantly different among any of the TUS parameter sets, including sham treatment, for the 10-minute incubation ($p = 0.612$, $F= 0.781$) or 1-hour incubation ($p = 0.940$, $F= 0.309$).

Figure 3.1

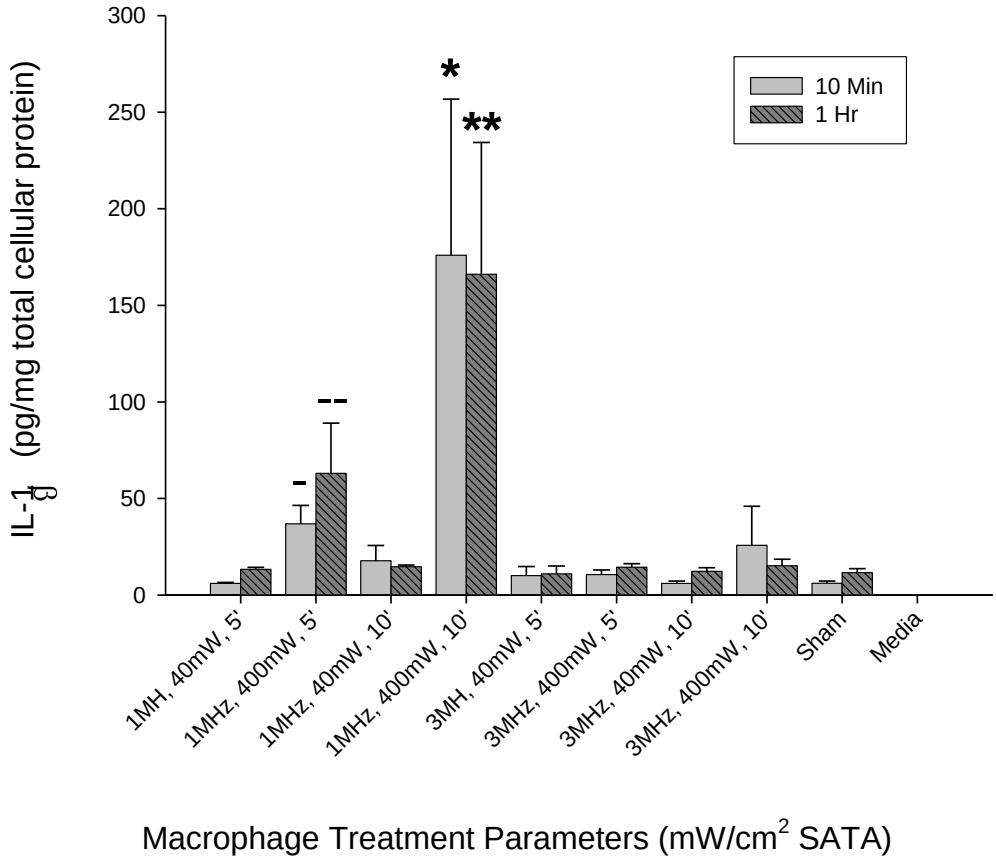
300
250
200
150
100
50
0
IL-1β (pg/mg total cellular protein)
10 Min
1 Hr
*
**
1MH, 40mW, 5'
1MHz, 400mW, 5'
1MHz, 40mW, 10'
1MHz, 400mW, 10'
3MH, 40mW, 5'
3MHz, 400mW, 5'
3MHz, 40mW, 10'
3MHz, 400mW, 10'
Sham
Media
Macrophage Treatment Parameters (mW/cm2 SATA)

Figure 3.1. *IL-1β release from TUS-treated macrophages incubated 10 minutes or 1 hour post-TUS in serum-free media*. Macrophages were treated with TUS and incubated for 10-minutes or 1-hour. Conditioned media was then assayed for the presence of cytokines/growth factors. One-way ANOVA revealed that IL-1β release was different among macrophages incubated for 10 minutes ($p = 0.012$, $F= 3.584$) and 1 hour ($p = 0.004$, $F= 4.465$) post TUS exposure. Post hoc analysis revealed significant differences in IL-1β release from macrophages among the TUS parameter sets. For both incubation periods, *1 MHz, 400mW/cm^2 SATA, 10-minute treatment* induced greater IL-1β release compared to all other parameter sets except *1 MHz, 400mW/cm^2, 5-minute treatment*. * and ** indicate significantly increased IL-1β in conditioned media at 10 minutes and 1 hour post-TUS, respectively, except where indicated by - and --. Values represent the average picograms of IL-1β per milligram of total cellular protein for each TUS parameter set ± SEM for n= 3 experiments.

Figure 3.2

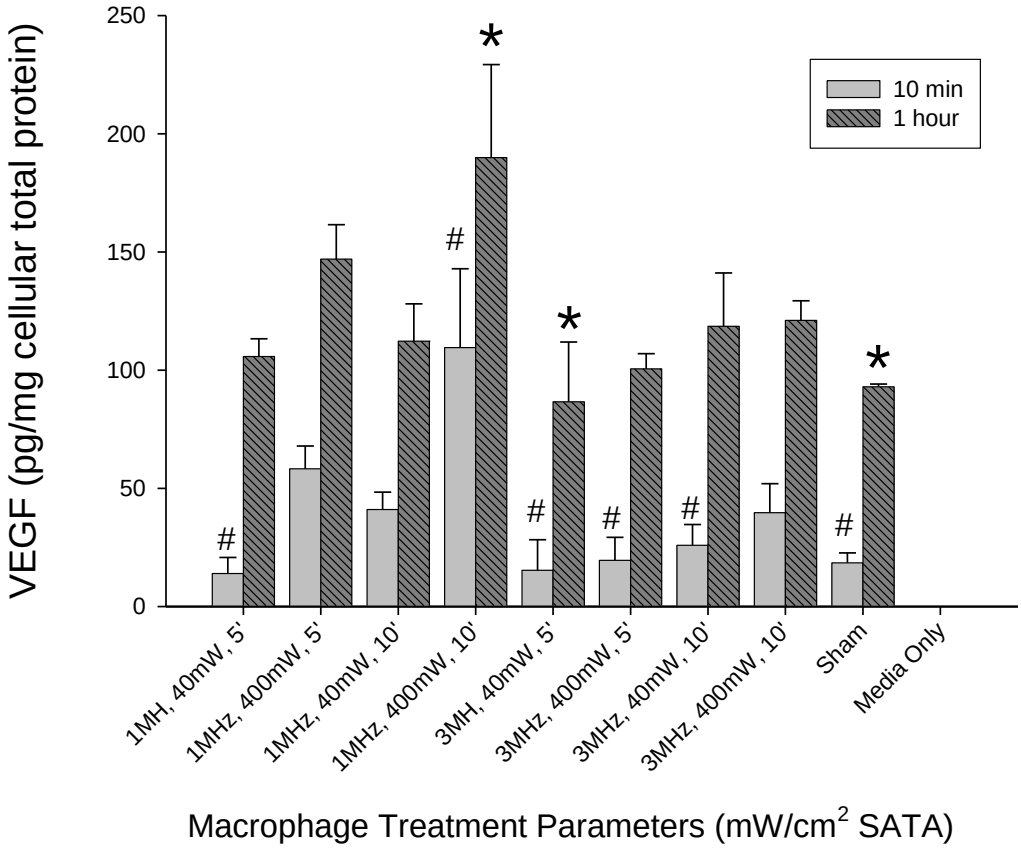
VEGF (pg/mg cellular total protein)
250
200
150
100
50
0
10 min
1 hour
#
*
1MH, 40mW, 5'
1MHz, 400mW, 5'
1MHz, 40mW, 10'
1MHz, 400mW, 10'
3MH, 40mW, 5'
3MHz, 400mW, 5'
3MHz, 40mW, 10'
3MHz, 400mW, 10'
Sham
Media Only
Macrophage Treatment Parameters (mW/cm2 SATA)

Figure 3.2. *VEGF release from TUS-treated macrophages at 10 minutes and 1 hour post-treatment*. Macrophages were treated with TUS and incubated for 10-minutes or 1-hour. Conditioned media was then assayed for the presence of cytokines/growth factors. One-way ANOVA revealed significant differences in VEGF release from macrophages treated with TUS and incubated for 10 minutes ($p = 0.003$, $F= 4.649$) and 1 hour ($p = 0.036$, $F = 2.740$) post-treatment. Post hoc analysis revealed that TUS at *1MHz, 400mW, 10-minutes* stimulated a significant increase in VEGF release at both post-TUS incubation periods. For 10-minute incubation, **#** represents significant differences compared to *1MHz, 400mW/cm^2, 10 minutes*. For 1-hour incubation, ***** indicates significant increases in VEGF release compared to *1MHz, 400mW/cm^2, 10 minutes*. Values represent the average picograms of VEGF per milligram of total cellular protein ± SEM for n= 3 experiments.

Figure 3.3

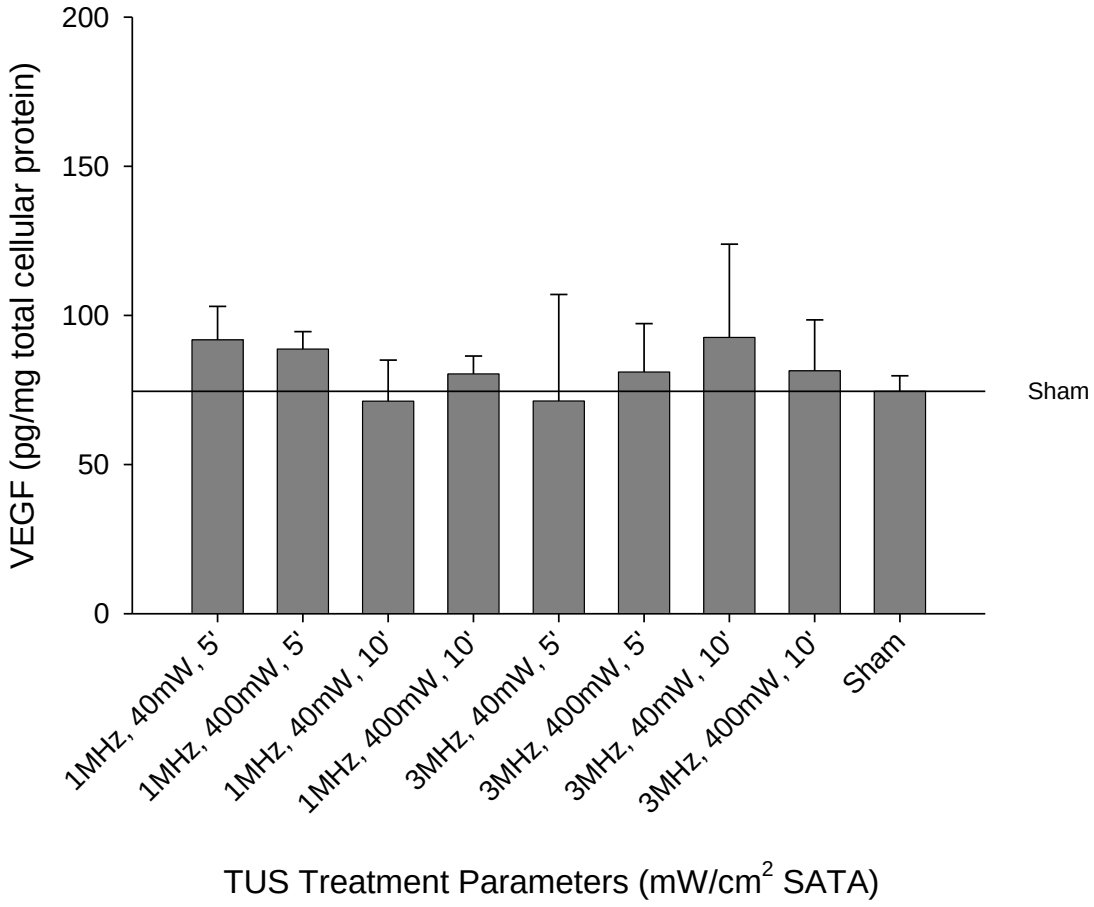
200
150
100
50
0
VEGF (pg/mg total cellular protein)
Sham
1MHz, 40mW, 5'
1MHz, 400mW, 5'
1MHz, 40mW, 10'
1MHz, 400mW, 10'
3MHz, 40mW, 5'
3MHz, 400mW, 5'
3MHz, 40mW, 10'
3MHz, 400mW, 10'
Sham
TUS Treatment Parameters (mW/cm2 SATA)

Figure 3.3. *Difference in VEGF levels following 1-hour compared to 10-minute post-TUS incubation*. VEGF release increased from 10-minutes to 1-hour post-TUS for all samples, including shams. VEGF levels for each sample at 10-minutes were subtracted from VEGF levels for the corresponding sample measured at 1-hour. The mean difference between sham samples *was 74.522 pg/mg total cellular protein*. Mean differences between experimental samples ranged from *71.203 to 92.626 pg/mg total cellular protein*. One-way ANOVA revealed no significant differences between VEGF levels from 10-minutes to 1-hour post-TUS for any TUS treatment parameter set ($p = 0.989$, $F= 0.190$). Data points represent the mean difference between VEGF levels from treated macrophages at 10-minutes compared to 1-hour post-TUS incubation ± SEM of $n = 3$ replicates.

Figure 3.4

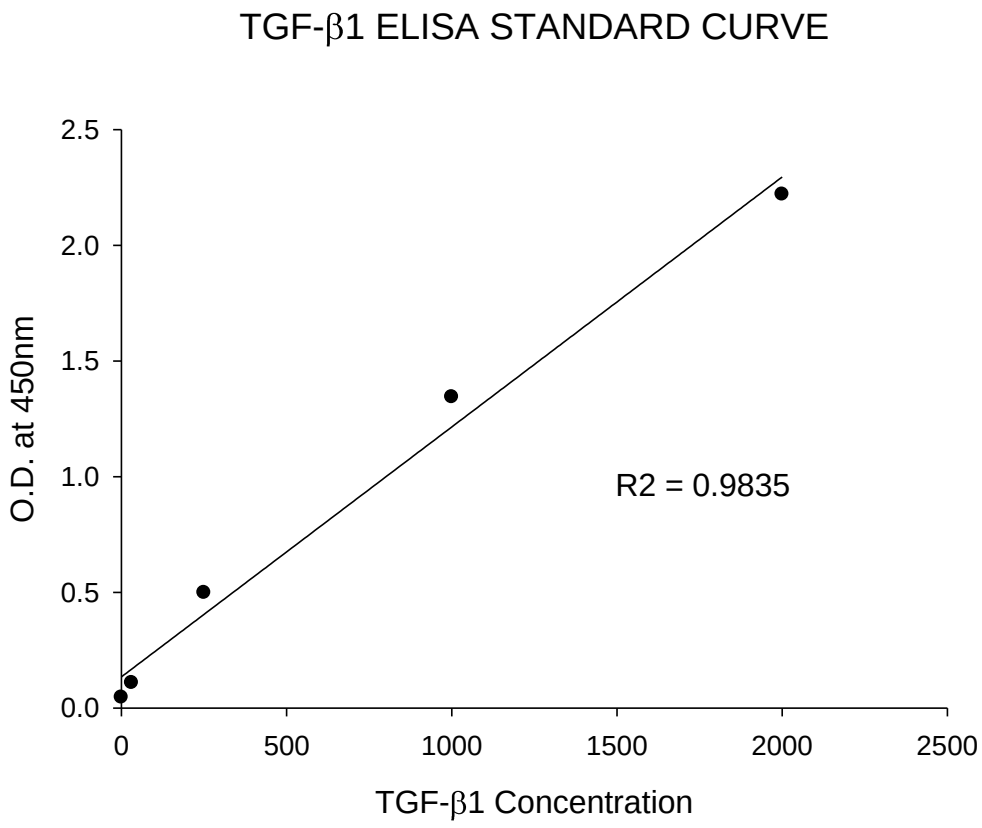
TGF-β1 ELISA STANDARD CURVE
O.D. at 450nm
2.5
2.0
1.5
1.0
0.5
0.0
0
500
1000
1500
2000
2500
TGF-β1 Concentration
R2 = 0.9835

Figure 3.4. *ELISA standard curve for TGF-β1*. Recombinant human TGF-β1 protein standard control samples were serially diluted and were added in duplicate to wells of a microplate coated with a monoclonal antibody to human TGF-β1. Conditioned media from macrophages treated with TUS and incubated for 10-minutes or 1-hour were also added in duplicate wells of the microplate. The remainder of the assay was completed as described in materials and methods. TGF-β1 was not detected in any of the experimental samples, while the TGF-β1in the serially diluted standard control samples was detected. R^2 value represents the coefficient of determination for the linear regression analysis of optical density vs. known concentrations of TGF-β1. Data points represent the mean of two measurements for each TGF-β1 concentration.

Figure 3.5

A

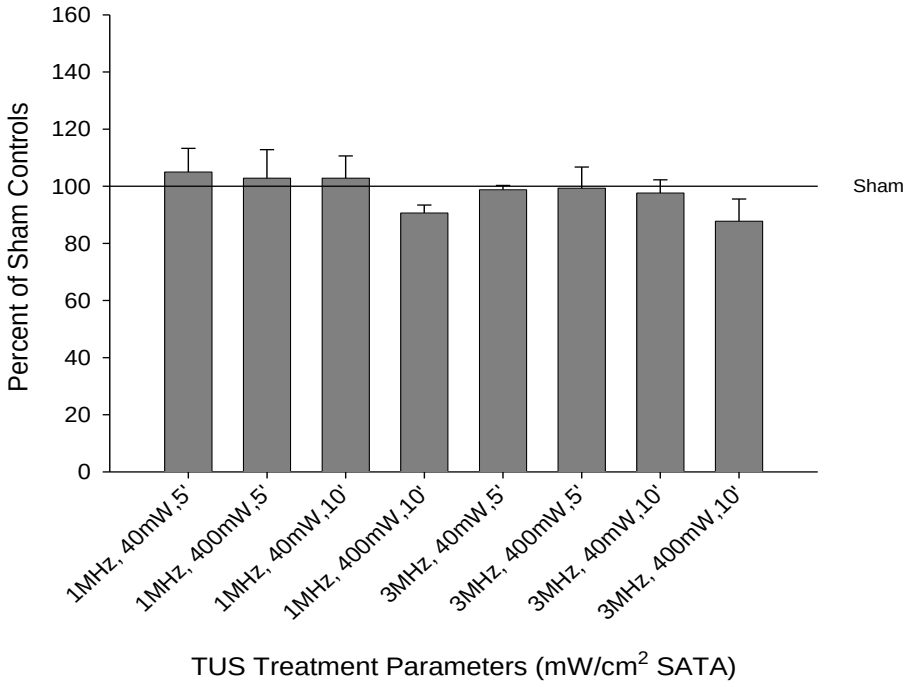
160
140
120
100
80
60
40
20
0
Percent of Sham Controls
Sham
1MHz, 40mW,5'
1MHz, 400mW,5'
1MHz, 40mW,10'
1MHz, 400mW,10'
3MHz, 40mW,5'
3MHz, 400mW,5'
3MHz, 40mW,10'
3MHz, 400mW,10'
TUS Treatment Parameters (mW/cm2 SATA)

B

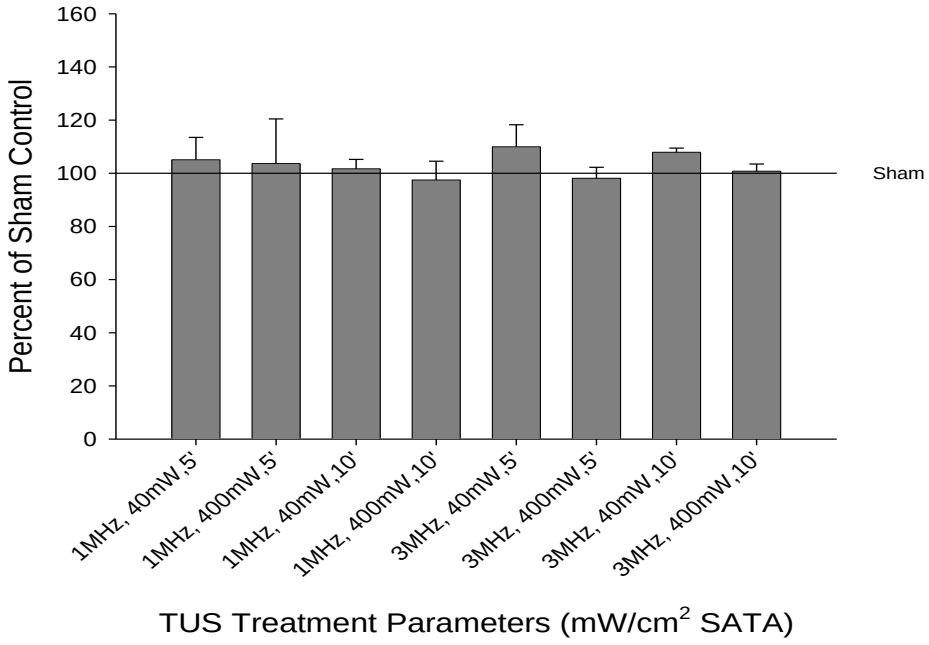
160
140
120
100
80
60
40
20
0
Percent of Sham Control
Sham
1MHz, 40mW,5'
1MHz, 400mW,5'
1MHz, 40mW,10'
1MHz, 400mW,10'
3MHz, 40mW,5'
3MHz, 400mW,5'
3MHz, 40mW,10'
3MHz, 400mW,10'
TUS Treatment Parameters (mW/cm2 SATA)

Figure 3.5. *Total cellular protein from macrophages following TUS exposure and post-TUS incubation for 10 minutes or 1 hour, as percent of sham controls*. Cellular protein content ranged from 87.5% to 104.9% of sham protein for 10-minute incubation samples, and ranged from 97.4% to 109.9% of sham protein for 1-hour incubation samples. One-way ANOVA revealed that total cellular protein was not significantly different among the TUS parameter sets, including sham treatment, for the (*A*) 10-minute incubation ($p = 0.612$, $F = 0.781$) and (*B*) 1-hour incubation ($p = 0.940$, $F = 0.309$). Values represent the mean ± SEM of milligrams cellular protein per milliliter as a percent of sham control milligrams cellular protein per milliliter for $n = 3$ samples at each parameter set and for both post-TUS incubation periods.

Discussion

Cytokines and growth factors play critical roles in the coordinated processes of tissue repair [89,199] and their release following TUS exposure is one of the hypothesized mechanisms of TUS-enhanced tissue healing [110,154,161,177]. TGF-β1 and VEGF enhance numerous cellular mechanisms of tissue healing [184,189,192,200,207,208,209], while IL-1β is known to potentiate inflammation and has been reported to be an important regulator of some of the cellular mechanisms of healing [183,210].

In the current study, macrophages exposed to TUS for 10 minutes at 1 MHz, 400mW/cm^2, responded by releasing IL-1β and VEGF but not TGF-β1. The release of IL-1β occurred within 10-minutes of sonication and there was no change when post-sonication incubation was extended to 1 hour (Fig. 3.1). Interleukin-1, originally identified as a leukocyte growth factor, exists in two distinct forms IL-1α and IL-1β. IL-1β is the predominant form, although the two have very similar functions in controlling local and systemic inflammation [211].

Mainly a product of monocytes and macrophages, IL-1 is an important regulator of the inflammatory processes following injury and infection, as well as being noted as a fibroblast mitogen [171,183,210]. Much of its pro-inflammatory properties are derived through activation of cyclooxygenase-2 (COX2) and subsequent release of prostaglandin-E2 (PGE_2) [204,212-214]. IL-1 is also involved in ECM catabolism through stimulation of matrix metalloproteinase (MMP) production by fibroblasts [215] and macrophages [216], and by promotion of neutrophil degranulation [217]. Furthermore, IL-1 induces synthesis of other

cytokines and growth factors that are involved with tissue healing in a paracrine and autocrine manner [171,210].

Young and Dyson found an acute macrophage response to TUS similar to the current investigation [161]. They reported that undifferentiated U937 macrophages released a fibroblast mitogen within 30 minutes of TUS exposure that was applied for 5 minutes (0.75 MHz, 500mW/cm^2 SATA, 100% duty cycle). The identity of the mitogen was not characterized, although IL-1β does exhibit mitogenic effects on fibroblasts [183,210]. IL-1β is capable of providing mitogenic stimulus to fibroblasts in culture [69], and increased levels could provide a stimulus for fibroblast proliferation as described by Young and Dyson [161]. Increased fibroblast number in the wound milieu could account for the accelerated rate of healing reported with in vivo investigations. However, we did not find any increase in fibroblast proliferation, as discussed previously in Chapter 2, which suggest that IL-1β may not have been the mitogen responsible for the fibroblast proliferation reported by Young and Dyson.

As evidence of a differential effect of TUS parameters on cellular response, Young and Dyson also reported that no secretory response was found within 30 minutes of sonication when TUS was applied using 3 MHz frequency for the same duration and at the same intensity, but they did report that TUS delivered at 3 MHz resulted in mitogen release at 12-hours post-exposure [161]. In agreement with those results, we did not find an increase in fibroblast mitogen (nor IL-1β or VEGF) release from macrophages within 1-hour of insonation (Figs. 2.2, 2.3, 3.1 and 3.2) at 3MHz, regardless of the other TUS parameters (Table 2.1). We did not explore whether U937 macrophages respond at time points

beyond 1-hour, thus it is not known if treated cells in the current model respond over longer periods of time post-TUS.

IL-1β release from TUS-treated, primary human monocytes has been previously reported [7]. TUS applied for 5 minutes (1 MHz, 80, 140 and 200mW/cm^2 SATA, 20% duty cycle) stimulated release of IL-1β, 18 hours after sonication. Unfortunately, the exact timing of the cellular response is not known since no earlier incubation time points were included. The monocytes also released IL-1β following a 5-minute sonication with a continuous-wave, 45 kHz wavelength and intensities of 15, 30, and 50mW/cm^2 SATA. At present, this low frequency (45 kHz) is not available on clinical TUS machines and has not been evaluated by others in relation to cytokine/growth factor release. However, the stimulation of cellular activity at this alternative ultrasound frequency indicates that a variety of combinations of wavelength, intensity and duty cycle affect cellular response to TUS.

VEGF is known to be a regulator of angiogenesis during tissue repair [218] and its importance to healing has been demonstrated in various models [101,193,193,208]. Addition of VEGF to full-thickness integument wounds accelerates tissue healing in vivo [101], while decreased levels of VEGF are associated with delayed angiogenesis and delayed healing [219]. Non-union fractures in rabbits were stimulated to heal following addition of VEGF to the injury site [193]. A study on normal fracture repair revealed that inhibition of VEGF at the fracture site resulted in decreased blood flow and non-union, while addition of VEGF increased blood flow at the fracture site [208]. Macrophages may play a role in VEGF release

during wound healing as they produce and release VEGF in situations of tissue damage and hypoxia [165,192,220].

Increased levels of VEGF were detected 10-minutes and 1-hour after applying TUS for 10 minutes at 1 MHz, 400mW/cm^2 (Fig. 3.2). One-hour post-TUS, VEGF levels were increased in all experimental and sham samples in comparison to the 10-minutes levels, which indicates that VEGF released between 10-minutes and 1-hour post-TUS was not dependent on TUS stimulation. The continued increase in VEGF levels was most likely due to constitutive release. The reasons for this hypothesis are first; the effect occurred across all of the TUS parameter sets, regardless of whether there was an initial increase in VEGF release. Also, increased levels of VEGF between 10-minutes and 1-hour incubation post-TUS were nearly identical to the VEGF increase that was detected in the sham samples over the same time period (Fig. 3.3). To support this hypothesis, statistical analysis revealed no differences among the increased levels of VEGF for any TUS treatment parameter sets over the additional 50 minutes of incubation time. Together with IL-1β release, these findings indicate that the macrophages responded acutely to TUS.

TUS enhancement of healing has also been associated with enhanced angiogenesis. TUS application (0.75 MHz, 100mW/cm^2 SATA, 20% PW, 5 minutes) accelerated angiogenesis in wounds in adult rat hind limbs after 5 days of treatment [135]. TUS treatment for 3 days (2 MHz, 50mW/cm^2 SATA,CW, 5 minutes) increased VEGF messenger ribonucleic acid (mRNA), overall vascularity, and blood flow in ischemic hind limbs of adult rats [154]. The cellular source of VEGF following in vivo TUS has not been reported, but macrophages are a source of VEGF in humans and mice [185,220]. The current

findings that macrophages release of VEGF following sonication, in addition to previously reported findings that monocytes release VEGF in response to TUS [177], suggest that monocytes/macrophages are at least partly responsible for the angiogenic response to in vivo TUS.

The current investigation did not find increased VEGF release from macrophages treated at 40 mW/cm^2 SATA, contrary to the report by Doan et al that primary monocytes released increased amounts of VEGF when exposed to TUS at intensities within the same range 20, 80 as well as at 200 mW/cm^2 SATA [7]. Doan et al utilized primary monocytes that were not differentiated toward a macrophage phenotype. The state of cellular differentiation can affect response to TUS [83,84,109] and is a possible explanation of the variance in findings of the current investigation and Doan et al. Also, no intensities higher than 200mW/cm^2 SATA were assessed in their investigation, thus it cannot be refuted with any certainty that the monocytes would have also responded to higher TUS intensities by releasing VEGF.

Roles of TGF-β in tissue repair include chemotaxis of reparative cells, stimulation of release of other cytokines, and enhancement of matrix deposition [130,206,221,222,223]. The addition of TGF-β to fibroblast cultures increased collagen production [191]. Wound healing in rats has been accelerated following topical application of TGF-β, and decreased in rats that are deficient in TGF-β [220].

Regarding TUS, in vitro exposure stimulated TGF-β secretion from osteoblasts and chondrocytes [90,110]. The increased release of TGF-β from chondrocytes was directly correlated with enhanced matrix molecule production and cellular proliferation [110]. In the

current investigation, TGF-β1 was not detected in the conditioned media of experimental or sham samples at 10-minutes or 1-hour post-TUS. The inability to detect TGF-β1 was not due to dysfunction of the ELISA as evidenced by the standard curve (Fig. 3.4) and by detection of TGF-β1 in the media of untreated, differentiated macrophages incubated for 24 hours in serum-free RPMI growth media (data not shown). As such, it appears that U937 macrophages do produce and release TGF-β1, but TUS does not stimulate its immediate release, as is it does for IL-1β and VEGF.

To further evaluate this finding, the presence of TGF-β1 in cell lysates from differentiated, non-treated U937 macrophages was evaluated. TGF-β1 was not present in detectable levels, which suggests that U937 macrophages do not readily store TGF-β1 protein intracellularly, and therefore TUS could not stimulate its immediate release. Supporting this, U937 macrophages have been reported to maintain constant levels of TGF-β1 mRNA levels, with TGF-β1 protein production occurring upon cell stimulation [184,224,225]. Similarly, TGF-β1 protein has been detected in the cytosol of primary macrophages, but its presence was dependent on prolonged exposure (24 hours or more) to cellular activation signals [226,227].

In conjunction with TUS-induced cytokine and growth factor release, acceleration of the healing process is hypothesized as a mechanism of TUS [32]. As evidence of this effect, in vivo TUS has been reported to enhance the early stages of healing (inflammatory, proliferative) resulting in replacement tissue that is of better quality than untreated, healing tissue [4,5,12,13,133]. Earlier clearance of macrophages and enhanced angiogenesis in TUS-

treated wounds also supports the acceleration hypothesis [135]. Enhanced angiogenesis stimulated by VEGF could provide the improved vascular response to healing and accelerate tissue healing related to TUS exposure. Improved angiogenesis of healing tissue following TUS has been reported in animal models for soft tissue and bone. The anabolic and proliferative effects of TGF-β1 on tissue healing are important for completion of the tissue healing process. Evidence suggests that TUS does not stimulate macrophage release of TGF-β1, rather its release may be induced from resident cells of the healing tissues as reported for osteoblasts and chondrocytes.

The mechanism that is responsible for transduction of ultrasound energy into signals for releasing cytokines and growth factors is not known. Calcium flux across the cell membrane, indicating increased membrane permeability, has been reported to occur in TUS-treated cells [50,65,158]. This ionic flux has been directly correlated with chondrocytes release of the ECM protein, aggrecan [49]. From this it follows that an increase in membrane permeability could provide the stimulus for release of intracellular contents from sonicated cells.

Genetic studies have identified numerous genes and their associated proteins that are up-regulated by TUS, suggesting that TUS energy was transduced into an intracellular signal that promotes genetic transcription and translation. This mechanism has been reported for VEGF and TGF-β in chondrocytes, periosteal cells and osteoblasts [10,11,64,90,110,154]. In the current investigation, the nearly immediate release of VEGF and IL-1β is unlikely to have occurred as a result of genetic transcription, translation and protein release.

Another possible mechanism of the release of VEGF and IL-1β in the current investigation is stimulation of exocytosis. Exocytosis of cytokines/growth factors occurs as a process of interactions between membrane proteins, cytosolic granules and cytoskeletal components [228-230]. Alteration of proteins associated with the membrane, vesicles and cytoskeleton following TUS could result in stimulation of exocytosis. As evidence of this possibility, TUS has been reported to alter membrane proteins (G-proteins and integrins) and associated second messenger proteins in fibroblasts and osteoblasts [123,125,231]. Thus, it may be that TUS affects exocytosis in addition to the longer-term affects on genetic transcription and translation. Investigations of a cellular mechanism responsible for TUS-stimulated release of cytokines and growth factors from macrophages have not been reported and elucidation of the mechanism is important to aid in the understanding of TUS affects on macrophage function and tissue healing.

Conclusion

U937 macrophages stimulated with TUS (1MHz, 400mW/cm^2, 20% duty cycle, 10-minute application) released IL-1β and VEGF into culture media within 10-minutes of exposure. From the findings of IL-1β and VEGF release, it is apparent that macrophages respond to TUS in a nearly immediate manner by releasing these molecules. Both IL-1β and VEGF are important paracrine regulators of the early stages of healing and as such, their release into the wound bed following TUS may very likely be part of the overall mechanism for TUS-accelerated healing that has been reported elsewhere.

U937 macrophages are capable of producing and releasing TGF-β1. This response was not stimulated in the post-TUS period up to 1-hour. The current study did not clarify whether TUS stimulates TGF-β1 release from macrophages by a mechanism other than that for IL-1β and VEGF, or if TUS-stimulated immediate release of TGF-β1 is precluded due to the lack of intracellular stores. In chondrocytes, TUS has been reported to increase TGF-β1 mRNA within 2 hours of treatment and to increase protein expression of TGF-β1 by 12 hours post-TUS [110]. No similar investigations have been reported in relation to macrophages. Mechanistically, therapeutic ultrasound units ultimately affect some property of cellular physiology (e.g., membrane permeability, free radical formation, stable cavitation, alteration of protein conformation, activation of second messenger systems). For macrophages, this mechanism has been hypothesized to be part immediate release and part stimulation of secretion. Given the differential expression of the cytokines and growth factors in response to TUS, reported here and by other investigators as discussed, it is important to provide a better characterization of the macrophage response to TUS.

Chapter 4

Mechanism of Interleukin-1β Release From Macrophages Treated With Specific Levels of Therapeutic Ultrasound

Abstract

Various cell types have been reported to respond to TUS by releasing cytokines and growth factors. Release of these paracrine mediators is thought to be part of the mechanism by which TUS enhances tissue healing. TUS exposure for 10-minutes at 1MHz, 400mW/cm^2 SATA, 20% pulsed-wave at 37°C stimulates the release of IL-1β from PMA-differentiated U937 macrophages. The purpose of this study was to investigate the possible contributions of non-specific increased cell membrane permeabilization and physiological processes in the release of IL-1β in response to TUS exposure at these parameters. Based on previous data compared to the total cellular IL-1β in macrophages not exposed to TUS, more than one-third of the total cellular content of IL-1β (197.648 ± 16.016 vs. 75.774 ± 33.057 pg IL-1β per 1 x 10^6 cells) was released in response to TUS. Non-specific cell permeabilization following TUS exposure was analyzed via measurement of LDH release into the media and microscopic evaluation of cells following staining with the fluorescent dyes calcein-AM and ethidium homodimer (EthD-1) to determine the proportion of cells permeabilized post-TUS. LDH release data indicates that

approximately 10% of the cells were permeabilized. Altered physiological processes were evaluated by exposing macrophages to TUS at 37°, 25° and 4° C. IL-1β release was attenuated at the lower temperatures. This attenuation in cytokine release at lowered temperatures suggests that, in addition to non-specific permeabilization, a specific mechanism of cell-mediated release of IL-1β was stimulated by TUS. Because there are at least four proposed mechanisms of IL-1β release from macrophages, further experimentation is necessary to identify which of these is affected by TUS.

Introduction

Many cell types, including osteoblasts, chondrocytes, fibroblasts, spleenocytes, monocytes, and endothelial cells release secretory products following TUS exposure at intensities ranging from 20 to 500mW/cm^2 SATA and exposure durations of 5 to 10 minutes [90,110,161,162,177,232]. In the current series of studies, activated macrophages were induced to release increased amounts of IL-1β and VEGF within 10-minutes with no further enhancement by 1-hour post-treatment, with TUS delivered for 10 minutes at 1MHz, 400 mW/cm^2 SATA, 20% duty cycle. Release of cellular products in response to TUS has been hypothesized to occur as release of material form preformed vesicles and as release of products synthesized de novo [11,64,161,162,177]. Given the rapid response in this series of studies, it is likely that TUS stimulated release of preformed material either via a form of cell-regulated exocytosis or at the result of cellular permeabilization.

TUS-induced cell membrane permeability changes following sonication have been related to a generalized increase in membrane porosity and to calcium flux across the membrane, which subsequently affects ion-gated channels [14,33,49,233,234]. The increased membrane porosity and calcium flux have been reported to be transient responses to TUS and cells have been shown to revert back to normal membrane function soon after sonication with minimal cell death occurring [235-239].

Changes in cell membrane permeabilization can be studied by measuring the release of lactate dehydrogenase (LDH) from cells and through visualization of cells following staining with dyes whose entrance into the cell is dependant on the degree of permeabilization. LDH is a cytosolic enzyme that is released from cells when their

membranes are damage [240], and therefore, has frequently been used as a marker of non-specific permeabilization that occurs as a result of cell membrane damage. The fluorescent cellular stains acetoxymethylester (calcein-AM) and ethidium homodimer-1 (EthD-1) provide a reliable method of staining cells with intact membranes (calcein-AM) and cells whose membranes have been permeabilized (EthD-1) [241,242]. Numerous normal physiological cellular processes are retarded with decreases in temperature away from normal physiological levels of 37°C. As such, temperature reduction was used to help delineate whether normal cellular processes were in part or in whole responsible for the rapid release of IL-1β from the TUS stimulated cells. The purpose of this study was to investigate the possible contributions of non-specific cell membrane permeabilization and physiological processes in the release of IL-1β in response to TUS exposure for 10 minutes at 1MHz, 400 mW/cm^2 SATA, 20% duty cycle.

Materials and Methods

Materials. Phorbol 12-myristate 13-acetate (PMA), dimethyl sulfoxide (DMSO), and lauryl sulfate (SDS) were obtained from Sigma Chemical Co., St. Louis, MO. Tris and the *DC* Protein Assay Kit were obtained from BioRad Laboratories, Hercules, CA. The BSA protein standard was purchased from Pierce Biotechnology Inc, Rockford, IL. Glycerol, sodium hydroxide, hydrochloric acid, and sterile pipets were purchased from Fisher Scientific, Pittsburgh, PA. Tissue culture plates and centrifuge tubes were purchased from Corning Inc., Corning NY. Microtubes were purchased from ISC Bioexpress, Kaysville, UT. Cell Proliferation Assay Kits were purchased from Chemicon

Intl., Temecula, CA. Disk sterile filters (0.22μM) were obtained from (Millipore, Billerica, MA). Human monocytic cells (U937) were purchased from American Type Culture Collection, Manassas, VA. Cell culture media reagents including RPMI-1640 culture media, sodium pyruvate, sodium bicarbonate, HEPES, L-glutamine, 0.25% trypsin, fetal calf serum, penicillin/streptomycin/amphotericin B, and phosphate buffered saline (PBS) were purchased from Invitrogen, Carlsbad, CA. LDH assay kit was obtained from BioVision Research Products, Mountain View CA. Calcein-AM and EthD-1 fluorescent stains were obtained from Molecular Probes Inc, Eugene, OR. Visualization and photography of fluorescent-stained cells was accomplished using a Nikon Eclipse TE300 Inverted microscope fitted with a Nikon DXM1200 digital still camera (Nikon Corp., Melville NY). Quantification of stained cells was completed using the Image Pro Plus Software Program, Silver Spring MD.

Cell Culture (U937 cells). All cell manipulations were conducted using sterile technique within a standard biological safety cabinet (Forma Scientific, Waltham, MA) and were described previously in Chapter 2 of this document.

U937 Macrophage Differentiation and Preparation for TUS Exposure. Differentiation of U937 cells into macrophages was completed according to the protocol previously described in Chapter 2 of this document.

TUS Treatment of U937 Macrophages for IL-1β and LDH Release at Physiological Temperature. Plated and differentiated macrophages were treated using a system similar to that described by Reher et al, and described in detail in Chapter 2 of this document [177]. Each experimental block was conducted on a single day using cells from the same stock

batch to reduce intra-assay variability (Table 2.1). A total of n = 3 experimental blocks were completed.

LDH Assay. LDH in the conditioned media was assessed with a commercially available colorimetric assay kit (Biovision Research Products) in which, LDH is quantified based on the enzymatic conversion of tetrazolium salt (WST-1) to a formazan dye. LDH initially catalyzes the oxidation of lactate to NADH (nicotinamide adenine dinucleotide). The NADH then reacts with WST-1 to produce the formazan dye, a process that results in the development of a yellow color. An increase in color intensity is directly correlated to an increase in LDH in the conditioned media samples and this intensity can be measured by assessing the optical density (OD) of each sample using a spectrophotometer at 450nm. The assay was completed according to the manufacturer protocol.

Conditioned media samples were thawed in a water bath and immediately placed on ice. 10ul of each conditioned media sample was added to duplicate wells of a clean 96-well microtiter plate. Next 100ul of WST-1 assay solution was added to each well and the reaction was allowed to proceed for 30 minutes up to 4 hours, until the OD of the 0.1ug/ml LDH positive control had an OD of approximately 2.0 at 450nm, as recommended by the manufacturer protocol. Sample plates were read on a microplate spectrophotometer (SpectraMax Plus, Molecular Device, Sunnyvale, CA) at 450nm with the reference wavelength set at 650nm. Samples were measured every 30 minutes until the positive control reached the recommended OD. OD values were then recorded with values representing the mean value of the sample duplicates. OD was normalized to total cellular protein.

For total cellular LDH analysis, macrophages were propagated and differentiated as previously described in Chapter 2. Following 24-hr serum free incubation, cell lysates were collected as described in Chapter 3. Analysis of total cellular LDH content was conducted using the protocol described above in this section. For all LDH analyses, A total of n = 3 experimental blocks were completed.

Total Protein Determination for Cell Lysates. Cell lysates from sonicated macrophages were assayed for total protein concentration using DC Protein Assay System (Bio-Rad Laboratories, Hercules, CA) as previously described in Chapter 3.

Treatment of Macrophages for Fluorescent Cell Staining. Cell staining based on membrane permeabilization, as a measure of cell viability, was completed using the Live/Dead Viability/Cytotoxicity Assay that includes the EthD-1 and calcein-AM fluorescent dyes. The assay allows simultaneous determination of viable and non-viable cells from one sample. EthD-1 is a cell impermeant dye that stains nucleic acids by intercalating between base pairs, while calcein-AM is a cell permeant dye that is retained in cells and fluoresces upon conversion to calcein after interacting with intracellular esterases [241-243]. Calcein-AM produces a bright green fluorescence at ~530nm, and EthD-1 produces a bright red fluorescence at ~635nm. Macrophages were stained following TUS treatment using parameters sets of *1 MHz, 40mW/cm^{2}SATA 20% PW; 1 MHz, 400mW/cm^2 SATA 20% PW; and sham*, all of which were applied for 10-minutes. Following macrophage sonication and incubation for 10-minutes or 1-hour, calcein-AM and EthD-1 were added to the culture plates containing cells and conditioned media at concentrations 0.8µM and 2µM, respectively and incubated with the cells for 30 minutes at room

temperature. After incubation, the media containing the dyes was decanted and the cells rinsed three times with 5ml of PBS and then visualized using the Nikon Eclipse TE300 fitted with a high-pressure 75-watt xenon lamp and a 10X objective lens. Each fluorophore was excited using a 495 nm excitation wavelength with fluorescence viewed at 530 nm for calcein-AM and 605 nm for EthD-1. Digital photographs were captured on the ACT-1 software (Nikon, Melville NY). Multiple photographic images were required to insure an adequate sampling of the treated macrophages coated on 60 x 15 mm plates. Specifically, the plate was divided into 9 equally sized areas within the body of the culture dish (Fig. 4.1). The 5 areas marked on the figure indicate the areas of each plate in which the stained cells were photographed. The field of view was manually centered in each area and three photographs were taken of each field: 1) normal light microscopy, 2) fluorescence of the calcein-AM, and 3) fluorescence of the EthD-1 (Figs. 4.2-4.4). The photographs were stored for later image analysis using the Image Pro Plus 4.1 software program. For the fluorescent photographs, the software identified the area, in pixels, of all the cells that were stained with calcein or EthD-1 within each field. For each photographic field, the area of all stained cells, calculated by the image program from the number of pixels, were summed to generate a total area for each fluorophore. The total areas from each of the five fields of the culture plate were summed to give a total area of each fluorophore per plate (the total number of pixels encompassing the stained cells). Thus, there was a total area for each plate for calcein-AM stained cells and a total area for EthD-1 stained cells. For each plate, the total area of the calcein-AM stained and EthD-1 stained cells were summed to generate a total area of cells analyzed. This total cellular area of the

plate was used to generate the percentage of viable cells (calcein-AM stained) by dividing the total calcein-AM stained area by the total cellular area and multiplying by 100. A total of n = 3 experimental blocks were completed and each experimental block was conducted on a single day using cells from the same stock batch.

To determine the ability of the combined calcein-AM and EthD-1 cell staining to represent the total area of cells present on each analyzed field, total area determination was also completed from normal light microscopy images. A sample of gray-scaled images of two randomly selected fields from each of five randomly selected plates were analyzed using the Image Pro Plus 4.1 software program and total cellular area (number of pixels) for the fields was recorded (total of ten fields analyzed). These values were then used to generate a percentage of total cellular area represented by the sum of the calcein-AM and EthD-1 stained cells compared to the normal light microscopy images (data not shown).

Treatment of Macrophages at Variable Temperatures. Macrophages were propagated, plated, differentiated and treated with TUS using the custom-designed apparatus as described in Chapter 2 except; macrophages were exposed to TUS for 10 minutes using *sham treatment (0 mW/cm^2 SATA) and treatment at 1MHz, 400mW/cm^2 SATA, 20% PW* at 4°, 25° and 37° C and then incubated for 10-minutes post-treatment at the respective temperatures. A thermostatically controlled water bath was utilized to maintain the appropriate exposure temperature. Post-TUS incubations were completed on ice (4° C), at room temperature (25° C) or in a humidified incubator maintained at 37° C. Following incubation, conditioned media were collected as described previously, and analyzed for the presence of IL-1β. A total of n = 3 experimental blocks were completed

and each experimental block was conducted on a single day using cells from the same stock batch.

ELISA for IL-1 β in Conditioned Media and Cell Lysates. Analysis of macrophage conditioned media and cell lysates for IL-1β was completed using commercially available, quantitative, sandwich enzyme-linked immunosorbent assays (ELISA; R & D Systems, Minneapolis, MN) as described in Chapter 3. The detection range for IL-1β was 3.9 - 250 pg/ml. IL-1β content was determined using the standard curve and recorded as pg/ml. The final concentrations (pg/ml) were then normalized to pg/1 x 10^6 cells/ml, based on the number of macrophages plated.

IL-1β content in total cell lysates of untreated macrophages. To determine the total amount of IL-1β in untreated macrophages, macrophages were propagated, plated and differentiated as described previously. Macrophages at concentrations of 0.5, 0.25 and 0.125 x 10^6, cells/ml in 5ml of media for a total of 2.5, 1.25 and 0.625 x 10^6 cells, respectively, were analyzed for IL-1β. Cell lysates were collected as described previously and then analyzed by ELISA. Data for IL-1β content in total cell lysates from untreated cells was normalized as picograms IL-1β per 1 x 10^6 cells. All macrophage cell lysates assessed were from the same batch of cells. The data reported represents the mean ± SEM of n = 3 for each cell concentration analyzed.

Data analysis/Statistics.

For macrophage sonication and subsequent determination of LDH release, each experimental block of TUS parameters was repeated for n = 5 replicates. For cell staining, variable temperature experiments, and ELISAs for IL-1β from treated and untreated macrophages, the experimental blocks were repeated for n = 3 replicates. All data are represented as the mean of the replicates ± SEM. Data from all experiments was analyzed using a one-way ANOVA with significance level set at $p < 0.05$ with post hoc testing completed using Tukey's HSD test.

Results

LDH release from macrophages. TUS exposure induced increased LDH release from macrophages ($p = 0.001$, $F = 7.734$) following 10-minutes post-treatment incubation. Post hoc analysis revealed that macrophages treated with TUS delivered at 1 MHz, 400mW/cm^2, 10 minutes released an increased amount of LDH compared to other levels of TUS, except TUS delivered at 1MHz, 400mW/cm^2, 5 minutes (Fig. 4.5A). At 1-hour post-treatment, TUS also induced increased LDH release ($p = 0.002$, $F= 4.057$) (Fig 4.5B). Based on post hoc testing, LDH release from macrophages treated at 1 MHz, 400mW/cm^2, 10 minutes was increased over all other TUS parameter sets except 1MHz, 400mW/cm^2, 5 minutes (Fig 4.5 A, B). Data represents the mean values for the optical density for the LDH assay normalized to the total cellular protein from each treated sample for n = 5 samples at each TUS parameter set.

Figure 4.6 represents the comparison of the total content of LDH in untreated macrophages and LDH release from macrophages treated with the stimulatory TUS parameters. Untreated macrophages plated at the same concentration as TUS-treated macrophages (2.5×10^6 cells) contained approximately ten-times the amount of LDH released in response to TUS, evidenced by the total cell lysate of untreated cells requiring a 10-fold dilution of samples to allow measurement of LDH content. This value provided the estimate that approximately $1/10^{th}$ of the total LDH was released in response to the stimulatory TUS parameters.

Macrophage viability as a measure of permeabilization. Macrophages treated with 1MHz TUS for 10-minutes at 0, 40 or 400mW/cm^2 SATA, 20% PW incubated for 10-minutes or 1-hour post-TUS and stained with the fluorescent dyes, calcein-AM and EthD-1 were analyzed for total area of intact cells (Figs. 4.2-4.4, 4.7). Following 10-minute post TUS incubation, the percentage of the total area of macrophages that were stained by calcein-AM was not significantly different when comparing sham, 1 MHz, 40mW/cm^2, and 1 MHz, 400mW/cm^2 (10 minute treatments) ($p = 0.128$, $F= 2.952$) (Fig. 4.7A). Following 1-hour post TUS incubation, the percentage of the total area of macrophages that were stained by calcein was significantly different among the treatment groups ($p = 0.002$, $F= 17.930$) (Fig. 4.7B). Post hoc testing revealed that calcein-AM staining was significantly less for TUS treatment at 1 MHz, 400mW/cm^2, 10 minutes compared to sham ($93.805\% \pm 1.637$ vs. $98.433\% \pm 0.336$, $p = 0.003$) and 1 MHz, 40mW/cm^2 , 10 minutes ($93.805\% \pm 1.637$ vs. $97.953\% \pm 0.336$, $p = 0.005$). These findings indicate that approximately 7-8% of the treated cells were permeabilized by the stimulatory TUS

parameter set and that percentage is comparable to the 10% of total LDH release, which also characterizes the extent of non-specific permeabilization due to TUS.

The total area of fluorescently stained cells (calcein-AM and EthD-1) was compared to total area of cells from normal light microscopy images from the same fields of the culture plates (10 total fields from 5 culture plates) containing treated macrophages. The total area of all fluorescently stained cells was 94.321% ± 1.578 of the total area of cells identified in the light microscopy images of n= 10 fields analyzed (data not shown).

IL-1β content in total cell lysates of untreated macrophages. Cell lysates from 2.5, 1.25 and 0.625 x 10^6 differentiated, untreated macrophages were analyzed for IL-1β using ELISA with data normalized as IL-1β per 1 x 10^6 cells. The concentration of IL-1β from the samples was 197.648 ± 16.016 pg/1 x 10^6 cells (range 178.161 - 229.408 pg/1 x 10^6 cells) (Fig. 4.8A). This data was used to compare IL-1β release from macrophages treated with various TUS parameter sets to the total IL-1β from untreated macrophages.

IL-1β content in conditioned media following TUS exposure. Macrophages exposed to various levels of TUS (Table 2.1) released significantly increased amounts of IL-1β at 10-minutes ($p= 0.005$, $F= 4.203$) and 1 hour post-TUS ($p= 0.004$, $F= 4.560$). Post hoc analysis revealed that TUS delivered at 1MHz, 400mW/cm^2 SATA, 10-minute treatment induced significantly greater IL-1β release when compared to all other TUS parameter sets at 10 minutes and 1 hour incubation post-TUS (Fig 4.8B) for n = 3 separate TUS experiments ($p < 0.05$). TUS-stimulated macrophages released 75.774 ± 33.057 pg IL-1β / 1 x 10^6 cells protein, compared to the total cellular content of 197.648 ± 16.016 pg

IL-1β /1 x 10^6 cells (Fig 4.8A,B). These findings indicate that approximately 1/3^{rd} of the total cellular IL-1β was released by macrophages in response to the stimulatory TUS parameter set.

Comparison of the release of greater than 30% of the total IL-1β to the 7-10% of non-specific permeabilization indicated by LDH and fluorescent staining suggests that another mechanism beyond non-specific membrane permeabilization is likely responsible for a portion of the IL-1β released by TUS-exposed macrophages.

Temperature effect on IL-1β release from macrophages treated with TUS at 1MHz, 400mW/cm^2 SATA, 20% PW, 10-minutes. The release of IL-1β in response to TUS was affected by temperature during TUS exposure and the post TUS incubation ($p < 0.001$, F= 15.081) (Fig. 4.9). Post hoc analysis indicated that macrophages released increased amounts of IL-1β when TUS (1MHz, 400mW/cm^2 SATA, 20% PW, 10 minutes) was carried out at 37°C when compared to all sham treatments and compared to TUS (1 MHz, 400mW/cm^2 SATA, 10 minutes) completed at 4°C, as indicated by ($p < 0.05$). TUS (1MHz, 400mW/cm^2 SATA, 20% PW, 10 minutes) delivered at 25° and 37° increased the release of IL-1β compared to sham treatments at the respective temperatures ($p < 0.05$). In addition, IL-1β release was greater at 37°C compared to 25°C and 25°C compared to 4°C and but neither trend was not statistically significant ($p = 0.08$, $p = 0.061$).

Figure 4.1

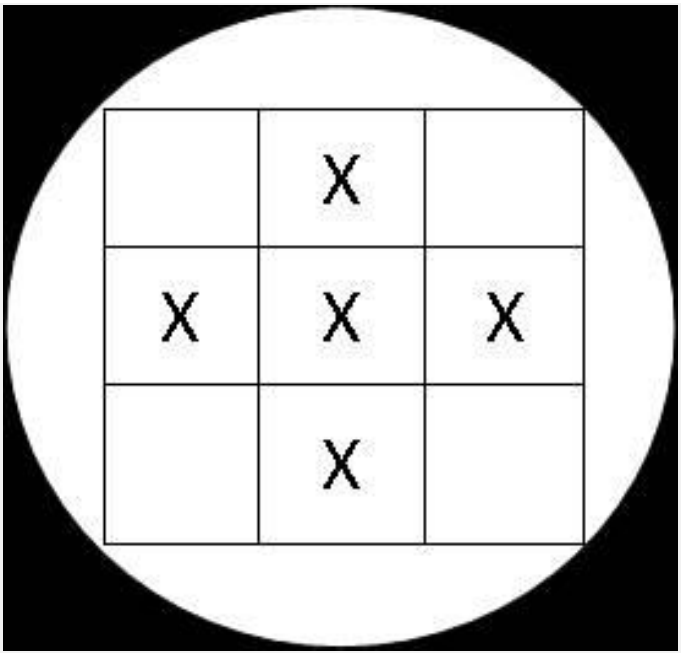

Figure 4.1. *Culture plate areas analyzed for cell staining.* Diagram representing the five selected fields that were photographed and analyzed for calcein-AM and ethidium homodimer staining of insonated macrophages. All culture plates of stained macrophages were analyzed from these fields. Data from the five fields were summed and the summed data was reported as representative of total area of stained cells for each plate.

Figure 4.2

A

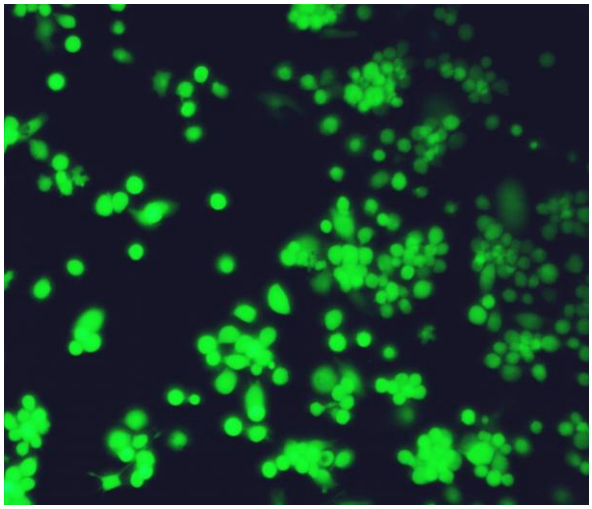

B

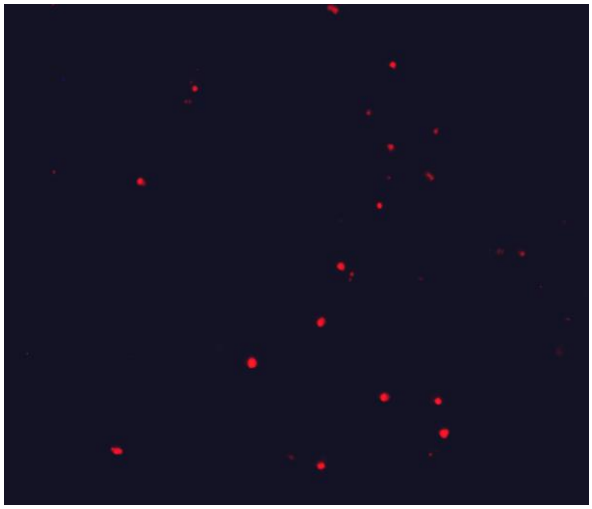

C

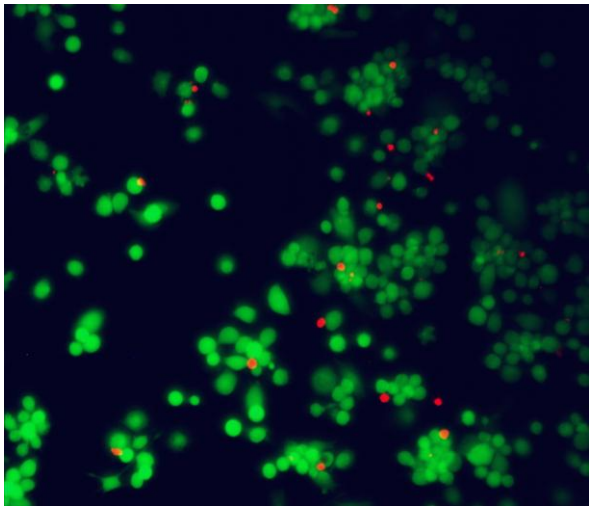

D

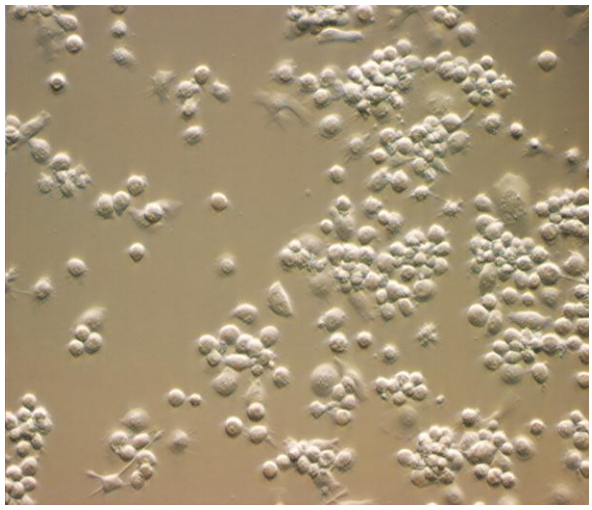

Figure 4.2. *Images of macrophages stained with calcein-AM, ethidium homodimer or unstained, following sham TUS exposure,* ***0 mW/cm^2 SATA****, 10 minutes and 10-minute or 1-hour post-TUS incubation.* Images were captured using a Nikon Eclipse TE300 microscope fitted with a high-pressure 75-watt xenon lamp for fluorescent imaging and a 10X objective lens. **A**) Macrophages incubated with 0.8μM calcein-AM, a membrane permeant dye that is converted to a green fluorescence based on intracellular esterase activity, demonstrating viable cells, **B**) Macrophages incubated with 2.0μM EthD-1, a dye which enters cells with damaged membranes and increases fluorescence after binding to nucleic acids, **C**) Overlay of images calcein-AM and EthD-1 stained cells, and **D**) Unstained macrophages imaged under normal light microscopy conditions. All three images are of macrophages from the same field and are representative of the images analyzed for cytotoxicity of the TUS treatment.

Figure 4.3

A

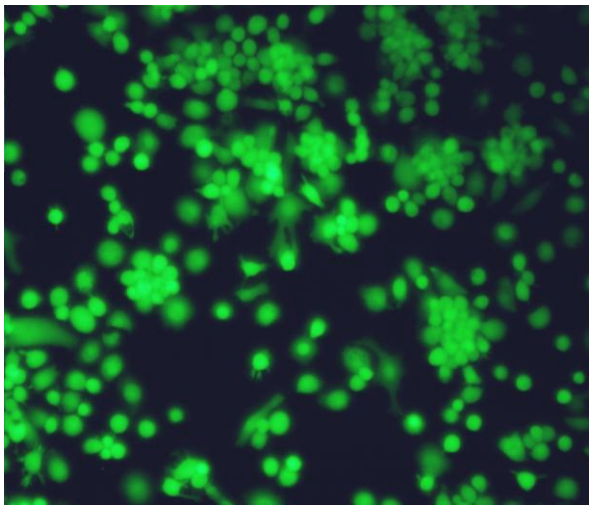

B

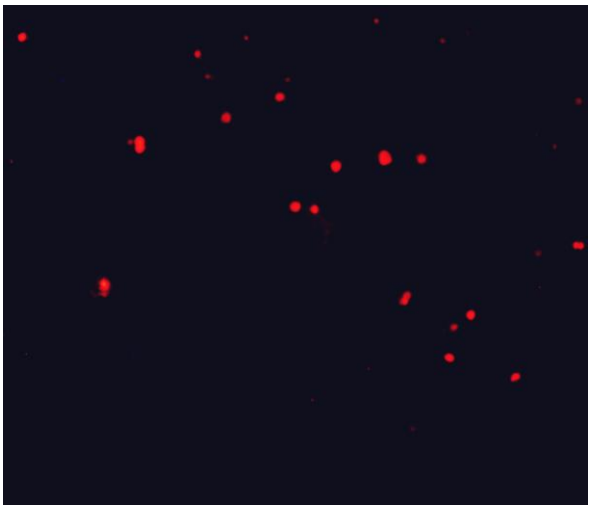

C

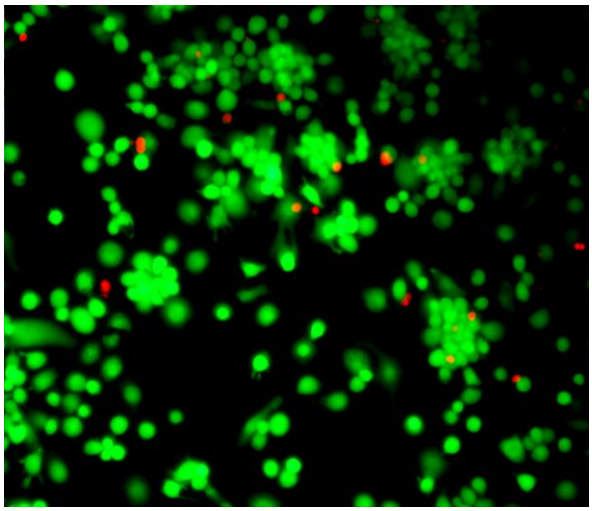

D

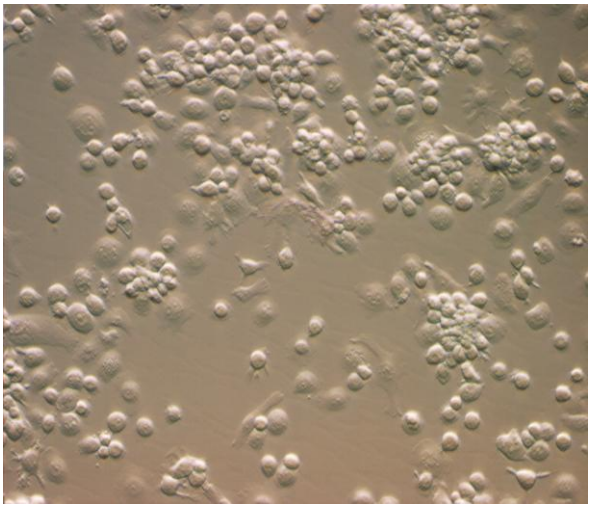

Figure 4.3. *Images of macrophages stained with calcein-AM, ethidium homodimer or unstained, following TUS exposure at 1MHz,* ***40mW/cm^2 SATA****, 20% PW 10 minutes and 10-minute or 1-hour post-TUS incubation.* Images were captured using a Nikon Eclipse TE300 microscope fitted with a high-pressure 75-watt xenon lamp for fluorescent imaging and a 10X objective lens. **A**) Macrophages incubated with 0.8μM calcein-AM, a membrane permeant dye that is converted to a green fluorescence based on intracellular esterase activity, demonstrating viable cells, **B**) Macrophages incubated with 2.0μM EthD-1, a dye which enters cells with damaged membranes and increases fluorescence after binding to nucleic acids, **C**) Overlay of images calcein-AM and EthD-1 stained cells and, **D**) Unstained macrophages imaged under normal light microscopy conditions. All three images are of macrophages from the same field and are representative of the images analyzed for cytotoxicity of the TUS treatment.

Figure 4.4

A

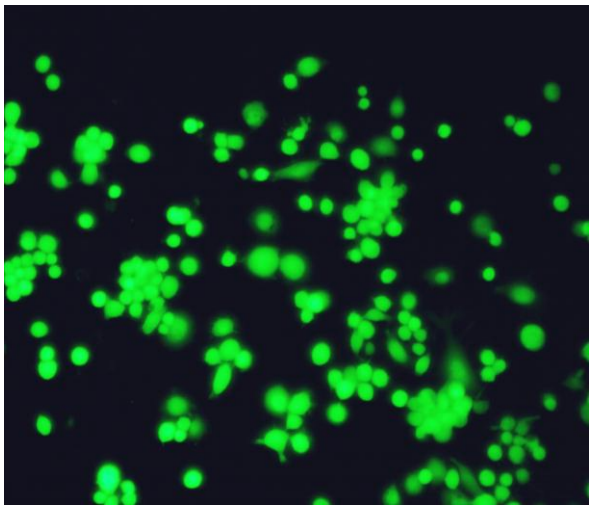

B

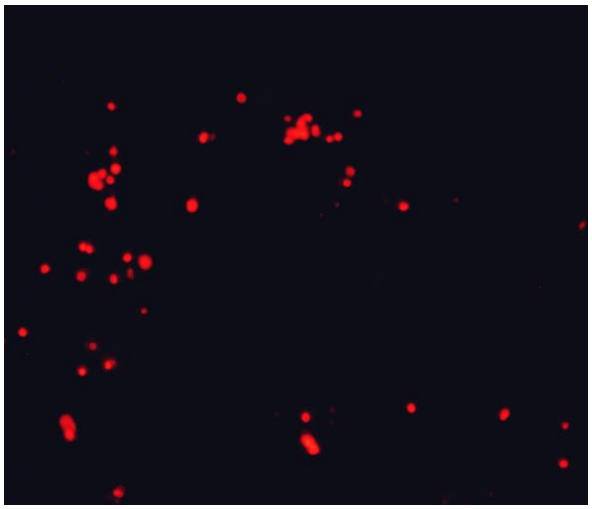

C

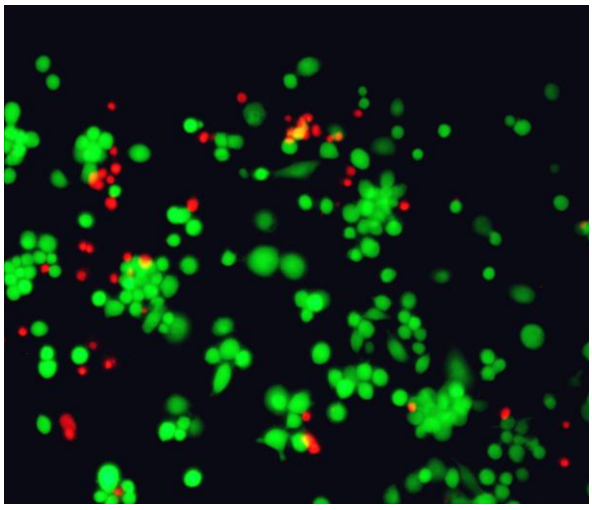

D

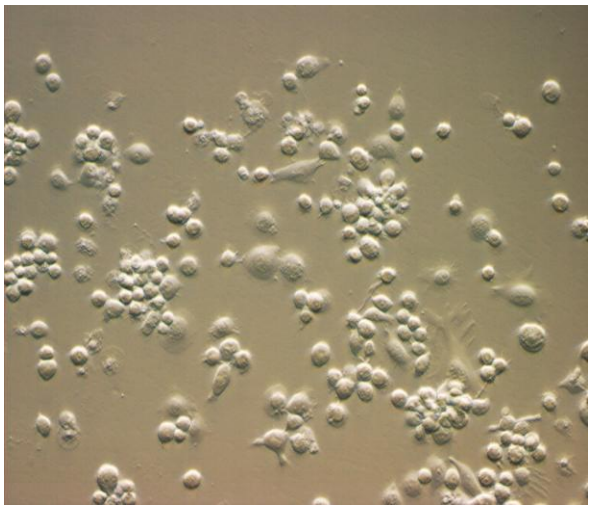

Figure 4.4. *Images of macrophages stained with calcein-AM, ethidium homodimer or unstained, following TUS exposure at 1MHz,* ***400mW/cm^2 SATA****, 20% PW 10 minutes and 10-minute or 1-hour post-TUS incubation.* Images were captured using a Nikon Eclipse TE300 microscope fitted with a high-pressure 75-watt xenon lamp for fluorescent imaging and a 10X objective lens. **A**) Macrophages incubated with 0.8μM calcein-AM, a membrane permeant dye that is converted to a green fluorescence based on intracellular esterase activity, demonstrating viable cells, **B**) Macrophages incubated with 2.0μM EthD-1, a dye which enters cells with damaged membranes and increases fluorescence after binding to nucleic acids, **C**) Overlay of images calcein-AM and EthD-1 stained cells, and **D**) Unstained macrophages imaged under normal light microscopy conditions. All three images are of macrophages from the same field and are representative of the images analyzed for cytotoxicity of the TUS treatment.

Figure 4.5

A

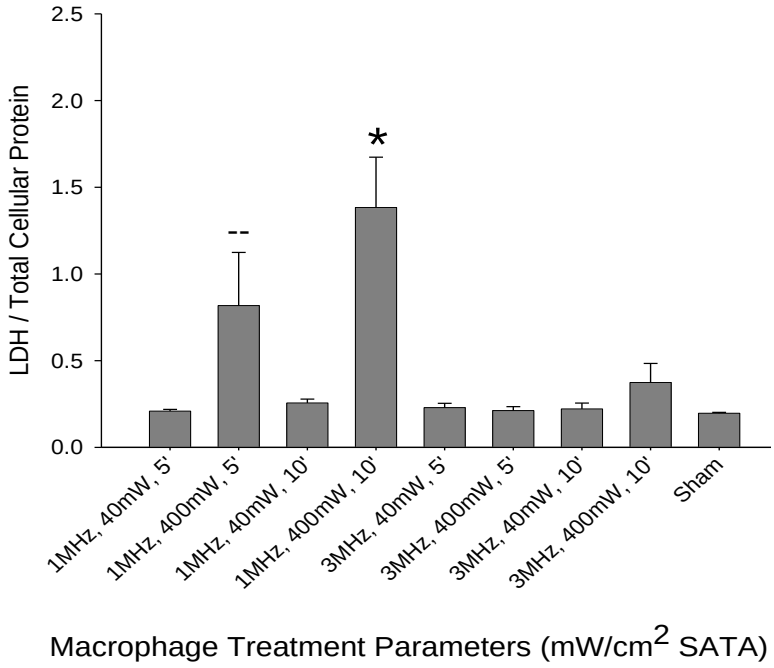
LDH / Total Cellular Protein
2.5
2.0
1.5
1.0
0.5
0.0
--
*
1MHz, 40mW, 5'
1MHz, 400mW, 5'
1MHz, 40mW, 10'
1MHz, 400mW, 10'
3MHz, 40mW, 5'
3MHz, 400mW, 5'
3MHz, 40mW, 10'
3MHz, 400mW, 10'
Sham
Macrophage Treatment Parameters (mW/cm2 SATA)

B

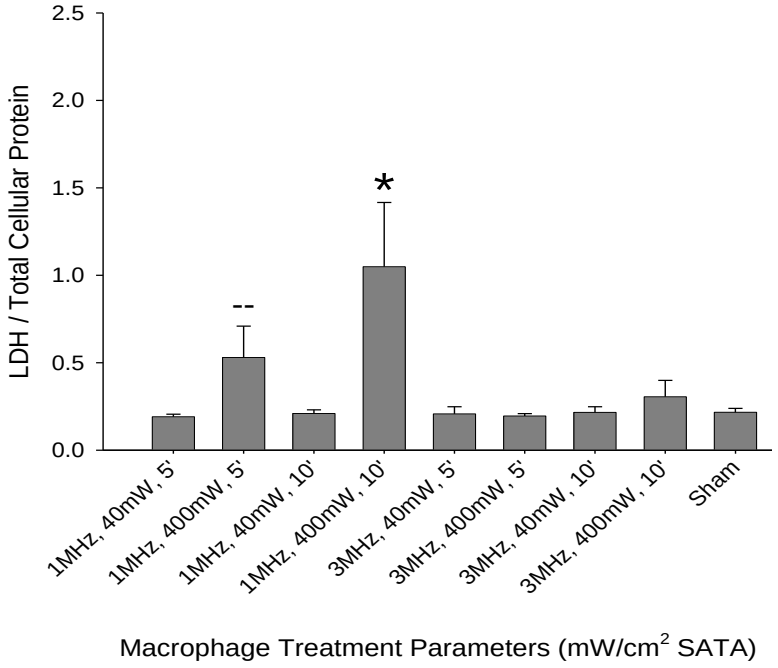
LDH / Total Cellular Protein
2.5
2.0
1.5
1.0
0.5
0.0
--
*
1MHz, 40mW, 5'
1MHz, 400mW, 5'
1MHz, 40mW, 10'
1MHz, 400mW, 10'
3MHz, 40mW, 5'
3MHz, 400mW, 5'
3MHz, 40mW, 10'
3MHz, 400mW, 10'
Sham
Macrophage Treatment Parameters (mW/cm2 SATA)

Figure 4.5. *Lactate dehydrogenase release from TUS-treated macrophages incubated for 10-minutes and 1-hour post-treatment.* **A**) TUS exposure induced increased LDH release from macrophages ($p = 0.001$, $F = 7.734$) following 10-minutes post-treatment incubation. Post hoc analysis revealed that macrophages treated with TUS delivered at 1 MHz, 400mW/cm^2, 20% PW, 10 minutes released an increased amount of LDH compared to other levels of TUS, except TUS delivered at 1MHz, 400mW/cm^2, 20% PW, 5 minutes as indicated by the ***** and **--** symbols. **B***) Lactate dehydrogenase release from TUS-treated macrophages incubated for 1-hour post-treatment.* At 1-hour post-treatment, LDH release from macrophages insonated at 1 MHz, 400mW/cm^2, 20% PW, 10 minutes were increased over all other TUS parameter sets except 1MHz, 400mW/cm^2, 20% PW 5 minutes, as indicated by the ***** and **--** symbols ($p = 0.002$, $F= 4.057$). Data represents the mean values the optical density for the LDH assay normalized to the total cellular protein from each insonated sample for $n = 5$ samples at each TUS parameter set. All significant differences were noted with $p < 0.05$.

Figure 4.6

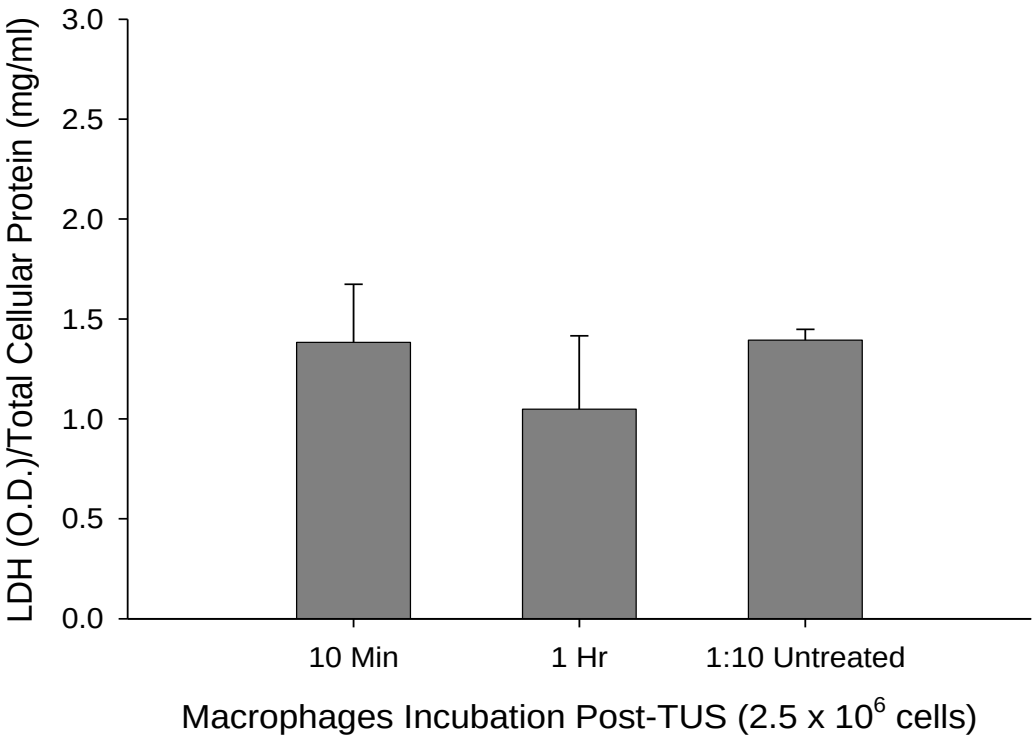
LDH (O.D.)/Total Cellular Protein (mg/ml)
3.0
2.5
2.0
1.5
1.0
0.5
0.0
10 Min
1 Hr
1:10 Untreated
Macrophages Incubation Post-TUS (2.5 x 10^6 cells)

Figure 4.6. *Comparison of Lactate Dehydrogenase in Conditioned Media from TUS-treated Macrophages and from Total Cell Lysates of Untreated Macrophages.* LDH was measured in conditioned media at 10-minutes and 1-hour post-treatment from macrophages exposed to TUS (1MHz, 400mW/cm^2 SATA, 20% PW, 10-minutes) and also in total cellular lysates of untreated macrophages. Data represents mean ± SEM of n = 3 separate samples.

Figure 4.7

A

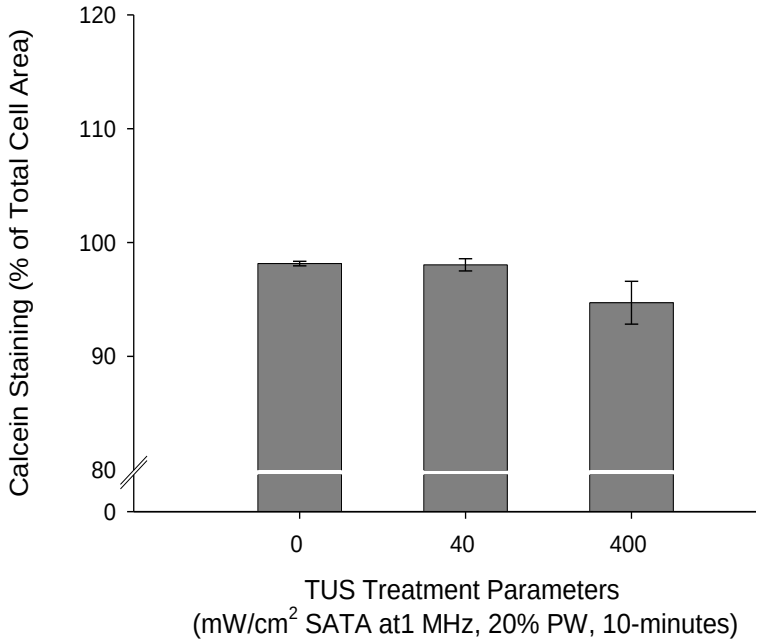
Calcein Staining (% of Total Cell Area)
120
110
100
90
80
0
0
40
400
TUS Treatment Parameters
(mW/cm2 SATA at1 MHz, 20% PW, 10-minutes)

B

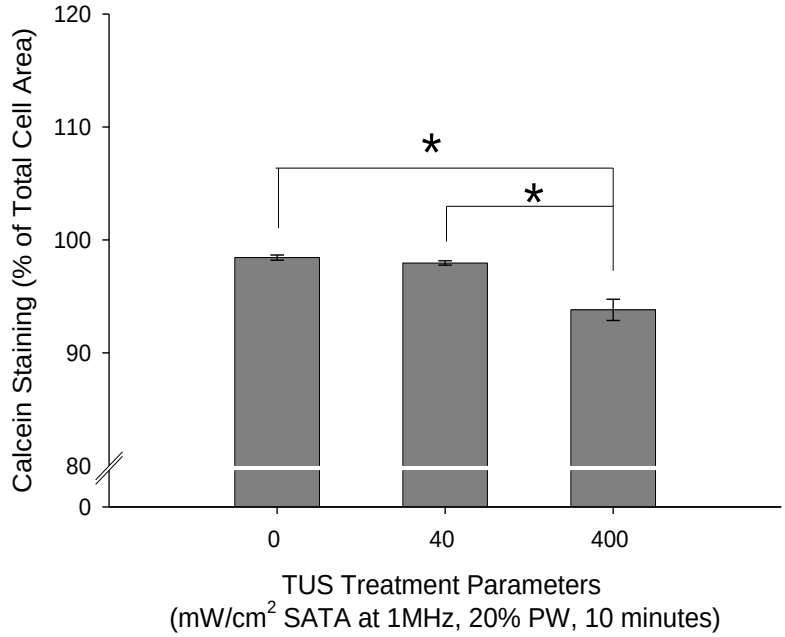
Calcein Staining (% of Total Cell Area)
120
110
100
90
80
0
*
*
0
40
400
TUS Treatment Parameters
(mW/cm2 SATA at 1MHz, 20% PW, 10 minutes)

Figure 4.7. Analysis of m*acrophage staining with fluorophores, following TUS exposure and 10-minute and 1-hour post-TUS incubation.* Macrophages were insonated for 10 minutes, at 1MHz, 40 or 400 mW/cm^2 SATA, 20% PW incubated for 10-minutes or 1-hour post-TUS and then stained with the cell permeant fluorescent dyes, calcein (viable cells) and EthD-1 (permeabilized cells). Images of the stained cells were analyzed for total area (total # of pixels) encompassing both calcein and EthD-1 stained cells. **A***)* At the 10-minute incubation time point, the percentage of the total area of macrophages that were stained by calcein were not significantly different when comparing sham, 1 MHz, 40mW/cm^2, and 1 MHz, 400mW/cm^2. 20% PW (10 minute treatments) ($p = 0.128$, $F= 2.952$). **B***)* At the 1-hour incubation time point the percentage of the total area of macrophages that were stained by calcein was significantly different among treatment groups ($p = 0.002$, $F= 17.930$). Specifically, calcein staining for TUS treatment at 1 MHz, 400mW/cm^2, 20% PW, 10-minutes was significantly decreased compared to sham and 1 MHz, 40mW/cm^2, 20% PW, 10-minutes ($p = 0.003$, $p = 0.005$ respectively). Data represent mean ± SEM of $n = 3$ samples at each treatment parameter set.

Figure 4.8

A

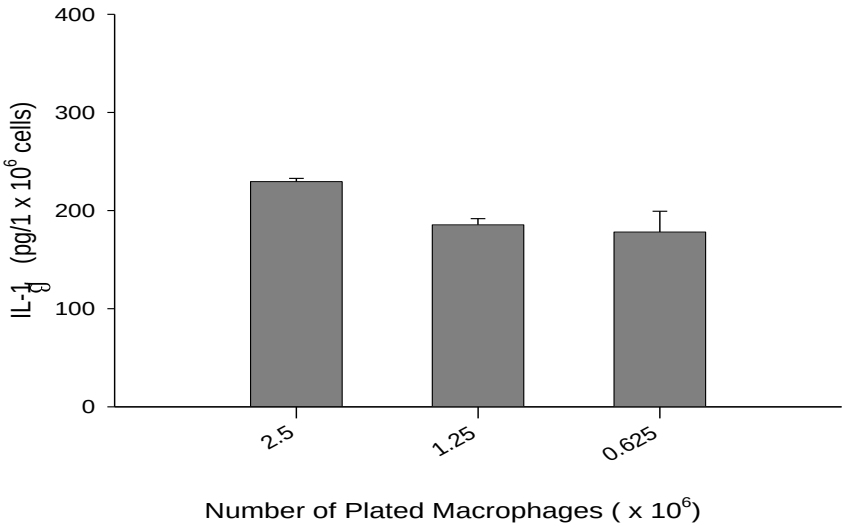
400
300
200
100
0
IL-1β (pg/1 x 10^6 cells)
2.5
1.25
0.625
Number of Plated Macrophages (x 10^6)

B

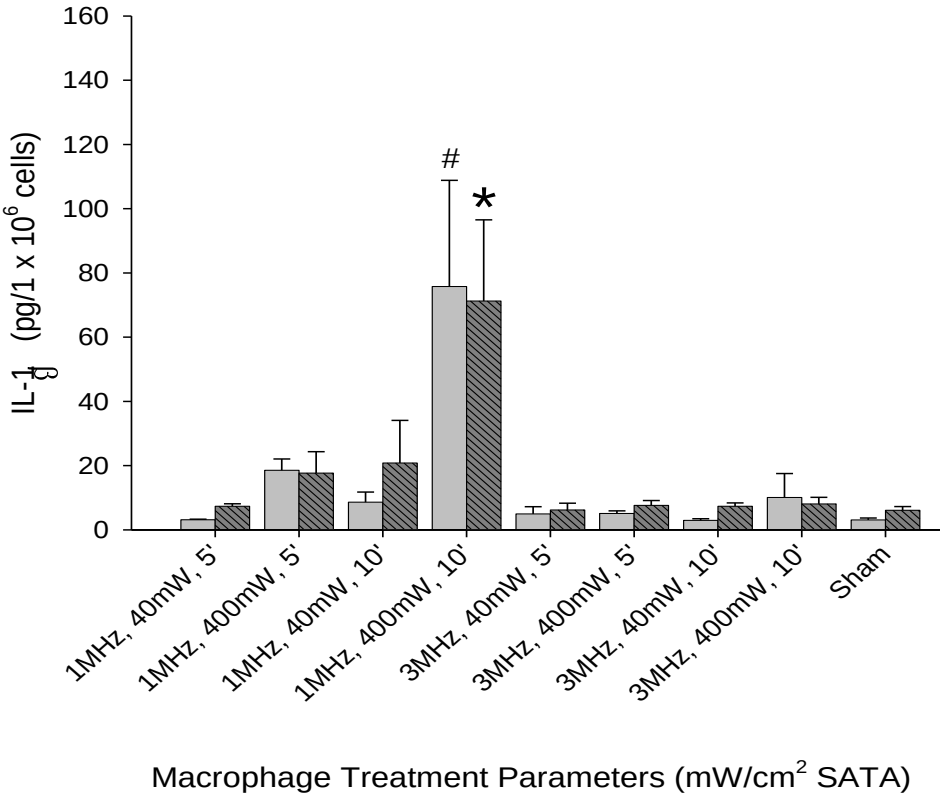
160
140
120
100
80
60
40
20
0
IL-1β (pg/1 x 10^6 cells)
#
*
1MHz, 40mW, 5'
1MHz, 400mW, 5'
1MHz, 40mW, 10'
1MHz, 400mW, 10'
3MHz, 40mW, 5'
3MHz, 400mW, 5'
3MHz, 40mW, 10'
3MHz, 400mW, 10'
Sham
Macrophage Treatment Parameters (mW/cm^2 SATA)

Figure 4.8. *IL-1β content in total cell lysates of untreated macrophages and conditioned media from macrophages exposed to various levels of TUS.* **A)** Total cell lysates from differentiated, untreated macrophages (2.5, 1.25 and 0.625 x 10^6 cells) were analyzed for IL-1β using ELISA, which determined pg/ml of IL-1β. The concentration of IL-1β is reported as IL-1β per 1 x 10^6 cells. IL-1β concentration ranged from 178.161 to 229.408 pg/1 x 10^6 cells, with a mean ± SEM of 197.648 ± 16.016. Data represents the mean ± SEM for n = 3 at each cell concentration. **B)** IL-1β released from 0.5 x 10^6 cells/ml (total of 2.5 x 10^6 cells plated) exposed to various levels of TUS and incubated for 10 minutes or 1-hour post-TUS. Release of IL-1β was significantly increased by TUS at 10-minutes post-TUS ($p= 0.005$, $F= 4.203$) and at 1 hour ($p= 0.004$, $F= 4.560$). Post hoc analysis revealed that TUS delivered at 1MHz, 400mW/cm^2 SATA, 20% PW, 10-minute treatment induced significantly greater IL-1β release ($p < 0.05$) when compared to all other TUS parameter sets at 10-minute and 1-hour incubation post-TUS, as indicated by # and *****. Data represents the mean ± SEM of picograms IL-1β released per 1 x 10^6 cells for n = 3 separate TUS experiments.

Figure 4.9

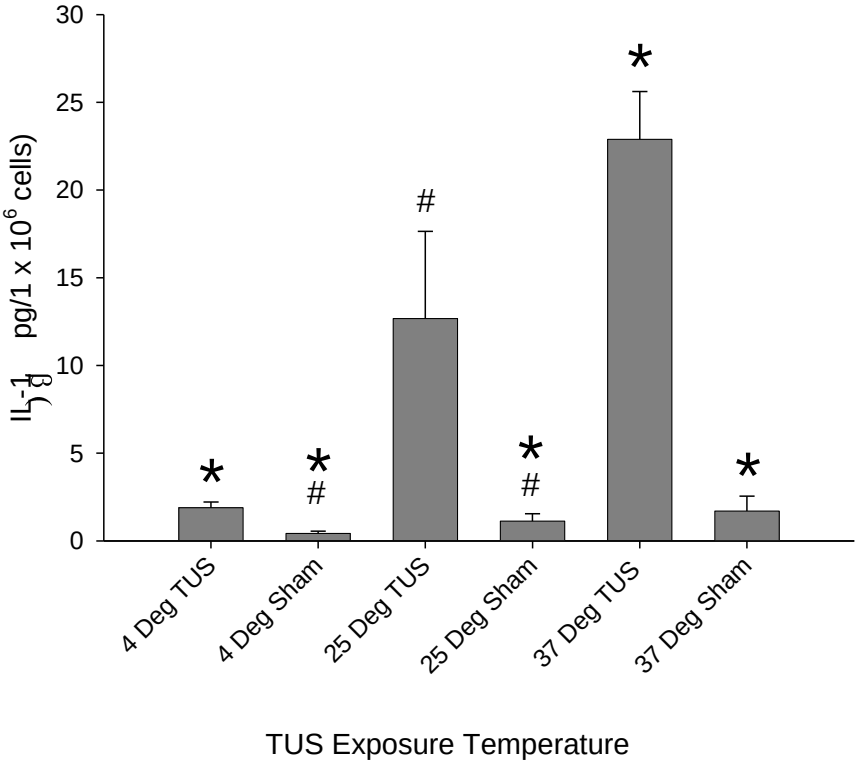
30
25
20
15
10
5
0
IL-1β pg/1 x 10^6 cells)
*
*
#
#
*
#
*
4 Deg TUS
4 Deg Sham
25 Deg TUS
25 Deg Sham
37 Deg TUS
37 Deg Sham
TUS Exposure Temperature

Figure 4.9. *IL-1β release from macrophages treated with TUS at variable temperatures.* Macrophages were treated for 10 minutes with sham TUS or TUS delivered at *1MHz, 400mW/cm^2 SATA, 20% PW* and incubated for 10-minutes post-exposure at 4°, 25° and 37°C. IL-1β release was compared between the groups of macrophages exposed to TUS at the variable temperatures. Macrophage release of IL-1β was affected by the TUS exposure and by the temperature of TUS exposure ($p < 0.001$, $F = 15.081$). Post hoc analysis indicated that macrophages released greater amounts of IL-1β when TUS (*1MHz, 400mW/cm^2 SATA, 10 minutes*) was applied at 37°C compared to sham treatments at each temperature and compared to TUS applied at 4°C, as indicated by *****, $p < 0.05$. IL-1β release following treatment at 25° was decreased compared 37°C treatment, but the trend was not statistically significant ($p = 0.08$). TUS applied at 25°C increased IL-1β release compared to sham treatments at 4° and 25°C, as indicated by **#**, $p < 0.05$. The trend of increased IL-1β release with TUS applied at 25°C compared to 37°C sham treatment was not statistically significant ($p = 0.055$). Data represents the mean ± SEM of $n = 3$ samples at each parameter set/temperature of TUS.

Discussion

TUS stimulates cellular activities that result in the release of various substances from cells in vitro. Monocytes and macrophages respond to TUS by release of cytokines and growth factors. Previously, we identified a set of specific TUS parameters (1MHz, 400mW/cm^2 SATA, 20% PW, 10-minute treatment) that induced the release of IL-1β from activated macrophages. In addition, we found that the macrophage response occurred within 10 minutes post-TUS. The goal of this investigation was to begin to characterize the possible cellular mechanism(s) responsible for the macrophage response to TUS using the treatment parameters identified in the earlier aspects of this series of investigations

Release from cells post TUS has been hypothesized to occur as a result of increased membrane permeability or enhanced metabolic processes of exocytosis or stimulation of protein synthesis and exocytosis [233]. The rapid release of IL-1β following TUS suggests that the response involved release of pre-formed protein rather than synthesis and release. This study analyzed TUS-induced release via two mechanisms, non-specific membrane permeabilization and exocytosis. LDH release and staining of intact and permeabilized membranes were used to assess non-specific permeabilization of cells. To explore exocytosis as a mechanism of response, the effect of varied temperature on TUS stimulation of IL-1β release was assessed. Because lowered temperature reduces many cellular metabolic processes, including Exocytosis [246], this method of analysis provided indirect evidence that exocytosis of IL-1β was stimulated by TUS.

LDH is an intracellular enzyme that is released from cells with damaged membranes and is used to identify cellular treatments that damage cell membranes [240,244].

Utilizing this marker, we found that membrane damage occurred in macrophages following exposure to the TUS parameter set (1MHz, 400mW/cm^2 SATA, 20% PW, 10-minute treatment) that stimulated release of IL-1β as evidenced by the increased levels of both LDH and IL-1β when macrophages were exposed to this TUS parameter set (Figs. 4.5, 4.8). Cell lysates from untreated macrophages plated at the same concentration as TUS-treated macrophages contained nearly ten-times the amount of LDH that was released due to TUS exposure (Fig. 4.6). This suggests that approximately 10% of treated cells had sufficient membrane damage to allow release of LDH into the culture media. However, it is possible that the 10% of total LDH release due to TUS represents non-specific permeabilization of all the cells so as to allow release of only a fraction of intracellular contents from all cells.

The extent of membrane permeabilization related to TUS exposure was also explored by directly examining cells following insonation. Using the fluorescent dyes calcein-AM and EthD-1, which identify healthy and membrane-damaged cells respectively, we found that TUS (1MHz, 400mW/cm^2 SATA, 20% PW, 10-minute treatment) induced a significant increase in cells with damaged membranes (Figs. 4.7). Quantification of cells with intact and damaged membranes revealed that approximately 5% more of the total cells treated with TUS using had membrane damage compared to sham treated cells. The total combined area from intact and damaged cells comprised approximately 94% of the total cell area measured from the unstained, gray-scaled images of the fluorescent stained cells. This indicates that there was a 5-6% under-estimation of the total area from the measurements of the fluorescent images. If the underestimation of

total area included only damaged cells that were not stained with EthD-1, the total percentage of damaged cells would approach 10-11% of cells. In this "worst case" scenario", this value is in the range of that we found in the analysis of LDH release compared to total LDH content in the experimental cells, lending further support to the conclusion that approximately 10% of the insonated cells had membrane damage.

Given the two analyses indicating approximately 10% of treated cells were permeabilized, we compared the release of IL-1β following TUS exposure to IL-1β content of untreated cells in order to estimate the portion of total IL-1β released from treated cells. Macrophage cell lysates contained 197.648 ± 16.016 pg IL-1β per 1 x 10^6 cells, and macrophages treated with the stimulatory TUS parameter set (1MHz, 400mW/cm^2 SATA, 20% PW, 10-minute treatment) released 75.774 ± 33.057 pg IL-1β per 1 x 10^6 cells. Comparing these two values, it appears that greater than one-third of the available IL-1β was released following TUS exposure (Fig. 4.8). This is substantially greater than what would be expected based on the permeabilization data that indicated damage to 10% of the cells. Thus, it appears that only a portion of IL-1β release was related to permeabilization of the cells, with the remaining portion of IL-1β release was due to stimulation of a form of cell-controlled exocytosis.

To investigate whether TUS induced metabolic cellular changes that may have contributed to IL-1β release, macrophages were exposed to TUS (1 MHz, 400 mW/cm^2 SATA, 20% PW, 10-minutes) at various temperatures (4°, 25° and 37° C). At temperatures below 37°C metabolic process are slowed [245,246], therefore, if IL-1β release

was in part due to cell-mediated metabolic processes, release following TUS would be reduced at the lower temperatures. The results confirmed this hypothesis. Compared to 37°C, IL-1β release was significantly reduced at 4°C and there was a trend towards reduced release at 25° C indicating that decreased temperature attenuated the effects of TUS on macrophages, most likely due to decreased physiological activity of cells associated with decreased temperatures (Fig 4.9). In support of this hypothesis, decreased IL-1β release from LPS-stimulated macrophages after incubation for two hours below physiological temperatures (32° C) compared to 37°C has been reported [259]. LPS is thought to stimulate several cell signaling mechanisms including tyrosine kinases, mitogen-activated protein kinase C, protein kinase A, G-proteins, and microtubules which can induce secretory responses [247-249].

One confounding factor in the data from macrophages exposed to TUS at different temperature was identified when IL-1β release due to TUS from the two separately conducted macrophage-TUS experiments was compared. In the normal-temperature TUS experiments, macrophages released 75.774 ± 33.057 pg IL-1β per 1 x 10^6 cells IL-1β (Fig. 4.6B), while in the subsequent variable-temperature experiments macrophages stimulated with the same TUS parameters (1 MHz, 400 mW/cm^2 SATA, 20% PW, 10-minutes) at physiological temperatures (37°C) released 22.889 ± 2.723 pg IL-1β per 1 x 10^6 cells (Fig. 4.9). This lower level of release represents nearly 11% of the total cellular IL-1β (Fig. 4.8A), which falls within the range of non-specific permeabilization indicated by LDH release and cell-staining data (Figs. 4.5, 4.7). There was a minimal difference in

release of IL-1β from the sham cells in the two experiments 3.096 ± 0.566 (mean ± SEM) compared to 1.703 ± 0.844 pg IL-1β per 1 x 10^6 cells, suggesting that the macrophages were overall less responsive to TUS, likely resulting in the decreased IL-1β release noted for insonated macrophages. Analysis of TUS intensity from the sonication device was maintained throughout experimentation, thus we concluded that the difference in response was not related to reduced ultrasound energy. Specifically, the Omnisound 3000 delivered 374.4 ± 4.1 mW/cm^2 over the course of the variable temperature experiments compared to 380 ± 3.347 mW/cm^2 from normal temperature experiments (Appendix B, Table B3), demonstrating a minimal reduction of TUS energy delivered for 400mW/cm^2.

Based on the results of this study, it appears that TUS exposure at (1 MHz, 400 mW/cm^2 SATA, 20% PW, 10-minutes) results in increased release of cytokines via both increased cellular permeabilization as well as through metabolic mechanisms. At least four metabolic mechanisms have been proposed for IL-1β release from macrophages, these include release of multivesicular bodies as exosomes, Ca^{2+}-dependent release of lysosomes and microvesicle shedding of membrane blebs, and direct release through the membrane via specific membrane transporters [250]. Given that changes in calcium flux in response has been reported in fibroblasts, chondrocytes, and epithelial cells in response to TUS exposure [49,50,65], it is reasonable to suspect that calcium-mediated mechanisms may be involved in IL-1β release from macrophages exposed to TUS. U937 macrophages do contain cell membrane-gated potassium (K+) channels [251-253]. However, additional research is need to determine whether a Ca^{2+} mediated process or some other metabolic

process is responsible for the IL-1β release from macrophages in response to TUS that is not accounted for by the increased permeability.

Conclusion

IL-1β release from macrophages in response to TUS appears to be due to a combination of non-specific permeabilization and some form of cell-mediated release mechanisms. Non-specific permeabilization was directly assessed using metabolic and cytological assays, while specific cell-mediated mechanisms were indirectly assessed by decreased response at sub-physiological temperatures. Additional experimentation is needed to determine the specific cell mediated mechanisms of IL-1β release from macrophages following exposure to TUS.

Chapter 5

DISCUSSION and CONCLUSION: Mechanism of Macrophage Response to TUS

The data presented here indicates that macrophages can play a role in TUS-stimulated tissue healing. Macrophages responded to TUS exposure at 1 MHz, 400mW/cm^2 SATA, 20% PW, 10-minute treatment by releasing IL-1β and VEGF. These secretory peptides are paracrine factors involved with control of inflammation and angiogenesis, which are integral activities for appropriate repair of damaged tissue [163,199]. Release of both mediators occurred within 10-minutes of TUS-exposure, and this immediate response is most likely due to release of preformed products. Macrophages are highly secretory cells, especially in the wound-healing milieu [164,168], and stimulation of mediator release by TUS could provide an acceleration of processes normally controlled by wound macrophages.

Initially, fibroblast proliferation was measured following incubation in media conditioned by TUS-stimulated macrophages. TUS did not stimulate any fibroblast mitogen release at any parameter set tested, as assessed by 24 and 48-hours of fibroblast incubation in macrophage conditioned media. This is contrary to the findings of Young and Dyson who reported that TUS-stimulated macrophage release of fibroblast mitogen within 30-minutes of treatment when TUS was delivered at 1MHz, 500mW/cm^2, SATA,

CW, 5-minutes [161]. While we could not confirm macrophage release of fibroblast mitogens, the findings of IL-1β and VEGF release within 10 minutes of TUS-exposure in the same cell type (U937 cells) studied by Young and Dyson does appear to support the idea of TUS-stimulated release of pre-formed products that was posited by Young and Dyson.

Methodological differences in the use of undifferentiated macrophages and CW-TUS compared to use of differentiated macrophages and PW-TUS in the current study may be the reason for the lack of fibroblast mitogen release noted here. Once differentiated, macrophages assume a different phenotype from monocyte precursors and their overall cellular activity is altered [168]. Indeed U937 cells differentiated with agents like PMA have been shown to respond differently to subsequent stimuli [254]. Thus, it is plausible that the PMA-differentiated macrophages assumed a phenotype that was unable to provide a mitogenic signal for fibroblasts in the short post-TUS time frame. Direct comparison of the response of U937 macrophages in various stages of differentiation to TUS would provide significant insight into this aspect of TUS stimulation.

Differences in cellular response to TUS have been attributed to different duty cycles [118]. However, no additional in vitro investigations on duty cycle have been reported, therefore there is no clear indication of what particular duty cycle is associated with stimulation of particular cellular functions. It may be that cells respond to PW-TUS signals differently than CW-TUS, which could result in a different release response. In support of this hypothesis, a study of the effect of variable TUS duty cycles indicated that

increased cell permeabilization is directly correlated to increasing duty cycle suggesting differential cellular response to duty cycle [238].

On the other hand, the difference in response to duty cycle could be a function of overall TUS energy transmitted to the cells. The fact that 5-minute exposures to TUS at 1 MHz, 400mW/cm^2 SATA, 20% PW in the current study did not induce a significant release supports this hypothesis. The stimulatory TUS at 10-minutes delivered twice as much energy compared to 5-minute treatment, which suggests that some energy threshold was required to generate the response reported in this investigation. In vitro investigations reporting TUS-stimulation have utilized exposure times ranging from 3 to 20 minutes [8,112,162,177]. However, within study comparison of cellular response based on treatment duration have not yielded consistent results of increased response due to increase energy applied [7,98,112].

TUS has been reported to induce membrane permeabilization [236,239] which could result in non-specific dumping of intracellular contents. The current investigation confirms this hypothesis of TUS action. Given the immediate release response, we analyzed macrophages for evidence of non-specific membrane permeabilization. To accomplish this, conditioned media was analyzed for the presence of LDH, and TUS-treated macrophages were visualized with fluorescent dyes that identify intact and membrane-damaged cells. The same stimulatory TUS parameters for IL-1β and VEGF release also induced LDH release (Figs 3.1, 3.2, 4.5). This finding indicates that non-specific permeabilization was involved in the macrophage response. Similar to IL-1β, significant levels of LDH were released at 10 minutes post-TUS without additional

measurable release at 1 hour. Further analysis of LDH content in experimental macrophages revealed that the extent of LDH release stimulated by TUS was approximately 10% of the total content in untreated macrophages (Fig. 4.6). This indicates either a low level of LDH release from all cells or a small fraction of the total cells being permeabilized.

Analysis of fluorescently-stained cells revealed that approximately 5% of cells were permeabilized by TUS exposure (Figs 4.2-4.4, 4.7). Quantification of stained cells underestimated the total cell area by nearly 6% (data not shown). As such, the data is presented with the recognition that up to 11% of the cells were actually permeabilized. Because that value was nearly the same as the percentage of LDH release, it appears that the staining data provides confirmation of permeabilization identified by LDH release. Furthermore, the staining data suggests that a limited number of cells were permeabilized as opposed to slight permeabilization of all cells.

In efforts to identify the mechanism of the immediate release, we chose to investigate further the mechanism of IL-1β release. VEGF release also appeared to be non-specifically increased during the incubation period from 10-minutes to 1-hour (Fig. 3.3). The fact that VEGF release was induced at the stimulatory parameters, and that it continued to be released by all samples including sham indicates that TUS can enhance an already active cell processes. Given the apparent constitutive release of VEGF, further analysis of this growth factor would likely have been confounded by the constantly active cells. TUS-induced IL-1β release appeared within 10-minutes and did not change over the remainder of the incubation period. Like VEGF release, this response indicated that TUS

induced an immediate cellular response (Figs. 3.1, 4.8). Because IL-1β release did not continue to any measurable extent over the final 50-minutes of incubation, analysis of mechanism of this cytokine provided a more discreet avenue of mechanism investigation.

Comparison of IL-1β release stimulated by TUS to total cellular content of IL-1β revealed that approximately one-third of measurable IL-1β was released in response to TUS (Fig. 4.8). This fraction of the total represents a larger portion than was expected based on the permeabilization data, and presents the possibility that another mechanism of release was stimulated by TUS. TUS-exposure at variable temperatures (4°, 25° and 37° C) revealed an inhibition of release that was increasingly pronounced as temperatures were lowered to 4° C (Fig. 4.9). Since lowered temperatures generally decrease cellular metabolic processes [245,255], which includes exocytosis, the inhibition at decreased temperature indicates that some form of exocytosis of IL-1β was likely stimulated by TUS.

Mechanisms of IL-1β exocytosis include release of multivesicular bodies as exosomes, Ca^{2+}-dependent release of lysosomes, Ca^{2+}-dependent microvesicle shedding of membrane blebs, and direct release through the membrane via specific membrane transporters [249,250]. TUS-stimulated exocytosis has been reported to be dependent on Ca^{2+} for chondrocytes and fibroblasts [49,50]. Since macrophage exocytosis is partially dependent on Ca^{2+}, it is reasonable to hypothesize that TUS stimulated either lysosome release or microvesicular shedding. However, cellular response to TUS is variable among cells, evidenced by reports of response involving angiotensin II receptors, phosphorylation of extracellular signal-regulated kinase (ERK) and increased expression of integrins (α2, α5,

and β1) in osteoblasts [125,256]. As further evidence of the plethora of possible TUS transducers in cells, fluid shear stress, which is likely the biophysical mechanism of TUS on cells, activates membrane-bound G-proteins creating second messenger signaling in endothelial cells [257]. Macrophages transduction of TUS energy by any of these mechanisms has not been directly explored, thus further directed experimentation is needed to confirm a Ca^{2+}-regulated mechanism of macrophage response.

TUS delivered at 1 MHz, 400mW/cm^2 SATA, 20% PW stimulates release of paracrine factors associated with tissue healing. Mechanistically, macrophages responded to TUS through at least two mechanisms; non-specific permeabilization and some form of cell-mediated exocytosis. Cell permeabilization is a well-known result of TUS exposure, however, immediate cell-mediated exocytosis in response to TUS has not been previously reported. Flux of calcium ions across the membrane is a possible mechanism of macrophage response, given previous reports of Ca^{2+}-regulated secretion from fibroblasts, chondrocytes and keratinocytes. Continued research regarding the mechanism of release response of macrophages should be focused on identifying the specific mechanism of IL-1β release, as well as characterizing the cellular response based on the differentiation state of the macrophages.

The current investigation explored only one facet of macrophage function during wound healing, release of cytokines and growth factors. Given the numerous functions of macrophages during healing (i.e., phagocytosis, release of proteases for matrix degradation, release of chemokines, induction of neutrophil apoptosis), the effects of TUS on those other aspects of macrophage activity should be explored. In addition, in vitro

assay of macrophage response to TUS cannot simulate the wound healing environment where many environmental factors influence cell activity and function. As such, the importance of macrophage function in TUS-treated, healing tissue should be explored using in vivo models where macrophages are depleted or rendered non-functional.

Lastly, since all experimental macrophages were induced to differentiate using PMA, its role in the current results should be acknowledged. In U937 cells, PMA arrests cell proliferation and stimulates expression of macrophage-like characteristics, but it does not completely recapitulate naturally occurring monocyte-to-macrophage differentiation [175,176]. As described in a biochemistry review by Nelson and Alkon (2009), PMA is one of the most potent of group of compounds that stimulates protein kinase C activation, which results in various changes in cellular function, including DNA transcription, protein synthesis, cell growth, cell proliferation and differentiation [260]. In addition, PKC activation leads to temporary down-regulation of PKC within the cell. This change renders second messenger systems within the cell less responsive to signaling, and as such can affect the cell's response to stimuli. Given its potency, it is reasonable to believe that PMA-induced activation of PKC likely affected cell functions beyond the intended use in the current investigation for monocyte-to-macrophage differentiation. As such, it is possible that the response of macrophages to TUS in the current series of experiments is partially due to alteration in PKC-regulated cell activities. Investigations using various differentiation agents and comparing macrophage response to TUS are be important for understanding the possible role PMA-induced activity may have played in the macrophage response to TUS reported here.

REFERENCES

REFERENCES

1. Warden SJ, McMeeken JM. Ultrasound Usage and Dosage in Sports Physiotherapy. *Ultrasound in Medicine and Biology.* 2002;28:1075-1080.

2. Bryant J, Milne R. Therapeutic Ultrasound in Physiotherapy. *Wessex Institute Development and Evaluation Committee Report No.: 90.* 1998; 1-21.

3. Byl NN, McKenzie AL, West JM, Whitney JD, Hunt TK, Scheuenstuhl HA. Low-Dose Ultrasound Effects on Wound Healing: A Controlled Study With Yucatan Pigs. *Archives of Physical Medicine and Rehabilitation.* 1992;73:656-664.

4. Sparrow KJ, Finucane SD, Owen JR, Wayne JS. The Effects of Low-Intensity Ultrasound on Medial Collateral Ligament Healing in the Rabbit Model. *The American Journal of Sports Medicine.* 2004;33:1048-1056.

5. Ng COY, Ng GYF, See EKN, Leung MCP. Therapeutic Ultrasound Improves Strength of Achilles Tendon Repair In Rats. *Ultrasound in Medicine and Biology.* 2003;29:1501-1506.

6. Yang K-H, Park S-J. Stimulation of Fracture Healing in a Canine Ulna Full-defect Model by Low-Intensity Pulsed Ultrasound. *Yonsei Medical Journal.* 2001;42:503-508.

7. Doan N, Reher P, Meghji S, Harris M. In Vitro Effects of Therapeutic Ultrasound on Cell Proliferation, Protein Synthesis, and Cytokine Production by Human Fibroblasts, Osteoblasts, and Monocytes. *Journal of Oral and Maxillofacial Surgery.* 1999;57:409-419.

8. Ramirez A, Schwane JA, McFarland C, Starcher B. The Effect of Ultrasound On Collagen Synthesis and Fibroblast Proliferation In Vitro. *Medicine and Science in Sports and Exercise.* 1997;29:326-332.

9. Sun J-S, Hong R-C, Chang WH, Chen L-T, Lin F-H, Liu H-C. In Vitro Effects of Low-Intensity Ultrasound Stimulation on the Bone Cells. *Journal of Biomedical Materials Research.* 2001;57:449-456.

10. Leung KS, Cheung WH, Zhang C, Lee KM, Lo HK. Low Intensity Pulsed Ultrasound Stimulates Osteogenic Activity of Human Periosteal Cells. *Clinical Orthopedics and Related Research.* 2004;418:253-259.

11. Parvizi J, Wu C-C, Lewallen DG, Greenleaf JF, Bolander ME. Low-Intensity Ultrasound Stimulates Proteoglycan Synthesis in Rat Chondrocytes by Increasing Aggrecan Gene Expression. *Journal of Orthopaedic Research.* 1999;17:488-494.

12. Cook SD, Salkeld SL, Popich-Patron LS, Ryaby JP, Jones DG, Barrack RL. Improved Cartilage Repair After Treatment With Low-Intensity Pulsed Ultrasound. *Clinical Orthopaedics and Related Research.* 2001;391S:S231-S234.

13. Leung MC, Ng GY, Yip KK. Effect Of Ultrasound on Acute Inflammation of Transected Medial Collateral Ligaments. *Archives of Physical Medicine and Rehabilitation.* 2004;85:963-966.

14. Maxwell L. Therapeutic Ultrasound: Its Effect on the Cellular and Molecular Mechanisms of Inflammation and Repair. *Physiotherapy.* 1992;78:421-425.

15. Fu SC, Sum WT, Hung LK, Wong MW-N, Qin L, Chan KM. Low-Intensity Pulsed Ultrasound on Tendon Healing. A Study of the Effect of Treatment Duration and Treatment Initiation. *The American Journal of Sports Medicine.* 2008;36:1742-1749.

16. Warden SJ, Avin KG, Beck EM, DeWolf ME, Martin KM. Low-Intensity Pulsed Ultrasound Accelerates and a Nonsteroidal Anti-Inflammatory Drug Delays Knee Ligament Healing. *The American Journal of Sports Medicine.* 2006;34:1094-1102.

17. Takikawa S, Matsui N, Kokubu T, Tsunoda M, Fujoika H, Mizuna K, Azuma, Y. Low-Intensity Pulsed Ultrasound Initiates Bone Healing in Rat Nonunion Fracture Model. *Journal of Ultrasound in Medicine.* 2001;20:197-205.

18. Kristiansen TK, Ryaby JP, McCabe J, Frey JJ, Roe LR. Accelerated Healing of Distal Radius Fractures with the Use of Specific, Low-Intensity Ultrasound. A Multicenter, Prospective, Randomized, Double-Blind, Placebo-Controlled Study. *Journal of Bone and Joint Surgery.* 1997;79A:961-973.

19. Cook SD, Ryaby JP, McCabe J, Frey JJ, Heckman JD, Kristiansen TK. Acceleration of Tibia and Distal Radius Fracture Healing in Patients Who Smoke. *Clinical Orthopaedics and Related Research.* 1997;337:198-207.

20. Gebauer GP, Lin SS, Beam HA, Vieira P, Parsons JR. Low-Intensity Pulsed Ultrasound Increases the Fracture Callus Strength in Diabetic BB Wistar Rats But Does Not Affect Cellular Proliferation. *Journal of Orthopaedic Research.* 2002;20: 587-592.

21. Ricardo M. The Effect of Ultrasound on the Healing of Muscle-Pediculated Bone Graft in Scaphoid Non-Union. *International Orthopaedics.* 2006;30:123-127.

22. Azuma Y, Ito M, Harada Y, Takagi H, Ohta T, Jingushi S. Low-Intensity Pulsed Ultrasound Accelerates Rat Femoral Fracture Healing by Acting on the Various Cellular Reactions in the Fracture Callus. *Journal of Bone and Mineral Research.* 2001;16:671-680.

23. Enwemeka CS, Rodriguez O, Mendosa S. The Biomechanical Effects of Low-Intensity Ultrasound on Healing Tendons. *Ultrasound in Medicine and Biology.* 1990;16:801-807.

24. Byl NN, McKenzie A., Wong T, West J, Hunt TK. Incisional Wound Healing: A Controlled Study of Low and High Dose Ultrasound. *Journal of Orthopaedic & Sports Physical Therapy.* 1993;18:619-628.

25. Warden SJ, Fuchs RK, Kessler CK, Avin KG, Cardinal RE, Stewart RL. Ultrasound Produced by a Conventional Therapeutic Ultrasound Unit Accelerates Fracture Repair. *Physical Therapy.* 2006;86:1118-1127.

26. Karnes JL, Burton HW. Continuous Therapeutic Ultrasound Accelerates Repair of Contraction-Induced Skeletal Muscle Damage in Rats. *Archives of Physical Medicine and Rehabilitation.* 2002;83:1-4.

27. Chang C-J, Hsu S-H. The Effects of Low-Intensity Ultrasound On Peripheral Nerve Regeneration In Poly(DL- Lactic Acid-Co-Glycolic Acid) Conduits Seeded With Schwann Cells. *Ultrasound in Medicine and Biology.* 2004;30:1079-1084.

28. Sparrow KJ. Therapeutic Ultrasound. *Modalities for Therapeutic Intervention*. 4th. ed. Philadelphia, PA.: FA Davis Co.; 2005:79-96.

29. Miller MW, Miller DL, Brayman AA. A Review of In Vitro Bioeffects of Inertial Ultrasonic Cavitation From a Mechanistic Perspective. *Ultrasound in Medicine and Biology.* 1996;22:1131-1154.

30. Barnett SB, Rott HD, ter Haar GR, Ziskin MC, Maeda K. The Sensitivity of Biological Tissue to Ultrasound. *Ultrasound in Medicine and Biology.* 1997;23:805-812.

31. Baker KG, Robertson VJ, Duck FA. A Review of Therapeutic Ultrasound: Biophysical Effects. *Physical Therapy.* 2001;81:1351-1358.

32. Dalecki D. Mechanical Bioeffects of Ultrasound. *Annual Review of Biomedical Engineering.* 2004;6:229-248.

33. Feril LB, Kondo T. Biological Effects of Low Intensity Ultrasound: The Mechanism Involved, and its Implications on Therapy and Biosafety of Ultrasound. *Journal of Radiation Research.* 2004;45:479-489.

34. Zderic V, Keshavarzi A, Andrew MA, Vaezy S, Martin RW. Attenuation of Porcine Tissues In Vivo After High-Intensity Ultrasound Treatment. *Ultrasound in Medicine and Biology.* 2004;30:61-66.

35. Speed CA. Review: Therapeutic Ultrasound in Soft Tissue Lesions. *Rheumatology*. 2001; 40:1331-1336.

36. Draper DO, Castel JC, Castel D. Rate of Temperature Increase in Human Muscle During 1MHz and 3MHz Continuous Ultrasound. *Journal of Orthopaedic and Sports Physical Therapy.* 1995;22:142-150.

37. Warden SJ. A New Direction for Ultrasound Therapy in Sports Medicine. *Sports Medicine.* 2003;33:95-107.

38. Barnett SB, Ter Haar GR, Ziskin MC, Nyborg WL, Maeda K, Bang J. Current Status of Research on Biophysical Effects of Ultrasound. *Ultrasound in Medicine and Biology.* 1994;20:205-218.

39. Chetverikova EP, Pashovkin TN, Rosanova NA, Sarvazyan AP, Williams AR. Interaction of Therapeutic Ultrasound With Purified Enzymes In Vitro. *Ultrasonics.* 1985;23:183-188.

40. Lehman JF, DeLateur B.J. Therapeutic Heat. *Therapeutic Heat and Cold*. 4th ed. Baltimore: Williams & Wilkins; 1990; 590-632.

41. Lehmann JF, DeLateur BJ, Warren CG, Stonebridge JB. Heating of Joint Structures by Ultrasound. *Archives of Physical Medicine and Rehabilitation.* 1968; 49(1) 28-30.

42. Draper DO, Schulthies S, Sorvisto P, Hautala A-M. Temperature Changes in Deep Muscles of Humans During Ice and Ultrasound Therapies: An In Vivo Study. *Journal of Orthopaedic and Sports Physical Therapy.* 1995;21:153-157.

43. Cambier D, D'Herde K, Witvrouw E, Beck M, Soenens S, Vanderstraeten G. Therapeutic Ultrasound: Temperature Increase at Different Depths by Different Modes in a Human Cadaver. *Journal of Rehabilitation Medicine.* 2001;33:212-215.

44. Demmink JH, Helders PJM, Hobaek H, Enwemeka C. The Variation of Heating Depth With Therapeutic Ultrasound Frequency in Physiotherapy. *Ultrasound in Medicine and Biology.* 2003;29:113-118.

45. Usuba M, Miyanaga Y, Miyakawa S, Maeshima T, Shirasaki Y . Effect of Heat in Increasing the Range of Knee Motion After the Development of a Joint Contracture: An Experiment With an Animal Model. *Archives in Physical Medicine and Rehabilitation.* 2006;87:247-253.

46. Reed BV, Ashikaga T, Fleming BC, Zimny NJ. Effects of Ultrasound and Stretch on Knee Ligament Extensibility. *Journal of Orthopaedic and Sports Physical Therapy.* 2000;30:341-347.

47. Wessling KC, DeVane DA, Hylton CR. Effects of Static Stretch Versus Static Stretch and Ultrasound Combined on Triceps Surae Muscle Extensibility in Healthy Women. *Physical Therapy.* 1987;67:674-679.

48. Dyson M. Non-thermal Cellular Effects of Ultrasound. *British Journal of Cancer.* 1982; 45:165-171.

49. Parvizi J, Parpura V, Greenleaf JF, Bolander ME. Calcium Signaling is Required for Ultrasound-Stimulated Aggrecan Synthesis by Rat Chondrocytes. *Journal of Orthopaedic Research.* 2002;20:51-57.

50. Mortimer AJ, Dyson M. The Effect of Therapeutic Ultrasound on Calcium Uptake in Fibroblasts. *Ultrasound in Medicine and Biology.* 1988;14:499-506.

51. Samal AB, Adzerikho ID, Mrochek AG, Loiko EN. Platelet Aggregation and Change in Intracellular Ca^{2+} Induced by Low Frequency Ultrasound In Vitro. *European Journal of Ultrasound.* 2000;11:53-59.

52. Miyamoto K, An HS, Sa RL, Akeda K, Okuma M, Otten L, Thonar E, Masuda K. Exposure to Pulsed Low Intensity Ultrasound Stimulates Extracellular Matrix Metabolism of Bovine Intervertebral Disc Cells Cultured in Alginate Beads. *Spine.* 2005;30:2398-2405.

53. Tsai WC, Chen JYS, Pang JHS, Hsu CC, Chieh LW. Therapeutic Ultrasound Stimulation of Tendon Cell Migration. *Connective Tissue Research.* 2008;49:367-373.

54. Maxwell L, Collecutt T, Gledhill M, Sharma S, Edgar S, Gavin JB. The Augmentation of Leucocyte Adhesion to Endothelium By Therapeutic Ultrasound. *Ultrasound in Medicine and Biology.* 1994;20:383-390.

55. Miller DL, Thomas RM, Frazier ME. Single Strand Breaks in CHO Cell DNA Induced By Ultrasonic Cavitation In Vitro. *Ultrasound in Medicine and Biology.* 1991;17:401-6.

56. Kaufman GE. Mutagenicity Of Ultrasound In Cultured Mammalian Cells. *Ultrasound in Medicine and Biology.* 1985;11:487-501.

57. Lawrie A, Brisken AF, Francis SE, Wyllie, D, Kiss-Toth, E, Qwarnstrom, EE, Dower SK, Crossman, DC, Newman CM. Ultrasound-Enhanced Transgene Expression in Vascular Cells is Not Dependent Upon Cavitation-Induced Free Radicals. *Ultrasound in Medicine & Biology.* 2003;29:1453-1461.

58. Mitragotri S, Edwards DA, Blankschtein D, Langer R. A Mechanistic Study of Ultrasonically-Enhanced Transdermal Drug Delivery. *Journal of Pharmaceutical*

Sciences. 1995;84:697-706.

59. Dinno M, Crum LA, Wu J. The Effect of Therapeutic Ultrasound on Electrophysiological Parameters of Frog Skin. *Ultrasound in Medicine and Biology.* 1989;15:461-470.

60. Webster DF, Pond JB, Dyson M, Harvey W. The Role of Cavitation in the in Vitro Stimulation of Protein Synthesis in Human Fibroblasts By Ultrasound. *Ultrasound in Medicine and Biology* . 1978;4:343-351.

61. Ter Haar GR, Daniels S. Evidence for Ultrasonically Induced Cavitation In Vivo. *Physics in Medicine and Biology.* 1981;26:1145-1149.

62. Ter Haar GR, Hopewell JW. Ultrasonic Heating of Mammalian Tissues In Vivo. *British Journal of Cancer.* 1982;45:65-67.

63. Gross DR, Miller DL, Williams AR. A Search for Ultrasonic Cavitation Within The Canine Cardiovascular System. *Ultrasound in Medicine and Biology.* 1985;11:85-97.

64. Harle J, Mayia F, Olsen I, Salih V. Effects of Ultrasound on Transforming Growth Factor-β Genes In Bone Cells. *European Cells and Materials.* 2005;10:70-77.

65. Al-Karmi AM, Dinno MA, Stoltz DA, Crum LA, Matthews JC. Calcium and The Effects of Ultrasound on Frog Skin. *Ultrasound in Medicine and Biology.* 1994;20:73-81.

66. Adinno MA, Al-Karmi AM, Stoltz DA, Matthews JC, Crum LA. Effect of Free Radical Scavengers on Changes in Ion Conductance During Exposure to Therapeutic Ultrasound. *Membrane Biochemistry.* 1993;10:237-247.

67. Pickworth MJW, Dendy PP, Leighton TG, Walton AJ. Studies of the Cavitational Effects of Clinical Ultrasound by Sonoluminescence: 2. Thresholds for Sonoluminescence From a Therapeutic Ultrasound Beam and The Effect of Temperature and Duty Cycle. *Physics in Medicine and Biology.* 1988;33:1249-1260.

68. Rubin C, Bolander M, Ryaby JP, Hadjiargyrou M. Current Concepts Review: The Use of Low-Intensity Ultrasound to Accelerate the Healing of Fractures. *Journal of Bone and Joint Surgery.* 2001;83A:259-270.

69. Yang K-H, Parvizi J, Wang S-J, Lewallen DG, Kinnick RR, Greenleaf AF, Bolander, ME. Exposure to Low-Intensity Ultrasound Increases Aggrecan Gene Expression in a Rat Femur Fracture Model. *Journal of Orthopaedic Research.* 1996;14:802-809.

70. Hantes ME, Mavrodontidis AN, Zalavras CG, Karantanas AH, Karachalios T, Malizos KN. Low-Intensity Transosseous Ultrasound Accelerates Osteotomy Healing In a Sheep Fracture Model. *The Journal of Bone and Joint Surgery* . 2004;86A:2275-2282.

71. Aynaci O, Onder C, Piskin A, Ozoran Y. The Effect of Ultrasound on the Healing of Muscle-Pediculated Bone Graft in Spinal Fusion. *Spine.* 2002;27:1531-1535.

72. Glazer PA, Heilmann MR, Lotz JC, Bradford DS. Use of Ultrasound in Spinal Arthrodesis: A Rabbit Model. *Spine.* 1998;23:1142-1148.

73. Cook SD, Salkeld SL, Patron LP, Ryaby JP, Whitecloud TS . Low-intensity Pulsed Ultrasound Improves Spinal Fusion. *The Spine Journal.* 2001;1:246-254.

74. Erdogan O, Esen E, Ustün Y, Kürkcü M, Akova T, Gönlüsen G, Uysal H, Cevlik F. Effect of Low-Intensity Pulsed Ultrasound on Healing of Mandibular Fractures: An Experimental Study in Rabbits. *Journal of Oral and Maxillofacial Surgery.* 2006;64:180-188.

75. Sakurakichi K, Tsuchiya H, Uehara K, Yamashiro T, Tomita K , Azuma Y. Effects of Timing of Low-Intensity Pulsed Ultrasound on Distraction Osteogenesis. *Journal of Orthopedic Research.* 2004;22:395-403.

76. Heckman JD, Ryaby JP, McCabe J, Frey JJ, Kilcoyne RF. Acceleration of Tibial Fracture-Healing by Non-Invasive, Low-Intensity Pulsed Ultrasound. *The Journal of Bone and Joint Surgery.* 1994;76A:26-34.

77. Leung K-S, Lee WS, Tsui HF, Lui PPL, Cheung WH. Complex Tibial Fracture Outcomes Following Treatment With Low-Intensity Pulsed Ultrasound. *Ultrasound in Medicine and Biology.* 2004;30:389-395.

78. Day SM, Ostrum RF, Chao EYS, Rubin CT, Aro HT, Einhorn TA. Bone Injury, Regeneration and Repair. *Orthopaedic Basic Science: Biology and Biomechanics of the Musculoskeletal System.* 2nd ed. Rosemont, IL: American Academy of Orthopaedic Surgeons; 2000:371-399.

79. Nolte PA, Van der Krans A, Patka P, Janssen IM, Ryaby JP, Albers GH. Low-Intensity Pulsed Ultrasound in the Treatment of Nonunions. *The Journal of Trauma.* 2001;51:693-702.

80. Gebauer D, Mayr E, Orthner E, Ryaby JP. Low-Intensity Pulsed Ultrasound: Effects on Nonunions. *Ultrasound in Medicine and Biology.* 2005;31:1391-1402.

81. Warden SJ, Bennell KL, Matthews B, Brown DJ, McMeeken M, Wark JD. Efficacy of Low-Intensity Pulsed Ultrasound in the Prevention of Osteoporosis

Following Spinal Cord Injury. *Bone.* 2001;29:431-436.

82. Yang R-S, Chen Y-Z, Huang T-H, et al. The Effects of Low-Intensity Ultrasound on Growing Bone After Sciatic Neurectomy. *Ultrasound in Medicine and Biology.* 2005;31:431-437.

83. Wiltink A, Nijweide PJ, Oosterbaan WA, Hekkenberg RT, Helders PJM. Effect of Therapeutic Ultrasound on Endochondral Ossification. *Ultrasound in Medicine and Biology.* 1995;21:121-127.

84. Nolte PA, Klein-Nulend J, Albers GHR, Marti RK, Semeins CM, Goei SW, Burger EH. Low-Intensity Ultrasound Stimulates Endochondral Ossification In Vitro. *Journal of Orthopaedic Research.* 2001;19:301-307.

85. Sun J-S, Tsuang Y-H, Lin F-H, Liu H-C, Tsai C-Z. Bone Defect Healing Enhanced by Ultrasound Stimulation: An In Vitro Tissue Culture Model. *Journal of Biomedical Materials Research.* 1999;46:253-261.

86. Bolander ME. Regulation of Fracture Repair by Growth Factors. *Proceedings of the Society for Experimental Biology and Medicine.* 1992;200:165-170.

87. Dimitriou R, Eleftherios T, Giannoudis PV. Current Concepts of Molecular Aspects of Bone Healing. *Injury.* 2005;36:1392-1404.

88. Kloth LC, McCulloch JM. The Inflammatory Response to Wounding, in *Wound Healing: Alternatives in Management.* Second ed. Philadelphia, PA: F.A. Davis Company; 1995; 3-15.

89. Evans C. Cytokines and the Role They Play in the Healing of Ligaments and Tendons. *Sports Medicine.* 1999;28:71-76.

90. Li JK, Chang WH, Lin JC, Ruaan R.C., Liu H.C., Sun JS. Cytokine Release From Osteoblasts In Response to Ultrasound Stimulation. *Biomaterials.* 2003;24:2379-2385.

91. Kalfas IH. Principles of Bone Healing. *Neurosurgical Focus.* 2001;10:1-4.

92. Kokubu T, Matsui N, Fujioka H, Tsunoda M, Mizuno K. Low Intensity Pulsed Ultrasound Exposure Increased Prostaglandin E2 Production Via the Induction of Cyclooxygenase-2 mRNA in Mouse Osteoblasts. *Biochemical and Biophysical Research Communications.* 1999;256:284-287.

93. Naruse K, Mikuni-Takagaki Y, Azuma Y, Ito, M, Oota, T, Kameyama, K, Itoman, M. Anabolic Response of Mouse Bone-Marrow-Derived Stromal Cell Clone ST2 Cells to Low-Intensity Pulsed Ultrasound. *Biochemical and Biophysical Research*

Communications. 2000;268:216-220.

94. Warden SJ, Favaloro JM, Bennell KL, McMeeken, JM, Ng, KW, Zajac, JD, Wark JD. Low-Intensity Pulsed Ultrasound Stimulates a Bone-Forming Response in UMR-106 Cells. *Biochemical and Biophysical Research Communications.* 2001;286:443-450.

95. Simon AM, Manigrasso MB, O'Connor JP. Cyclo-Oxygenase 2 Function is Essential for Bone Fracture Healing. *Journal of Bone and Mineral Research.* 2002;17:963-976.

96. Sena K, Leven RM, Mazhar K, Sumner DR, Viridi AS. Early Gene Response To Low-Intensity Pulsed Ultrasound in Rat Osteoblastic Cells. *Ultrasound in Medicine and Biology.* 2005;31:703-708.

97. Harle J, Salih V, Mayia F, Knowles JC, Olsen I. Effects of Ultrasound on the Growth and Function of Bone and Periodontal Ligament Cells In Vitro. *Ultrasound in Medicine and Biology.* 2001;27:579-586.

98. Harle J, Salih V, Knowles JC, Mayia F, Olsen I. Effects of Therapeutic Ultrasound on Osteoblast Gene Expression. *Journal of Materials in Science: Materials in Medicine.* 2001;12:1001-4.

99. Sant'Anna EF, Leven RM, Virdi AS, Sumner DR. Effect of Low-Intensity Pulsed Ultrasound and BMP-2 on Rat Bone Marrow Stromal Cell Gene Expression. *Journal of Orthopaedic Research.* 2005;23:646-652.

100. Street J, Bao M, deGuzman L, et al. Vascular Endothelial Growth Factor Stimulates Bone Repair by Promoting Angiogenesis and Bone Turnover. *Proceedings of the National Academy of Sciences.* 2002;99:9656-9661.

101. Saaristo A, Tammela T, Farkkila A, Kärkkäinen M, Suominen E, Herttuala S, Alitalo K. Vascular Endothelial Growth Factor-C Accelerates Diabetic Wound Healing. *The American Journal of Pathology.* 2006;169:1080-1087.

102. Beris AE, Lykissas MG, Papageorgiou CD, Georgoulis AD. Advances in Articular Cartilage Repair. *Injury.* 2005;36S:S14-S23.

103. Huang M-H, Ding H-J, Chai C-Y, Huang Y-F, Yang R-C. Effects of Sonication of Articular Cartilage in Experimental Osteoarthritis. *The Journal of Rheumatology.* 1997;24:1978-1984.

104. Huang M-H, Yang R-C, Ding H-J, Chai C-Y. Ultrasound Effet on Level of Stress Proteins and Arthritic Histology in Experimental Arthritis. *Archives of Physical Medicine and Rehabilitation.* 1999;80:551-556.

105. Feder ME, Hofman GE. Heat-Shock Proteins, Molecular Chaperones and the Stress Response: Evolutionary and Ecological Physiology. *Annual Reviews in Physiology.* 1999;61.:243-282.

106. Locke M, Nussbaum E. Continuous and Pulsed Ultrasound Do Not Increase Heat Shock Protein 72 Content. *Ultrasound in Medicine and Biology.* 2001;27:1413-1419.

107. Nishikori T, Ochi M, Uchio Y, et al. Effects of Low-Intensity Pulsed Ultrasound on Prolliferation and Chondroitin Sulfate Synthesis of Cultured Chondrocytes Embedded in Atelocollagen Gel. *Journal of Biomedical Materials Research.* 2002;59:201-206.

108. Zhang Z-J, Huckle J, Francomano CA, Spencer RGS. The Effects of Pulsed Low-Intensity Ultrasound on Chondrocyte Viability, Proliferation, Gene Expression and Matrix Production. *Ultrasound in Medicine and Biology.* 2003;29:1645-1651.

109. Zhang Z-J, Huckle J, Francomano CA, Spencer RGS. The Influence of Pulsed Low-Intensity Ultrasound on Matrix Production of Chondrocytes at Different Stages of Differentiation: An Explant Study. *Ultrasound in Medicine and Biology.* 2002; 28:1547-1553.

110. Mukai S, Ito H, Nakagawa Y, Akiyama H, Miyamoto M, Nakamura T. Transforming Growth Factor-β1 Mediates the Effects of Low-Intensity Pulsed Ultrasound in Chondrocytes. *Ultrasound in Medicine and Biology.* 2005;31:1713-1721.

111. Poiraudeau S, Monteiro I, Anract P, Blanchard O, Revel M, Corvol MT. Phenotypic Characteristics of Rabbit Intervertebral Disc Cells. *Spine.* 1999;24:837-844.

112. Iwashina T, Mochida J, Miyazaki T, Watanabe T, Iwabuchi S, Ando K, Hotta T, Sakai, D. Low-Intensity Pulsed Ultrasound Stimulates Cell Proliferation and Proteoglycan Production in Rabbit Intervertebral Disc Cells Cultured in Alginate. *Biomaterials.* 2006;27:354-361.

113. Frieder S, Weisberg J, Fleming B, Stanek A. A Pilot Study: The Therapeutic Effect of Ultrasound following Partial Rupture of Achilles Tendons in Male Rats. *The Journal of Orthopaedic And Sports Physical Therapy.* 1988;10:39-46.

114. Jackson BA, Schwane JA, Starcher BC. Effect of Ultrasound Therapy on the Repair of Achilles Tendon Injuries in Rats. *Medicine and Science in Sports and Exercise.* 1991;23:171-176.

115. Demir H, Menku P, Kirnap M, Calis M, Ikizceli I. Comparison of the Effects of

Laser, Ultrasound, and Combined Laser + Ultrasound Treatments in Experimental Tendon Healing. *Lasers in Surgery and Medicine.* 2004;35:84-89.

116. Enwemeka CS. The Effects of Therapeutic Ultrasound on Tendon Healing. A Biomechanical Study. *American Journal of Physical Medicine and Rehabilitation.* 1989;68:283-287.

117. Ng GYF, Ng COY, See KN. Comparison of Therapeutic Ultrasound and Exercises For Augmenting Tendon Healing in Rats. *Ultrasound in Medicine and Biology.* 2004;30:1539-1543.

118. Da Cunha A, Parizotto NA, Vidal Bde. The Effect of Therapeutic Ultrasound on Repair of the Achilles Tendon (Tendo Calcaneus) of the Rat. *Ultrasound in Medicine and Biology.* 2001;27:1691-1696.

119. Koeke PU, Parizotto NA, Carrinho PM, Salate ACB. Comparative Study of the Efficacy of the Topical Application of Hydrocortisone, Therapeutic Ultrasound, and Phonophoresis on the Tissue Repair Process in Rat Tendons. *Ultrasound in Medicine and Biology.* 2005;31:345-350.

120. Gan BS, Huys S, Sherebrin MH, Scilley CG. The Effects of Ultrasound Treatment on Flexor Tendon Healing in the Chicken Limb. *British Journal of Hand Surgery.* 1995;20B:809-814.

121. Stevenson JH, Pang CY, Lindsay WK, Zuker RM. Functional, Mechanical, and Biochemical Assessment of Ultrasound Therapy on Tendon Healing in the Chicken Toe. *Plastic and Reconstructive Surgery.* 1985;77:965-970.

122. Turner SM, Powell ES, Ng CSS. The Effect of Ultrasound on the Healing of Repaired Cockerel Tendon: Is Collagen Cross-Linkage a Factor? *Journal of Hand Surgery.* 1989;14B:428-433.

123. Chen YJ, Wang CJYKD, Chang P-R, et al. Pertussis Toxin-sensitive Gαi Protein and ERK-Dependent Pathways Mediate Ultrasound Promotion of Osteogenic Transcription in Human Osteoblasts. *Federation of European Biochemical Societies.* 2003;554:154-158.

124. Turner CH, Forwood MR, Otter MW. Mechanotransduction in Bone: Do Bone Cells Act as Sensors of Fluid Flow? *The FASEB Journal.* 1994;8:875-878.

125. Yang R-S, Lin W-L, Chen Y-Z, et al. Regulation by Ultrasound Treatment on the Integrin Expression and Differentiation of Osteoblasts. *Bone.* 2005;36:276-283.

126. Leung MC, Ng GY, Yip KK. Therapeutic Ultrasound Enhances Medial Collateral Ligament Repair in Rats. *Ultrasound in Medicine and Biology.* 2006;32:449-452.

127. Takakura Y, Matsui N, Yoshiya S, Fujioka H, Muratsu H. Tsunoda M, Kurosaka M. Low-Intensity Pulsed Ultrasound Enhances Early Healing of Medial Collateral Ligament Injuries in Rats. *Journal of Ultrasound in Medicine.* 2002;21:283-288.

128. Frank CB, Hart DA, Shrive NG. Molecular Biology and Biomechanics of Normal and Healing Ligaments - A Review. *Osteoarthritis and Cartilage* . 1999;7:130-140.

129. Mutsaers SE, Bishop JE, McGrouther G , Laurent GJ. Mechanisms of Tissue Repair: from Wound Healing to Fibrosis. *International Journal of Biochemistry & Cell Biology.* 1997;29:5-17.

130. Diegelmann RF, Evans MC. Wound Healing: An Overview of Acute, Fibrotic, and Delayed Healing. *Frontiers in Bioscience.* 2004;9:283-289.

131. Weiss EL. Connective Tissue in Wound Healing. *Wound Healing: Alternatives in Management.* 2nd ed. Philadelphia: F.A. Davis Company; 1995:17-31.

132. Davidson JM. Wound Repair. *Journal of Hand Therapy.* 1998;11:80-94.

133. Demir H, Solmaz Y, Kirnap M, Yaray K. Comparison of the Effects of Laser and Ultrasound Treatments on Experimental Wound Healing in Rats. *Journal of Rehabilitation Research & Development* . 2004;41:721-728.

134. Taskan I, Ozyazgan I, Tercan M, Kardas HY, Balkanli S, Saraymen R, Zorlu Ü, Özügül Y. A Comparative Study of the Effect of Ultrasound and Electrostimulation on Wound Healing in Rats. *Plastic and Reconstructive Surgery.* 1997;100:966-972.

135. Young SR, Dyson M. Effect of Therapeutic Ultrasound on the Healing of Full-Thickness Excised Skin Lesions. *Ultrasonics.* 1990;28:175-180.

136. Dyson M, Suckling J. Stimulation of Tissue Repair by Ultrasound: A Survey of the Mechanisms Involved. *Physiotherapy.* 1978;64:105-108.

137. Lundeberg T, Nordstrom F, Brodda-Jansen G, Eriksson SV, Kjartansson J, Samuelson UE. Pulsed Ultrasound Does Not Improve Healing of Venous Ulcers. *Scandanavian Journal of Rehabilitation Medicine.* 1990;22:195-197.

138. Eriksson SV, Lundeberg T, Malm M. A Placebo Controlled Trial of Ultrasound Therapy in Chronic Leg Ulceration. *Scandanavian Journal of Rehabilitation Medicine.* 1991;23:211-213.

139. McDiarmid T, Burns PN, Lewith GT, Machin D. Ultrasound and the Treatment of Pressure Sores. *Physiotherapy.* 1985;71:66-70.

140. Ter Riet G, Kessels AGH, Knipschild P. A Randomized Clinical Trial of

Ultrasound in the Treatment of Pressure Ulcers. *Physical Therapy.* 1996;76 :1301-1312.

141. Mulder G, Brazinsky B, Seeley JE. Factors Complicating Wound Healing. *Wound Healing: Alternatives in Management.* Second Edition ed. Philadelphia, PA: F.A. Davis Company; 1995:47-59.

142. Jarvinen TAH, Jarvinen TLN, Kaariainen M, Kalimo H, Jarvinen M. Muscle Injuries. Biology and Treatment. *The American Journal of Sports Medicine.* 2005;33:745-764.

143. Hurme T, Kalimo H, Lehto M, Järvinen M. Healing of Skeletal Muscle Injury: An Ultrastructural and Immunohistochemical Study. *Medicine and Science in Sports and Exercise.* 1991;23:801-810.

144. Rantanen J, Thorsson O, Wollmer P, Hurme T, Kalimo H. Effects of Therapeutic Ultrasound on the Regeneration of Skeletal Myofibers After Experimental Muscle Injury. *The American Journal of Sports Medicine.* 1999;27:54-59.

145. Markert CD, Merrick MA, Kirby TE, Devor ST. Nonthermal Ultrasound and Exercise In Skeletal Muscle Regeneration. *Archives in Physical Medicine and Rehabilitation.* 2005;86:1304-1310.

146. Heybeli N, Yesildag A, Oyar O, Gulsoy UK, Tekinsoy MA, Mumcu EF. Diagnostic Ultrasound Treatment Increases the Bone Fracture-Healing Rate in an Internally Fixed Rat Femoral Osteotomy Model. *Journal of Ultrasound in Medicine.* 2002;21:1357-1363.

147. Johnson EO, Zoubos AB, Soucacos PN. Regeneration and Repair of Peripheral Nerves. *Injury.* 2005;36:S24-S29.

148. Crisci AR, Ferreira AL. Low-Intensity Pulsed Ultrasound Accelerates the Regeneration of the Sciatic Nerve After Neurotomy in Rats. *Ultrasound in Medicine and Biology* . 2002;28:1335-1341.

149. Raso VVM, Barbieri CH, Mazzer N, Fasan VS. Can Therapeutic Ultrasound Influence the Regeneration of Peripheral Nerves? *Journal of Neuroscience Methods.* 2005;142:185-192.

150. Mourad PD, Lazar DA, Curra FP, Mohr BC, Andrus KC, Avellino AM, McNutt LD, Crum LA, Kliot M. Ultrasound Accelerates Functional Recovery After Peripheral Nerve Damage. *Neurosurgery.* 2001;48:1136-1141.

151. Sussman C, Bates-Jensen BM. Wound Healing Physiology: Acute and Chronic. *Wound Care: A Collaborative Practice Manual for Health Professionals*. 3rd ed.

Baltimore, MD: Lippincott Williams & Wilkins; 2007.

152. Hogan RD, Burke KM, Franklin TD. The Effect of Ultrasound on Microvascular Hemodynamics in Skeletal Muscle: Effects During Ischemia. *Microvascular Research.* 1982;23:370-379.

153. Young SR, Dyson M. The Effect of Therapeutic Ultrasound on Angiogenesis. *Ultrasound in Medicine and Biology.* 1990;16:261-269.

154. Barzelai S, Sharabani-Yosef O, Holbova R, et al. Low-Intensity Ultrasound Induces Angiogenesis in Rat Hind-Limb Ischemia. *Ultrasound in Medicine and Biology.* 2006;32.:139-145.

155. Hsu S, Huang T. Bioeffect of Ultrasound on Endothelial Cells In Vitro. *Biomolecular Engineering.* 2004;21:99-104.

156. Isenberg JS, Ridnour LA, Espey MG, Wink DA, Roberts DD. Nitric Oxide in Wound-Healing. *Microsurgery.* 2005;25 :442-451.

157. Broughton G, Janis JE, Attinger CE. The Basic Science of Wound Healing. *Plastic and Reconstructive Surgery.* 2006;117:12S-34S.

158. Robinson IM, Kinnick RR, Greenleaf JF, Fernandez JM. Stimulation of Secretion From Bovine Adrenal Chromaffin Cells by Microsecond Bursts of Therapeutic Levels of Ultrasound. *Journal of Physiology.* 1996;492:257-263.

159. Fyfe MC, Chahl LA. Mast Cell Degranulation and Increased Vascular Permeability Induced by 'Therapeutic' Ultrasound in the Rat Ankle Joint. *British Journal of Experimental Pathology.* 1984;64:671-676.

160. Noli C, Miolo A. The Mast Cell in Wound Healing. *Veterinary Dermatology.* 2001;12:303-313.

161. Young SR, Dyson M. Macrophage Responsiveness to Therapeutic Ultrasound. *Ultrasound in Medicine and Biology.* 1990;16:809-816.

162. Johns LD, Colloton P, Neuenfeldt J, Krupo K. Pre-exposure Effects of 1 and 3 MHz Therapeutic Ultrasound on ConA Activated Spleenocytes. *Cytokine.* 2003;22:55-61.

163. Eming SA, Krieg T, Davidson JM. Inflammation in Wound Repair: Molecular and Cellular Mechanisms. *Journal of Investigative Dermatology.* 2007;127:514-525.

164. Duffield JS. The Inflammatory Macrophage: A Story of Jekyll and Hyde. *Clinical Science.* 2003;104:27-38.

165. Amerongen MJ, Harmsen MC, van Rooijen N, Petersen AH, van Luyn MJA. Macrophage Depletion Impairs Wound Healing and Increase Left Ventricular Remodeling After Myocardial Injury in Mice. *The American Journal of Pathology*. 2007;170:818-829.

166. Leibovich SJ, Ross R. The Role of the Macrophage in Wound Repair. *American Journal of Pathology.* 1975;78:71-91.

167. Maruyama K., Asai J, Li M, Thorne T, Losordo DW, D'Amore PA. Decreased Macrophage Number and Activation Lead to Reduced Lymphatic Vessel Formation and Contribute to Impaired Diabetic Wound Healing. *The American Journal of Pathology*. 2007;170:1178-1191.

168. Mosser DM. The Many Faces of Macrophage Activation. *Journal of Leukocyte Biology.* 2003;73:209-212.

169. Enwemeka CS. Inflammation, Cellularity and Fibrillogenesis in Regenerating Tendon: Implications for Tendon Rehabilitation. *Physical Therapy.* 1989;69:816-825.

170. Spindler KP, Murray MM, Detweiler KB , Tarter JT, Dawson JM, Nanney LB, Davidson JM. The Biomechanical Response to Doses of TGF-β2 in the Healing Rabbit Medial Collateral Ligament. *Journal of Orthopaedic Research.* 2003;21:245-249.

171. Park JE, Barbul A. Understanding the Role of Immune Regulation in Wound Healing. *The American Journal of Surgery.* 2004;187 :11S-16S.

172. Leibovich SJ, Ross R. A Macrophage-Dependent Factor That Stimulates the Proliferation of Fibroblast In Vitro. *The American Journal of Pathology.* 1976;84:501-514.

173. Orita H, Campeau JD, Nakamura RM, diZerega GS. Modulation of Fibroblast Proliferation and Transformation by Activated Macrophages During Postoperative Peritoneal Reepithelialization. *American Journal of Obstetrics and Gynecology.* 1986;155:905-911.

174. Shimokado K, Raines EW, Madtes DK, Barrett TB, Benditt EP, Ross R. A Significant Part of Macrophage-Derived Growth Factor Consists of at Least two Forms of PDGF. *Cell.* 1985;43:277-286.

175. Hewison M, Brennan A, Singh-Ranger R, Walters JC, Katz DR, O'Riordan JLH. The Comparative Role of 1,25-Dihydroxycholecalciferol and Phorbol Esters in the Differentiation of the U937 Cell Line. *Immunology.* 1992;77:304-311.

176. Verhoeckx KC, Bijlsma S, De Groene EM, Witkamp RF, van der Greef J, Rodenburg RJ. A Combination of Proteomics, Principal Component Analysis and Transcriptomics is a Powerful Tool for the Identification of Biomarkers for Macrophage Maturation in the U937 Cell Line. *Proteomics.* 2004;4:1014-1028.

177. Reher P, Doan N, Bradnock B, Meghji S, Harris M. Effect of Ultrasound on the Production of IL-8, Basic FGF and VEGF. *Cytokine.* 1999;11:416-423.

178. Marcopoulou C, Vavouraki H, Dereka X, Vrotsos IA. Proliferative Effect of Growth Factors TGF-beta1, PDGF-BB, and rhBMP-2 on Human Gingival Fibroblasts and Periodontal Ligament Cells. *Journal of the International Academy of Periodontology.* 2003;5:63-70.

179. Mumford J, Carnes D, Cochran D, Oates TW. The Effects of Platelet-Derived Growth Factor-BB on Periodontal Cells in an In Vitro Wound Model. *Journal of Periodontology.* 2001;72:331-340.

180. Chan Y, Chen A, Yuan L, et al. Effects of Hyperbaric Oxygen and Platelet Derived Growth Factor on Medial Collateral Ligament Fibroblasts. *Undersea Hyperbaric Medicine.* 2007;34:181-190.

181. Loveland B, Johns T, Mackay I, Vaillant F, Wang Z, Hertzog PJ. Validation of the MTT Dye Assay for Enumeration of Cells in Proliferative and Antiproliferative Assays. *Biochemistry International.* 1992;27:501-510.

182. Slavin J. The Role of Cytokines in Wound Healing: A Review Article. *Journal of Pathology.* 1996;178:5-10.

183. Geiser T, Jarreau P, Atabai K, Matthay MA. Interleukin-1β Augments In Vitro Alveolar Epithelial Repair. *American Journal of Physiology: Lung Cellular and Molecular Physiology.* 2000;279:L1184-L1190.

184. Assoian RK, Fleurdelys BE, Stevenson HC, Miller PJ, Madtes DK, Raines EW, Ross R, Sporn MB. Expression and Secretion of Type β Transforming Growth Factor by Activated Human Macrophages. *Proceedings of the National Academy of Science, USA.* 1987;84:6020-6024.

185. Itaya H, Imaizumi T, Yoshida H, Koyama M, Suzuki S, Satoh K. Expression of Vascular Endothelial Growth Factor in Human Monocytes/Macrophages Stimulated by Lipopolysaccharide. *Journal of Thrombosis and Haemostasis.* 2001;85:171-176.

186. Archambault J, Tsuzaki M, Herzog W, Banes AJ. Stretch and Interleukin-1β Induce Matrix Metalloproteinases in Rabbit Tendon Cells In Vitro. *Journal of Orthopaedic Research.* 2002;20:36-39.

187. Sakaki H, Matsumiya T, Kusumi A, Imaizumi T, Satoh H, Yoshida H, Satoh H, Kimura H. Interleukin-1β Induces Matrix Metalloproteinase-1 Expression in Cultured Human Gingival Fibroblasts: Role of Cyclooxygenase-2 and Prostaglandin E2. *Experimental Oral Pathology.* 2004;10:87-93.

188. Menke A, Yamaguchi H, Gress TM, Adler G. Extracellular Matrix is Reduced by Inhibition of Transforming Growth Factor Beta 1 in Pancreatitis in the Rat. *Gastroenterology.* 1997;113:295-303.

189. Puolakkainen PA, Reed MJ, Gombotz WR, Twardzik DR, Abrass IB , Sage HE. Acceleration of Wound Healing In Aged Rats by Topical Application of Transforming Growth Factor-Beta 1. *Wound Repair and Regeneration.* 1995;3:330-339.

190. Cromack DT, Porras-Reyes B, Purdy JA, Pierce GF, Mustoe TA. Acceleration of Tissue Repair by Transforming Growth Factor Beta 1: Identification of In Vivo Mechanism of Action With RadioTherapy-Induced Specific Healing Deficits. *Surgery.* 1993;113:36-42.

191. Klein MB, Yalamanchi N, Pham H, Longaker MT, Chang J. Flexor Tendon Healing In Vitro: Effects of TGF-β on Tendon Cell Collagen Production. *The Journal of Hand Surgery.* 2002;27A:615-620.

192. Nissen NN, Polverini PJ, Koch AE, Volin MV, Gamelli RL, Dipietro LA. Vascular Endothelial Growth Factor Mediates Angiogenic Activity During the Proliferative Phase of Wound Healing. *American Journal of Pathology.* 1998;152:1445-1452.

193. Eckardt H, Ding M, Lind M, Hansen ES, Christensen KS, Hvid I. Recombinant Human Vascular Endothelial Growth Factor Enhances Bone Healing in an Experimental Nonunion Model. *The Journal of Bone and Joint Surgery.* 2005;87B:1434-1438.

194. Smith KL, Dean SJ. Tissue Repair of the Epidermis and Dermis. *Journal of Hand Therapy.* 1998;11:95-104.

195. Swift ME, Kleinman HK, DiPietro LA. Impaired Wound Repair and Delayed Angiogenesis in Aged Mice. *Laboratory Investigation.* 1999;79(12):1479-1487.

196. Cohen BJ, Danon D, Roth GS. Wound Repair in Mice as Influenced by Age and Antimacrophage Serum. *Journal of Gerontology.* 1987;42:295-301.

197. Low QEH, Drugea IA, Duffner LA, Quinn DC, Cook DN, Rollins BJ, Kovacs EJ, DiPietro LA. Wound Healing in MIP-1α -/- and MCP-1 -/- Mice. *American Journal of Pathology.* 2001;159:457-463.

198. Ziegler TR. *Growth Factors and Wound Healing*, In: Ziegler TR, Pierce GF, and Herndon DN (eds). Growth Factors and Wound Healing: Basic Science and Potential Clinical Applications. Norwell, MA: Massachusetts Serono Symposia; 1997, 104-150.

199. Barrientos S, Stojadinovic O, Golinko MS, Brem H, Tomic-Canic M. Growth Factors and Cytokines in Wound Healing. *Wound Repair and Regeneration.* 2008;16:139-145.

200. Nakamura T, Hara Y, Tagawa M, Yuge T, Fukuda H, Nigi H. Recombinant Human Basic Fibroblast Growth Factor Accelerates Fracture Healing by Enhancing Callus Remodeling in Experimental Dog Tibial Fracture. *The Journal of Bone and Mineral Research.* 1998;13:942-949.

201. Chan BP, Chan KM, Maffulli N, Webb S, Lee KKH. Effect of Basic Fibroblast Growth Factor: An In Vitro Study of Tendon Healing. *Clinical Orthopaedics and Related Research.* 1997;342:239-247.

202. Hildebrand KA, Woo SL-Y, Smith DW, Allen CR, Deie M, Taylor BJ, Schmidt CC. The Effects of Platelet-Derived Growth Factor-BB on Healing of the Rabbit Medial Collateral Ligament. *The American Journal of Sports Medicine.* 1998;26:549-554.

203. Iwabuchi S, Ito M, Hata J, Chikanishi T, Azuma Y, Haro H. In Vitro Evaluation of Low-Intensity Pulsed Ultrasound in Herniated Disc Resorption. *Biomaterials.* 2005;26:7104-7114.

204. Dinarello CA. Proinflammatory Cytokines. *Chest.* 2000;118:503-508.

205. Pierce GF, Mustoe TA, Lingelbach J, Masakowski VR, Griffin GL, Senior RM, Deuel TF. Platelet-Derived Growth Factor and Transforming Growth Factor-β Enhance Tissue Repair Activities by Unique Mechanisms. *The Journal of Cell Biology.* 1989;109:429-440.

206. Saadeh PB, Mehrara BJ, Steinbrech DS, Dudziak ME, Greenwald JA, Luchs JS, Spector JA, Ueno H, Gittes GK, Longaker MT. Transforming Growth Factor Beta 1 Modulates the Expression of Vascular Endothelial Growth Factor by Osteoblasts. *American Journal of Physiology Cell Physiology.* 1999;277:C268-C637.

207. Byrne AM, Bouchier-Hayes DJ, Harmey JH. Angiogenic and Cell Survival Functions of Vascular Endothelial Growth Factor (VEGF). *Journal of Cellular and Molecular Medicine.* 2005;9:777-794.

208. Chu TW, Wang ZG, Zhu PF, Jiao WC, Wen JL, Gong SG. Effect of Vascular Endothelial Growth Factor in Fracture Healing. *Zhongguo Xiu Fu Chong Jian Wai*

Ke Za Zhi. 2002;2:75-78.

209. Woo SL-Y, Smith DW, Hildebrand KA, Zeminski JA, Johnson LA . Engineering the Healing of the Rabbit Medial Collateral Ligament. *Medical and Biological Engineering and Computing.* 1998;36:359-364.

210. Raines E, Dower S, Ross R. Interleukin-1 Mitogenic Activity for Fibroblasts and Smooth Muscles Cells is Due to PDGF-AA. *Science.* 1989;243:393-396.

211. Dinarello CA. Interleukin-1. *Cytokine & Growth Factor Reviews.* 1997;8 :253-265.

212. Andrei C, Margiocco P, Poggi A, Lotti L, Torrisi M, Rubartelli A. Phospholipases C and A2 Control Lysosome-Mediated IL-1beta Secretion. *Proceedings of the National Academy of Sciences.* 2004;101:9745-9750.

213. Andrei C, Margiocco P, Poggi A, Lotti LV, Torrisi MR, Rubartelli A. Phospholipases C and A2 Control Lysosome-Mediated IL-1beta Secretion: Implications for Inflammatory Processes. *Proceedings of the National Academy of Sciences.* 2004;101:9745-9750.

214. Kim CH, Kang BS, Lee TK, Park WH, Kim JK, Park YG, Kim HM, Lee YC. IL-1Beta Regulates Cellular Proliferation, Prostaglandin E2 Synthesis, Plasminogen Activator Activity, Osteocalcin Production, and Bone Resorptive Activity of the Mouse Calvarial Bone Cells. *Immunopharmacology and Immunotoxicology.* 2002;24:395-407.

215. Martensson K, Chrysis D, Sävendahl L. Interleukin-1β and TNF-α Act in Synergy to Inhibit Longitudinal Growth in Fetal Rat Metatarsal Bones. *Journal of Bone and Mineral Research.* 2004;19:1805-1812.

216. Siwik DA, Chang DLF, Colucci WS. Interleukin-1β and Tumor Necrosis Factor-α Decrease Collagen Synthesis and Increase Matrix Metalloproteinase Activity in Cardiac Fibroblasts In Vitro. *Circulation Research.* 2000;86:1259-1265.

217. Mizel SB, Dayer J-M, Krane SM, Mergenhagen SE. Stimulation of Rheumatoid Synovial Cell Collagenase and Prostaglandin Production by Partially Purified Lymphocyte-Activating Factor (Interleukin 1). *Proclamations of the National Academy of Sciences, USA.* 1981;78:2474-2477.

218. Ribatti D. The Crucial Role of Vascular Permeability Factor/Vascular Endothelial Growth Factor in Angiogenesis: A Historical Review. *British Journal of Haematology.* 2004;128:303-309.

219. Sadoun E, Reed MJ. Impaired Angiogenesis in Aging is Associated with Alterations in Vessel Density, Matrix Composition, Inflammatory Response, and

Growth Factor Expression. *The Journal of Histochemistry & Cytochemistry.* 2003;51:1119-1130.

220. Xiong M, Elson G, Legarda D, Leibovich SJ. Production of Vascular Endothelial Growth Factor by Murine Macrophages: Regulation by Hypoxia, Lactate, and the Inducible Nitric Oxide Synthase Pathway. *American Journal of Pathology.* 1998;153:587-598.

221. Huang Q, Goh JC, Hutmacher DW, Lee EH. In Vivo Mesenchymal Cell Recruitment by a Scaffold Loaded With Transforming Growth Factor Beta 1 and the Potential For In Situ Chondrogenesis. *Tissue Engineering.* 2002;8:469-482.

222. Bira Y, Tani K, Nishioka Y, Miyata J, Sato K, Hayashi A, Nakaya Y, Sone S. Transforming Growth Factor Beta Stimulates Rheumatoid Synovial Fibroblasts via the Type II Receptor. *Modern Rheumatology.* 2005;15:108-113.

223. Ballock R.T., Heydemann A, Wakefield LM, Flanders KC, Roberts AB, Sporn MB. TGF-Beta 1 Prevents Hypertrophy of Epiphyseal Chondrocytes: Regulation of Gene Expression for Cartilage Matrix Proteins and Metalloproteases. *Developmental Biology.* 1993;158:414-429.

224. Defacque H, Piquemal D, Basset A, Marti J, Commes T. Transforming Growth Factor-β1 is an Autocrine Mediator of U937 Cell Growth Arrest and Differentiation Induced by Vitamin D3 and Retinoids. *Journal of Cellular Physiology.* 1999;109-119.

225. Khalil N, Bereznay O, Sporn M, Greenberg AH. Macrophage Production of Transforming Growth Factor β and Fibroblast Collagen Synthesis in Chronic Pulmonary Inflammation. *Journal of Experimental Medicine.* 1989;170:727-737.

226. McIntire RH, Morales PJ, Petroff MG, Colonna M, Hunt JS. Recombinant HLA-G5 and -G6 Drive Myelomonocytic Cell Production of TGF-β1. *Journal of Leukocyte Biology.* 2004;1220-1228.

227. Toossi Z, Gogate P, Shiratsuchi H, Young T, Ellner JJ. Enhanced Production of TGFβ by Blood Monocytes from Patients with Active Tuberculosis and Presence of TGFβ in Tuberculous Granulomatus Lung Lesions. *Journal of Immunology.* 1995;154:465-473.

228. Stow JL, Low PC, Offenhäuser C, Sangermani D. Cytokine Secretion in Macrophages and Other Cells: Pathways and Mediators. *Immunobiology.* 2009; 214(7):601-612.

229. Tapper H. The Secretion of Preformed Granules by Macrophages and Neutrophils. *Journal of Leukocyte Biology.* 1996;59:613-622.

230. Janmey PA. The Cytoskeleton and Cell Signaling: Component Localization and Mechanical Coupling. *Physiological Reviews.* 1998;78:763-781.

231. Zhou S, Schmelz A, Seufferlein T, Li Y, Zhao J, Bachem MG. Molecular Mechanisms of Low Intensity Pulsed Ultrasound in Human Skin Fibroblasts. *The Journal of Biological Chemistry.* 2004;279:54463-54469.

232. Ito M, Azuma Y, Ohta T, Komoriya K. Effects of Ultrasound and 1,25-Dihydroxyvitamin D_3 on Growth Factor Secretion in Co-Culture of Osteoblasts and Endothelial Cells. *Ultrasound in Medicine and Biology.* 2000;26:161-166.

233. Chapman IV, MacNally NATS. Ultrasound-Induced Changes in Rates of Influx and Efflux of Potassium Ions in Rat Thymocytes In Vitro. *Ultrasound in Medicine and Biology* . 1980;6:59-61.

234. Dinno MA, Dyson M, Young SR, Mortimer AJ, Hart J, Crum LA. The Significance of Membrane Changes in The Safe and Effective Use of Therapeutic and Diagnostic Ultrasound. *Physics in Medicine and Biology* . 1989;34:1543-1552.

235. Zhou Y, Shi J, Cui C, Deng C. Effects of Extracellular Calcium on Cell Membrane Resealing in Sonoporation. *Journal of Controlled Release.* 2008;126:34-43.

236. Deng CX, Sieling F, Pan H, Cui J. Ultrasound-induced Cell Membrane Porosity. *Ultrasound in Medicine and Biology.* 2004;30:519-526.

237. McNeil P, Terasaki M. Coping With The Inevitable: How Cells Repair a Torn Surface Membrane. *Nature Cell Biology.* 2001;3:E124-E129.

238. Pan H, Zhou Y, Izadnegahdar O, Cui J, Deng CX. Study of Sonoporation Dynamics Affected By Ultrasound Duty Cycle. *Ultrasound in Medicine and Biology.* 2005;31:849-856.

239. Pong M, Umchid S, Guarino AJ, et al. In Vitro Ultrasound-Mediated Leakage From Phospholipid Vesicles. *Ultrasonics.* 2006;45:133-145.

240. Danpure CJ. Lactate Dehydrogenase and Cell Injury. *Cell Biochemistry and Function.* 1984;2:144-148.

241. Decherchi P, Cochard P, Gauthier P. Dual-Staining Assessment of Schwann Cell Viability Within Whole Peripheral Nerves Using Calcein-AM and Ethidium Homodimer. *Journal of Neuroscience Methods.* 1997;71:205-213.

242. Sato KHK, Amano K, Mitusi-Saito M, et al. Membrane Permeabilization Induced By Discodermin A, a Novel Marine Bioactive Peptide. *Toxicon.* 2001;39:259-264.

243. Papadopoulos NG, Dedoussis GV, Spanakos G, Gritzapis AD, Baxevanis CN, Papamichail M. An Improved Fluorescence Assay for the Determination of Lymphocyte-Mediated Cytotoxicity Using Flow Cytometry. *Journal of Immunological Methods.* 1994;177:101-111.

244. Mitchell DB, Santone KS, Acosta D. Evaluation of Cytotoxicity in Cultured Cells by Enzyme Leakage. 1980;6:113-116.

245. Boutilier G. Mechanisms of Cell Survival in Hypoxia and Hypothermia. *The Journal of Experimental Cell Biology.* 2001;204:3171-3181.

246. Si QS, Nakamura Y, Kataoka K. Hypothermic Suppression of Microglial activation in Culture: Inhibition of Cell Proliferation and Production of Nitric Oxide and Superoxide. *Neuroscience.* 1997;81:223-229.

247. Sweet MJ, Hume DA. Endotoxin Signal Transduction in Macrophages. *Journal of Leukocyte Biology.* 1996;60:8-26.

248. Yasuda T. Hyaluron Inhibits Cytokine Production by Lipopolysaccharide-Stimulated U937 Macrophages Through Down-Regulation of NF-κB via ICAM-1. *Inflammation Research.* 2007;56:246-253.

249. Eder C. Mechanisms of Interleukin-1beta Release. *Immunobiology.* 2009; 214(7):543-553.

250. Qu Y, Franchi L, Nunez G, Dubyak GR. Nonclassical IL-1beta Secretion Stimulated by P2X7 Receptors Is Dependent on Inflammasome Activation and Correlated with Exosome Release in Murine Macrophages. *The Journal of Immunology.* 2007;179:1913-1925.

251. Gallin EK. Ionic Channels In Leukocytes. *Journal of Leukocyte Biology.* 1986;39:241-254.

252. Kanno T, Takishima T. Chloride and Potassium Channels in U937 Human Monocytes. *Journal of Membrane Biology.* 1990;116:149-161.

253. Li SW, Westwick J, Poll CT. Receptor-operated Ca^{2+} Influx Channels In Leukocytes: A Therapeutic Target? *Trends in Pharmacological Sciences.* 2002;23:63-70.

254. Hogquist KA, Unanue ER, Chaplin DD. Release of IL-1 From Mononuclear Phagocytes. *The Journal of Immunology.* 1991;147:2181-2186.

255. Maekawa S, Aibiki M, Si QS, Nakamura Y, Shirakawa Y. Differential Effects of Lowering Culture Temperature on Mediator Relase from Lipolpolysaccharide-

Stimulated Neonatal Rat Microglia. *Critical Care Medicine.* 2002;30:2700-2704.

256. Bandow K, Nishikawa Y, Ohnishi T, et al. Low-Intensity Pulsed Ultrasound (LIPUS) Induces RANKL, MCP-1 and MIP-1beta Expression in Osteoblasts Through the Angiotensin II Type I Receptor. *Journal of Cellular Physiology.* 2007;211:392-398.

257. Gudi S, Nolan JP, Frangos JA. Modulation of GTPas activity of G-proteins by Fluid Shear Stress and Phospholipid Composition. *Proceedings of the National Academy of Science.* 1998;95:2515-2519.

258. Nelson TJ, Alkon DL. Neuroprotective Versus Tumorigenic Protein Kinase C Activators. *Trends in Biochemical Sciences.* 2008;34(3):136-145.

259. Fairchild KD, Viscardi RM, Hester L, Singh IS, Hasday JD. Effects of Hypothermia and Hyperthermia on Cytokine Production by Cultured Human Mononuclear Phagocytes From Adults and Newborns. *Journal of Interferon and Cytokine Research.* 2000;20(12):1049-1055.

260. Nelson TJ, Alkon, DL. Neuroprotective Versus Tumorigenic Protein Kinase C Activators. *Trends in Biochemical Sciences*. 2009;34(30):136-145.

APPENDIX A

Preliminary Experimentation With Macrophages Exposed to TUS and Incubated 24-hours Post-Treatment

PREFACE: This appendix includes preliminary experimentation of therapeutic ultrasound-induced (TUS) growth factor and cytokine release from macrophages. Due to the limitations of the experimental methodology, the data included herein was not included as part of the current series of investigations previously describe.

Therapeutic ultrasound has been reported to enhance tissue healing in models including integument, ligaments, tendons and bones. TUS-enhanced healing is thought to occur via alteration of cellular activities during the inflammatory and early proliferative phases of healing. Specific cellular responses to TUS have been investigated in numerous cell types including osteoblasts, periosteal cells, chondrocytes, fibroblasts, endothelial cells, and leukocytes. Despite the volume of investigations into TUS effects on healing, few investigations of TUS effects on macrophages have been reported. Because macrophages are important mediators of inflammation and early proliferative phase of healing, where TUS effects are thought to be greatest, the following set of experiments was undertaken to explore the growth factor and cytokine release response of macrophages treated with TUS.

Materials and Methods

Materials and Reagents. Phorbol 12-myristate 13-acetate (PMA), dimethyl sulfoxide (DMSO), and lauryl sulfate (SDS) were obtained from Sigma Chemical Co., St. Louis, MO. Tris and DC Protein Assay Kit were from BioRad Laboratories, Hercules CA. Glycerol, HEPES, sodium hydroxide, hydrochloric acid, heat-inactivated fetal calf serum (HIFCS) and sterile pipets were from Fisher Scientific, Pittsburgh, PA. BSA protein standard was obtained from Pierce Biotechnology Inc., Rockford, IL. Human monocytic cells (U937) and human gingival fibroblasts (HGF-1) were purchased from American Type Culture Collection, Manassas, VA. Sterile tissue culture plates and centrifuge tubes were from Corning Inc., Corning NY. Cell culture media reagents including: RPMI-1640 culture media and Dulbecco's Modified Eagle's Medium (DMEM), sodium pyruvate, sodium bicarbonate, HEPES, L-glutamine, 0.25% trypsin, fetal calf serum and penicillin/streptomycin/amphotericin B were purchased from Invitrogen, Carlsbad, CA. ELISA antigen detection kits for IL-1β, VEGF, and TGF-β1 were acquired from R & D Systems, Minneapolis MN. All other reagents were obtained from Invitrogen Corp., Carlsbad, CA.

U937 Cell Culture. All cell manipulations were conducted using sterile technique as described in Chapter 2.

Cell differentiation and preparation for sonication. U937 cells induced to differentiate into macrophages through the addition of phorbol 12-myristate 13-acetate (PMA) [175]. Differentiation of U937 monocytes was conducted as described in Chapter 2, ***except:*** Following 24-hour differentiation in PMA-containing media, cells were incubated

24hr in RPMI-growth media supplemented with 5% HIFCS. Differentiated macrophages were subsequently exposed to TUS in RPMI-growth media supplemented with 5% HIFCS.

TUS Treatment of U937 Macrophages. For all experimental TUS exposures, culture plates (samples) containing cells were treated using a system similar to that described by Reher et al [177] as described in Chapter 2 (Fig. 2.1). Sham treated samples were included for 5 and 10-minute exposure times (Table A1). Each experimental block (set of TUS treatments) included each TUS parameter group (Table A1) for total of 14 parameter sets per experimental block. The order of application of each TUS parameter set was randomized for each experimental block to reduce the possibility of experimenter bias as previously described in Chapter 2. A total of n = 6 experimental blocks were completed.

Preparation of Fibroblasts for Experimentation with Conditioned Media. HGF-1 aliquots were thawed, washed in plain DMEM and resuspended in DMEM growth media and propagated under humidified incubation conditions as described in Chapter 2. From each batch of fibroblasts, three separate 96-well plates were seeded with cells (for 24, 48 and 72 hour incubations). Seeded cells were placed in the humidified incubator for 4 hours to allow adherence to the culture plate as described in Chapter 2. At the end of the incubation period in serum-free DMEM, media was removed from each well and replaced with 100μL of macrophage conditioned media and the fibroblasts were returned to the incubator for 24, 48 or 72 hours. Fibroblast proliferation was assessed at the end of each incubation period as described in Chapter 2.

Fibroblast Proliferation Assay. Fibroblast proliferation following incubation in macrophage conditioned media was analyzed using a Cell Proliferation Assay Kit as described in Chapter 2.

Validation of WST-1 Assay for Cell Proliferation. The validity of the WST-1 assay used to assess fibroblast proliferation was examined in relation to direct cell counts as described in Chapter 2, ***except:*** 1) the validation assay included fibroblasts incubated for 72hrs prior to assay. 2) After the 24 hr incubation period in serum-free DMEM growth media, the media was replaced with 100μl of RPMI growth media supplemented with 5% HIFCS, which was identical to macrophage RPMI growth media utilized in the TUS exposures.

ELISA assays for IL-1β, VEGF and TGF-β1. Analysis of conditioned media for these growth factors was completed using commercially available, quantitative, sandwich enzyme-linked immunosorbent assays (ELISA; R & D Systems, Minneapolis, MN) as described in Chapter 3, ***except:*** Initial assays were completed for each cytokine ELISA to determine the need to dilute conditioned media samples (Table A2). Dilution factors were identified for IL-1β at 1:10 and for VEGF at 1:20 in order to have measurements were within the detection range of the ELISA. For TGF-β1 samples were assayed undiluted. Following ELISA, data collected was recorded as pg/ml of media, with final concentrations in the conditioned media being calculated by multiplying the dilution factor x ELISA value. The final cytokine growth factor concentrations (pg/ml) were then normalized to total protein concentration (mg/ml) in the conditioned media, generating values reported as pg cytokine/mg total protein.

***Data Analysis/Statistics*.**

Each experiment was repeated for n=6 replicates. Fibroblast proliferation in response to macrophage conditioned media was assayed in duplicate wells and the mean of the two values was reported. Conditioned media assayed for growth factors by ELISA, and conditioned media analyzed for total protein concentration were analyzed in duplicate, with the average being reported. All values for statistical analysis are reported as mean ± standard error of the mean (SEM). Three-way analysis of variance (ANOVA) was used to evaluate for differences in fibroblast proliferation and growth factor release among various macrophage conditioned media to account for the effect of the independent variables: treatment intensity (mW SATA), treatment frequency (1MHz, 3MHz) and treatment duration (5min, 10min) (Sigma Stat version 2.03; Systat Software, Inc., Point Richmond, CA). Post hoc analysis of significant differences was performed using Tukey's HSD. A p-value of $< .05$ was considered significant for all values. Data analysis for WST-1 assay validation was completed using a correlation analysis on the variables of OD and cell counts and was reported as R^2 (coefficient of determination).

Table A1

5 minutes		
	1 MHz	**3 MHz**
0 mW/cm^2 (sham)	40 mW/cm^2	40 mW/cm^2
	100 mW/cm^2	100 mW/cm^2
	400 mW/cm^2	400 mW/cm^2
10 minutes		
	1 MHz	**3 MHz**
0 mW/cm^2 (sham)	40 mW/cm^2	40 mW/cm^2
	100 mW/cm^2	100 mW/cm^2
	400 mW/cm^2	400 mW/cm^2

Table A1. *TUS Exposure Parameters for 24-hour post-TUS macrophage incubation*. Exposure parameter combinations utilized for sonication of macrophages. All intensity values are reported as SATA at 20% duty cycle. Sham treatments were completed for 5 minute and 10-minute exposures, in which the culture plates were secured in the sonication apparatus but the ultrasound unit was not turned on. For each experimental block, the order of application of TUS parameter sets to macrophages was randomized.

Table A2

Growth Factor	**Minimum (pg/ml)**	***Maximum (pg/ml)***
IL-1β	*3.9*	250
TGF-β1	*31.2*	2000
VEGF	15.6	1000

Table A2. *Detection ranges of the ELISA assays*. Detection ranges of ELISA assay kits (pg/ml) that were utilized to determine growth factor release by sonicated macrophages incubated for 24-hours post-TUS.

Results

Fibroblast Proliferation in Macrophage Conditioned Media. Proliferation of fibroblasts was measured following 24, 48, and 72-hour incubation in conditioned media from TUS-treated macrophages. Three-way ANOVA revealed that TUS intensity, TUS wavelength frequency, and TUS treatment duration had no effect on fibroblast proliferation in macrophage conditioned media indicating no release of a fibroblast mitogenic factor at any level of TUS (Figs. A1 – A3).

Validation of WST-1 assay for Fibroblast Proliferation. Fibroblasts were plated at serially diluted concentrations (8, 4, 2 and 1 x 10^3 cells/well) and were incubated for (A) 24 hours, (B) 48 hours or (C) 72 hours in serum-free macrophage growth media. Cell proliferation assayed by WST-1 assay was compared to direct cell counting. WST-1 proliferation assay was strongly correlated with increasing cell number for (A) 24-hours, $R^2 = 0.998$, (B) 48 hours, $R^2 = 0.978$, and (C) 72 hours, $R^2 = 0.939$ (Figs. A1.4A-C).

Total protein determination. Total protein concentration of cell lysates was used as an indirect measure of cell number and was then utilized for normalization of the cytokine release data. Protein concentrations of samples were pooled based on the TUS treatment intensity from among the 1 and 3 MHz and the 5 and 10-minute treatments. Total protein concentrations were slightly less among treatment groups compared to sham control (Fig. A5), but the difference between groups was not statistically significant in comparison of any groups (ANOVA, p= 0.985, F = 0.391,).

TUS effects on release of IL-1β. IL-1β was measured by ELISA in the macrophage-conditioned media 24 hours after TUS exposure. Values on figure A6

represent mean ± SEM of n = 6 replicates that have been normalized to total protein in macrophage cell lysate. Three-way ANOVA revealed no significant differences in IL-1β release based on any TUS parameter: intensity, p = 0.176, wavelength frequency, p = 0.471, and duration, p = 0.110.

TUS Effects on VEGF. VEGF was measured in the conditioned media of TUS-treated macrophages following 24-hour post-treatment incubation**.** VEGF in the conditioned media was normalized to total cellular protein isolated from sonicated macrophages. Values in figure A7 represent mean ± SEM for n = 6 replicates. Three-way ANOVA for the effects of TUS parameters revealed no significant effect on VEGF release based on TUS intensity, p = 0.772, wavelength frequency, p = 0.744, or treatment duration, p = 0.751.

TUS effects on TGF-β1 release from sonicated macrophages. TGF-β1 was measured in conditioned media following TUS exposure and 24-hour post-TUS incubation. TGF-β1 levels were normalized to total cellular protein isolated from lysates of sonicated macrophages. All values are expressed as mean of n = 6 samples ± SEM. Similar to IL-1β and VEGF, TGF-β1 was detected in all samples including sham control (Fig. A8). Three-way ANOVA revealed a significant effect of TUS wavelength frequency, where 1 MHz exposure was associated with increased TGF-β1 release, when compared to release in response to 3 MHz exposure (p = 0.025). There was a trend toward increased TGF-β1 release for 10-minute treatments compared to 5-minute treatments (p = 0.061) and for treatments administered at 400mW/cm^2 (p = 0.082) although those trends did not reach statistical significance.

Figure A1

A

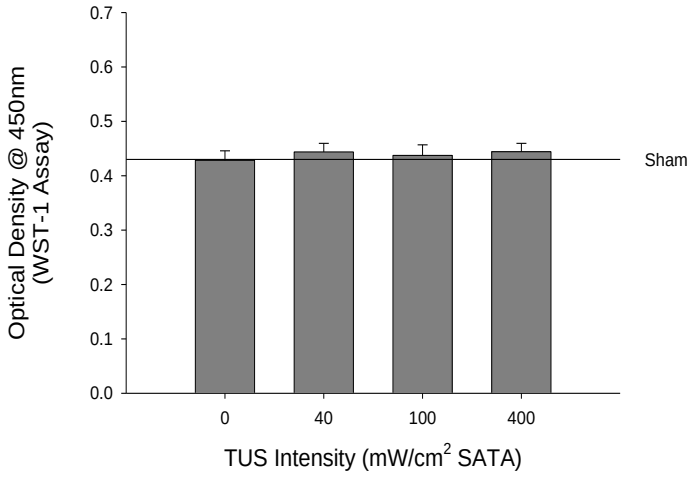

B

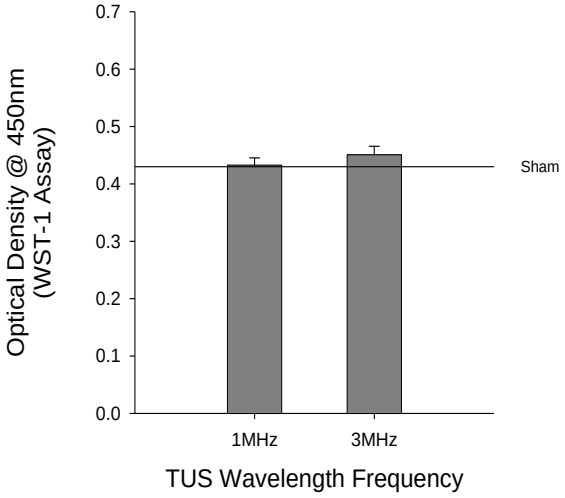

C

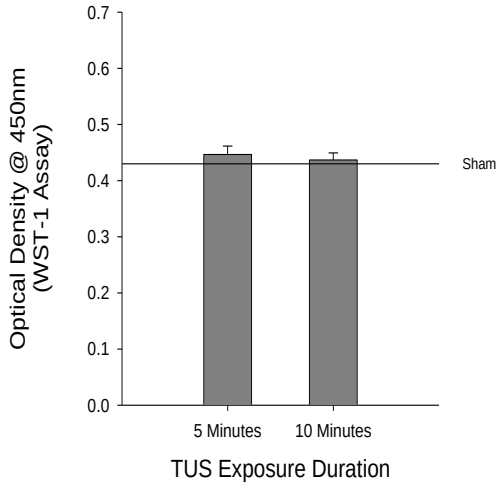

Figure A1. *Fibroblast proliferation in response to 24-hour incubation in macrophage conditioned media*. Fibroblast proliferation was assessed using WST-1 assay and reported as optical density units. Collapsed data across the TUS wavelengths and treatment durations demonstrates the three-way ANOVA analysis for intensity. (A) No level of TUS stimulated macrophage release of fibroblast mitogens into the conditioned media ($p = 0.577$). *Effect of TUS wavelength frequency (B).* Collapsed data across the TUS intensities and treatment durations demonstrates the lack of an effect by exposure wavelength ($p = 0.176$). *Effect of TUS treatment duration (C).* Collapsed data for TUS treatment duration demonstrates no effect of treatment time among all the TUS intensities and wavelength frequencies investigated ($p = 0.230$). All data represent mean ± SEM of $n = 6$ experiments

Figure A2

A

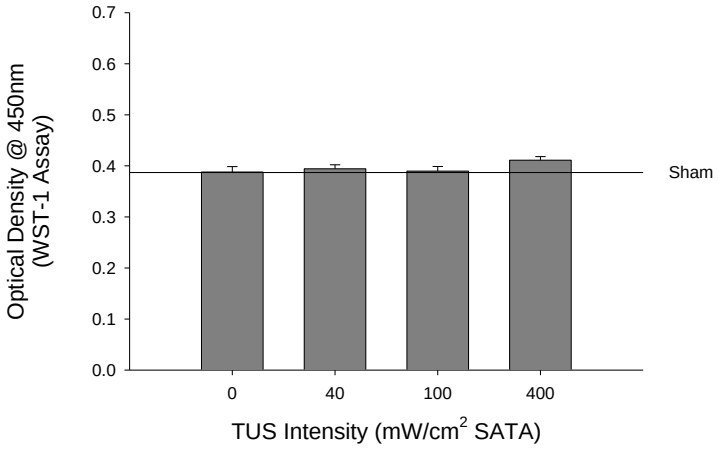

B

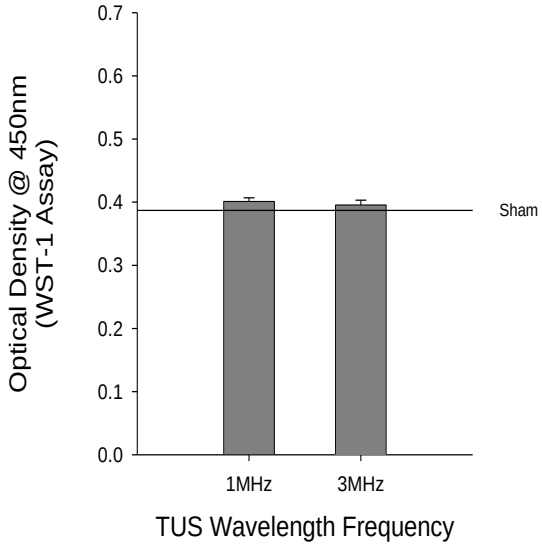

C

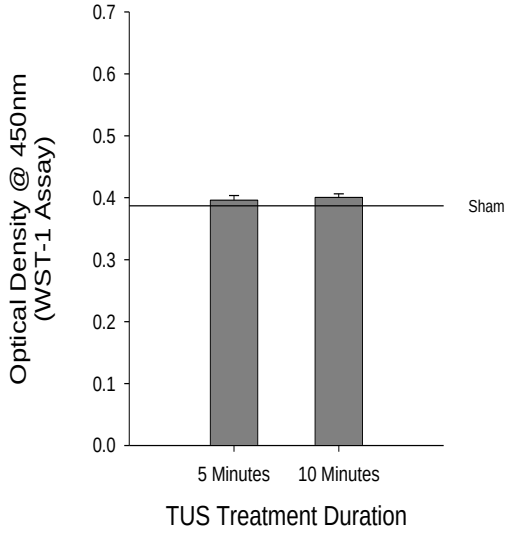

Figure A2 *Fibroblast proliferation in response to 48-hour incubation in macrophage conditioned media*. Fibroblast proliferation was assessed using WST-1 assay and reported as optical density units. Collapsed data across the TUS intensity, wavelengths and treatment durations demonstrates the three-way ANOVA analysis for each TUS parameter variable. No intensity, wavelength frequency or treatment duration of TUS-exposure stimulated macrophage release of fibroblast mitogens into the conditioned media at 48 hours. Collapsed data across *(A)* TUS Intensity ($p = 0.247$), *(B)* TUS wavelength ($p = 0.628$) and *(C)* TUS treatment duration ($p = 0.862$), demonstrates three-way ANOVA analysis of the effect on each variable on macrophage release of fibroblast mitogens. All data represent mean ± SEM of $n = 6$ experiments.

Figure A3

A

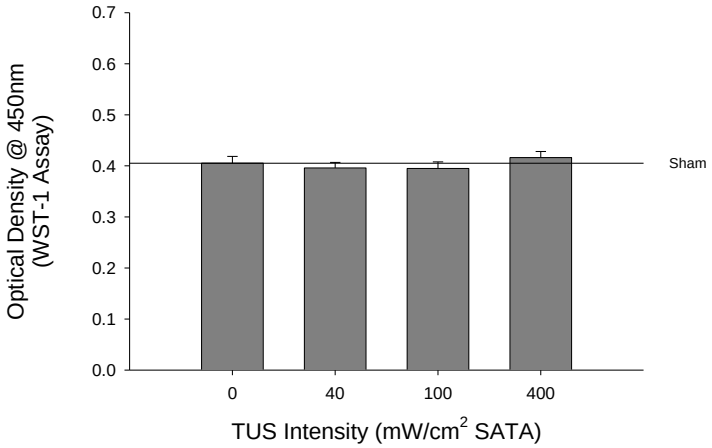

B

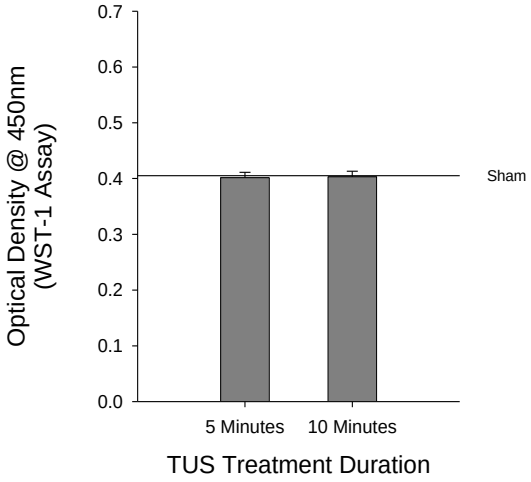

C

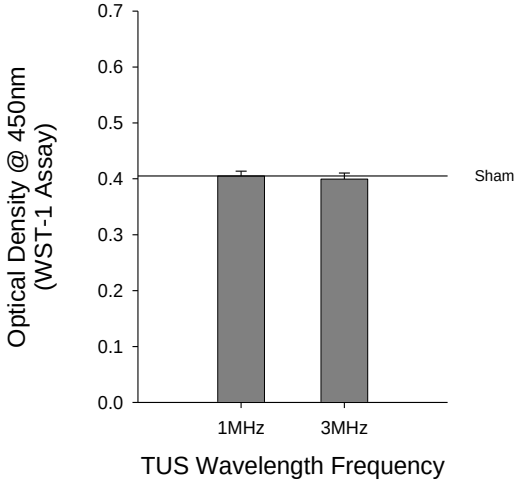

Figure A3. *Fibroblast proliferation in response to 72-hour incubation in macrophage conditioned media.* Fibroblast proliferation was assessed using WST-1 assay and reported as optical density units. Collapsed data across the TUS intensity, wavelengths and treatment durations demonstrates the three-way ANOVA analysis for each TUS parameter. Collapsed data across *(A)* TUS Intensity ($p = 0.480$), *(B)* TUS wavelength ($p = 0.685$) and *(C)* TUS treatment duration ($p = 0.587$), demonstrates three-way ANOVA analysis of the effect on each variable on macrophage release of fibroblast mitogens. No significant effect of TUS on release of fibroblast mitogen was found among any of the TUS treatment parameters at 72 hours. All data represent mean ± SEM of $n = 6$ experiments.

Figure A4

A

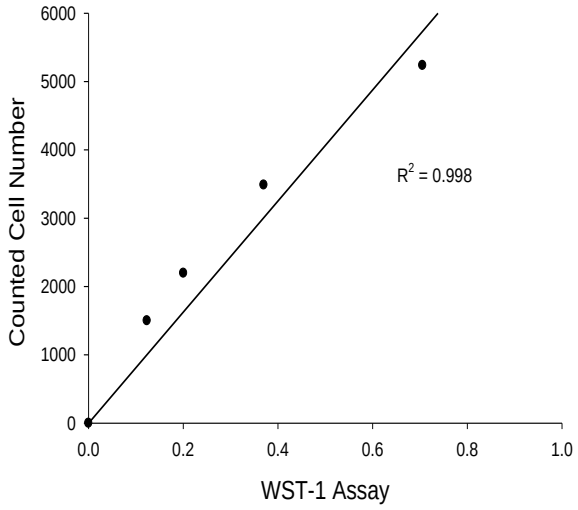

B

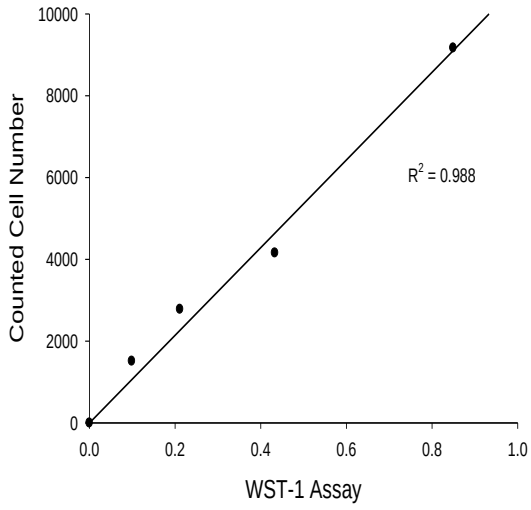

C

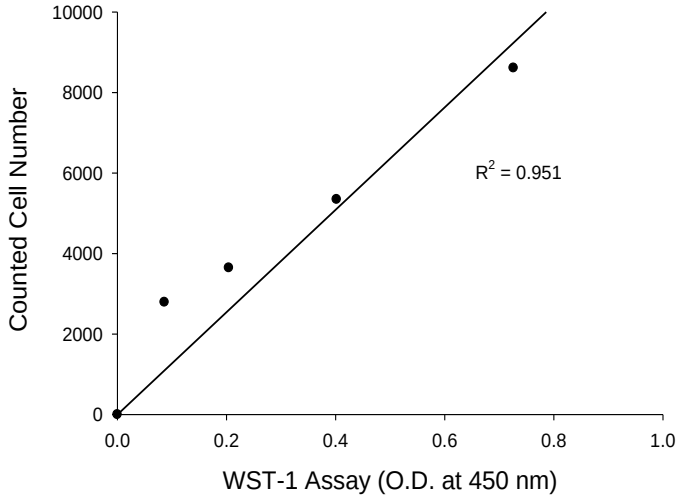

Figure A4. *Validation of WST-1 assay for Fibroblast Proliferation*. Comparison of direct cell counting and WST-1 colorimetric assay for determination of cellular proliferation. Fibroblasts were plated at serially diluted concentrations (8, 4, 2 and 1 x 10^3 cells/well) and were incubated for (A) 24 hours, (B) 48 hours or (C) 72 hours in macrophage growth media. Cell proliferation assayed by WST-1 assay was compared to direct cell counting. WST-1 proliferation assay was strongly correlated with increasing cell number for (A) 24-hours, $R^2 = 0.998$, (B) 48 hours, $R^2 = 0.978$, and (C) 72 hours, $R^2 = 0.939$.

Figure A5

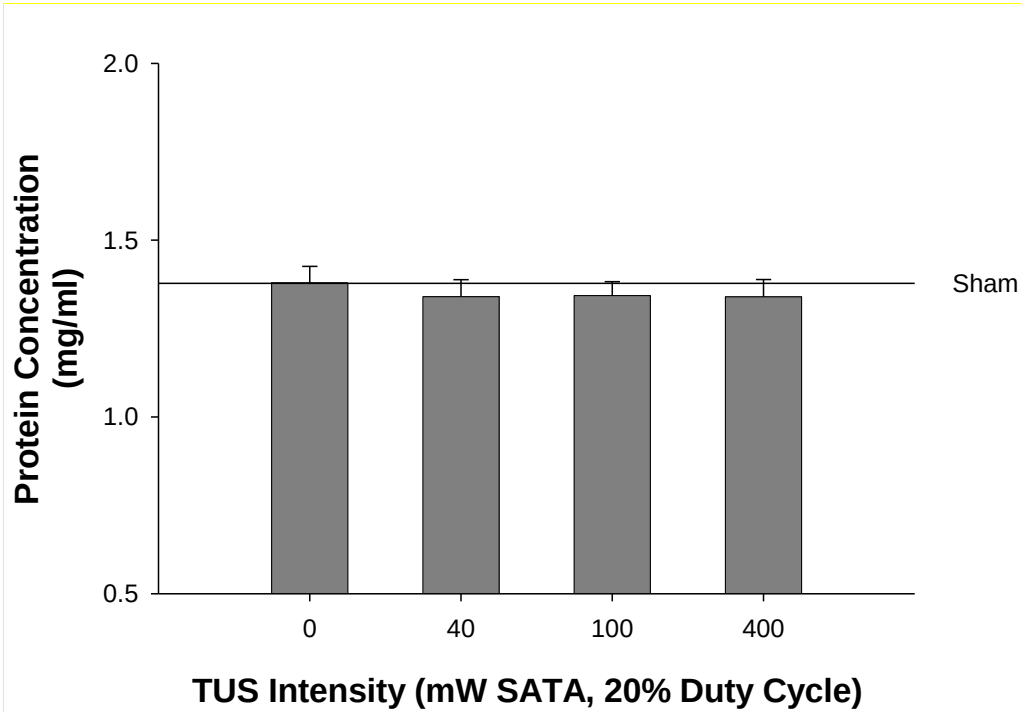
Protein Concentration (mg/ml)
2.0
1.5
1.0
0.5
Sham
0
40
100
400
TUS Intensity (mW SATA, 20% Duty Cycle)

Figure A5. *Protein concentration of macrophage cell lysates following TUS exposure and 24 hr incubation period.* Experimental samples from the same TUS treatment intensity were pooled from 1 MHz and 3 MHz frequency and from 5 and 10-minute treatments. Values are expressed as mg/ml ± SEM. Percentages indicate comparison of the protein content of sonicated samples compared to protein content of control samples and range between 97.1 – 97.5% of sham).

Figure A6

A

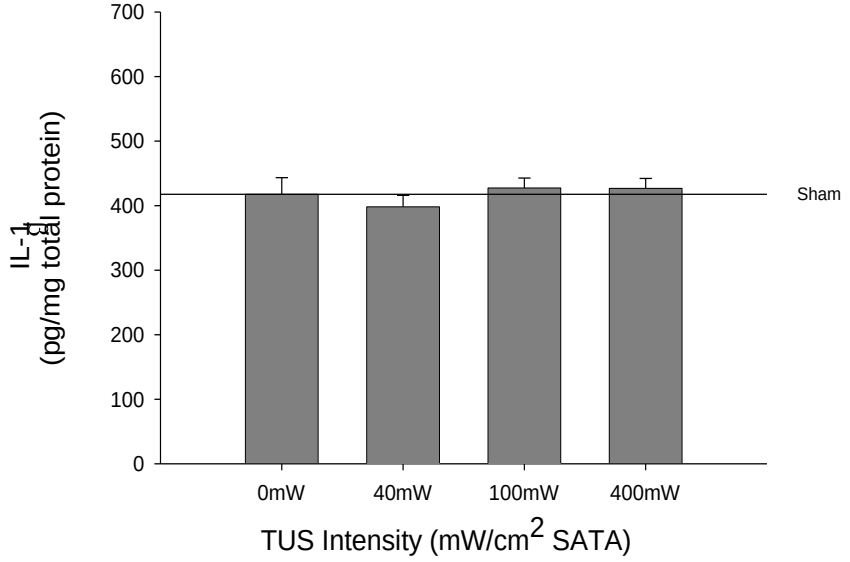

B

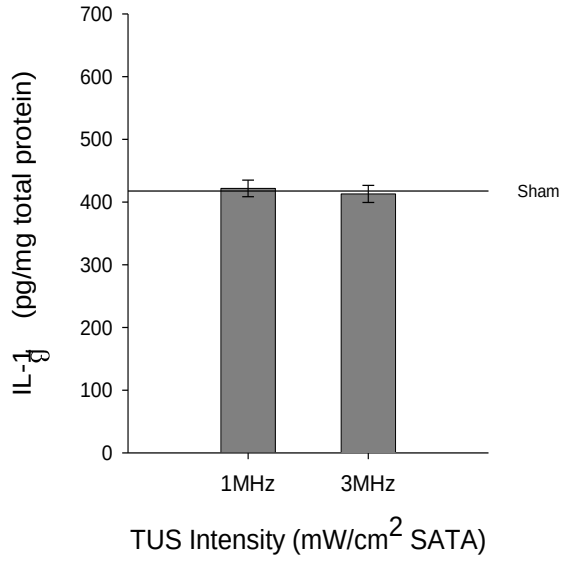

C

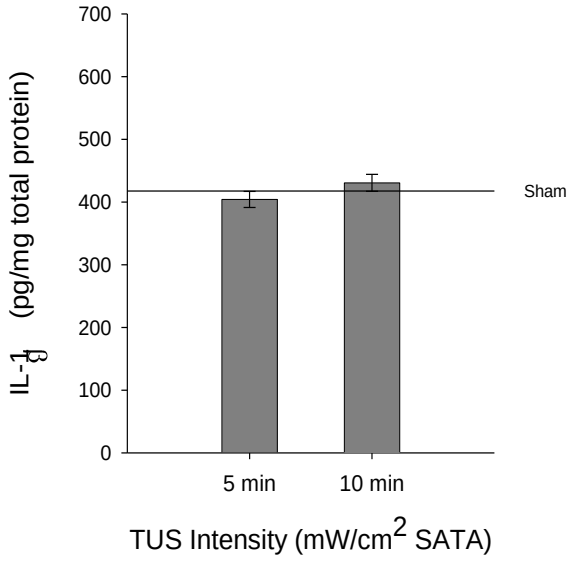

Figure A6. *IL-1β release from macrophages 24-hours after exposure to TUS*. IL-1β was measured by ELISA in the conditioned media 24 hrs after TUS exposure. Values represent mean ± SEM of n = 6 replicates that have been normalized to total protein in cell lysates. Three-way ANOVA revealed no significant differences in IL-1β release based on any TUS parameter: intensity, $p = 0.176$, wavelength frequency, $p = 0.471$, and duration, $p = 0.110$. Figures A-C exhibit the pooled values for IL-1β release based on TUS intensity, TUS treatment duration and TUS wavelength frequency. **(A)** *Comparison of TUS Intensity*. Data has been collapsed for each intensity among the 5 and 10 minute treatment durations and among the 1 MHz and 3 MHz wavelength frequencies. **(B)** *Comparison of TUS Treatment Duration*, Collapsed data for 5 and 10-minute treatments among all intensities and wavelengths, and **(C)** *Comparison of TUS Wavelength Frequency*, Collapsed data for 1 and 3 MHz among all intensities and treatment durations.

Figure A7

A

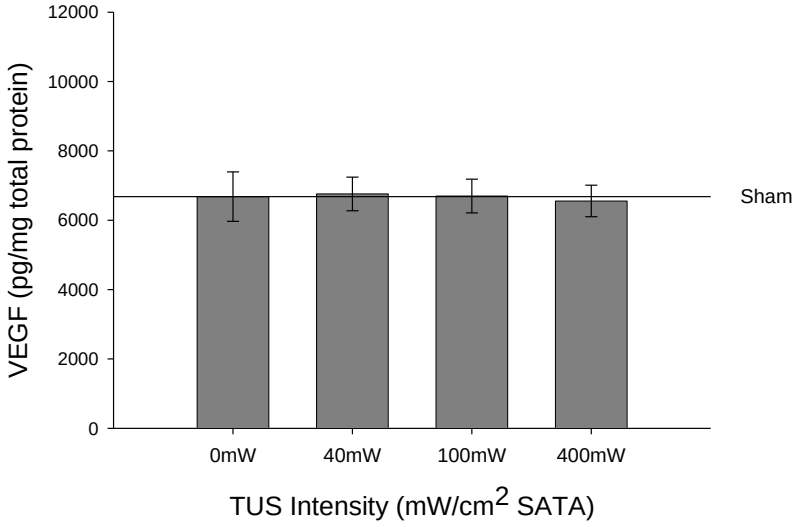

B

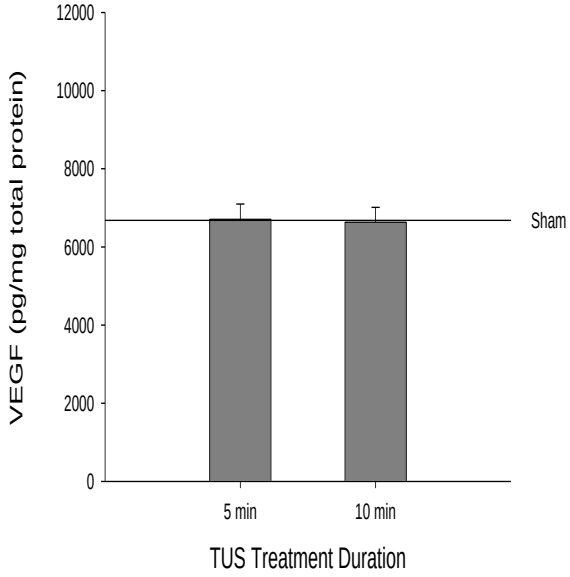

C

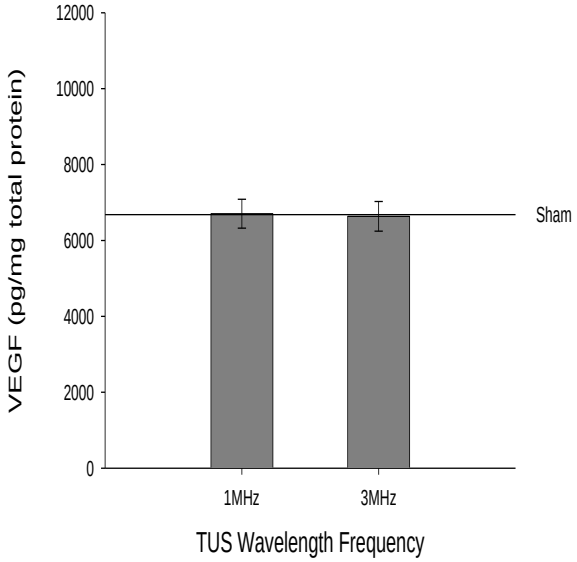

Figure A7. *VEGF release from macrophages 24-hours after exposure to TUS.* VEGF was measured in the macrophage conditioned media following 24-hour incubation following sonication**.** VEGF in the conditioned media was normalized to total cellular protein isolated from sonicated macrophages; values represent mean ± SEM for n = 6 replicates. **(A)** Pooled values for each TUS intensity among 5 and 10-minute treatments and 1 and 3 MHz application. TUS intensity had no effect on VEGF release from treated macrophages at 24-hours post-TUS ($p = 0.772$). **(B)** Pooled values for 1 and 3 MHz among each TUS intensity and 5 and 10-minute treatments. There was no effect of either TUS wavelength frequency on VEGF release at 24-hours post-TUS ($p=0.744$). **(C)** Pooled values for 5 and 10-minute treatments among each intensity and wavelength frequency. Treatment duration had no effect on VEGF release 24-hours post-TUS ($p = 0.751$).

Figure A8

A

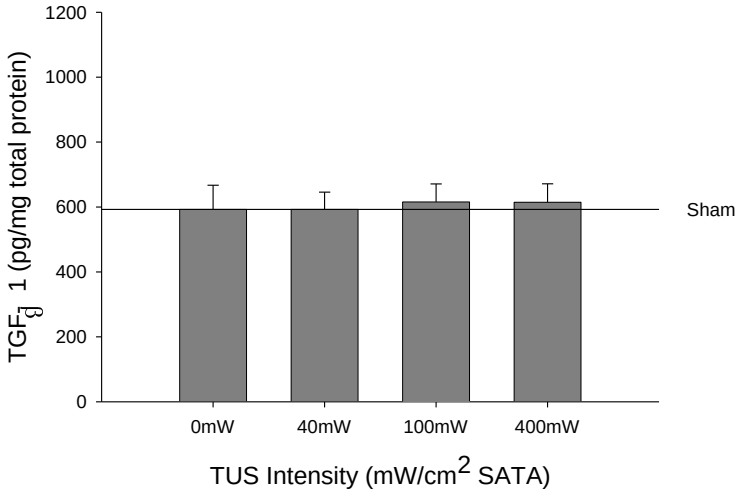

B

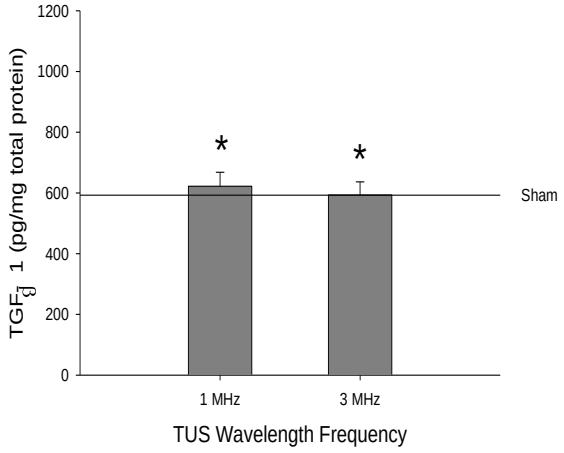

C

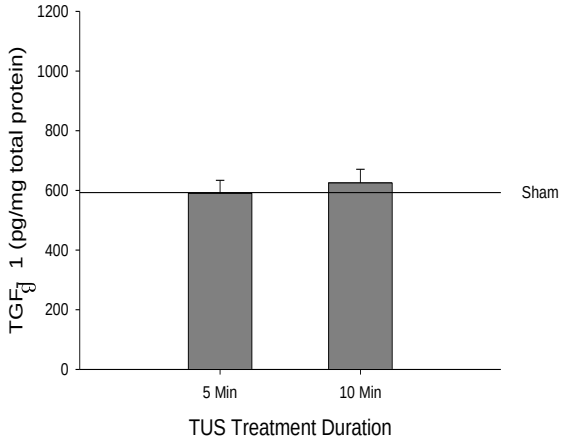

Figure A8. *TGF-β1 release from macrophages 24-hours after exposure to TUS.* TGF-β1 was measured in conditioned media following TUS exposure and 24-hour post-TUS incubation. TGF-β1 levels were normalized to total cellular protein isolated from lysates of sonicated macrophages. All values are expressed as mean of n = 6 samples ± SEM. Values are pooled for each independent variable (**A**) TUS intensities among the wavelength and durations, (**B**) TUS wavelength among all intensities and durations, and (**C**) TUS treatment duration among all intensities and wavelengths. Three-way ANOVA revealed a significant effect of TUS wavelength frequency indicated by *, where 1 MHz exposure was associated with increased TGF-β1 release, when compared to release in response to 3 MHz exposure ($p = 0.025$). Treatment intensities and treatment duration did not demonstrate a significant effect on TGF-β1 release ($p=0.061$ and $p=0.082$, respectively). However, there was a trend toward increased TGF-β1 release for 10-minute treatments compared to 5-minute treatments and for treatments administered at 400mW/cm^2.

Discussion

Three-way ANOVA revealed no differences in fibroblast proliferation following incubation up to 72 hours in conditioned media from TUS-treated macrophages based on any TUS variable assessed (Figs. A1-A3). As such, it appeared that macrophages did not respond to TUS at 20% pulsed-wave, 40-400 mW/cm^2 SATA, 5 or 10 minute exposure by releasing mitogenic factor(s) for fibroblasts.

In addition, TUS parameters did not affect the release of IL-1β (Fig. A6) and VEGF (Fig. A7) from macrophages exposed to TUS and incubated 24 hours post-treatment. TGF-β1 release from macrophages was affected by TUS wavelength frequency, where 1 MHz exposure increased release when compared to TUS delivered at 3 MHz. Despite statistical significance, the difference in release of TGF-β1 induced by TUS at 1 MHz compared to 3 MHz (622.058 ± 46.060 pg/mg total protein vs. 593.205 ± 43.392 pg/mg total protein) is quite small in comparison to total release.

Limitations. The original experimental design included sham-treatments that provided a negative control against the other experimental samples. However, the experimental design lacked a positive control for fibroblast proliferation. It is possible that the fibroblasts in our model were at their peak proliferative ability prior to addition of macrophage conditioned media. Under those conditions, additional mitogenicity from the macrophage conditioned media would not enhance proliferation, and no differences among treatment groups would be identified. Also, it is possible that the growth factors that are normally contained within the 5% HIFCS contributed to increased fibroblast proliferation across all samples. This effect may have overridden the effect of any added mitogens

present in the macrophage conditioned media, resulting in the equal number of fibroblasts in all experimental groups. Furthermore, a negative control of unconditioned media is desirable to allow analysis of the experimental media on fibroblast proliferation and determine any proliferative or inhibitory effects of media alone.

Concerning cytokine and growth factor data, the conditioned media containing 5% HIFCS may have provided measurable amounts of the proteins assessed. Since no unconditioned, 5% HIFCS-containing media was analyzed by ELISA, the possibility of serum/media altering the ELISA assays cannot be refuted.

For all assessments, the incubation period of macrophages following TUS exposure may have contributed to the non-stimulatory results noted above. Incubating macrophages for 24 hr may have allowed a constitutive release of mitogens to overwhelm the immediate release due to TUS, thereby eliminating the ability to determine whether any changes in TUS-treated macrophages actually occurred. To insure the validity of the "negative" proliferative data and cytokine release data, these experimental limitations are addressed by changes in and additions to the original experimental protocol and resulted in refinement of methodology described in Chapters 2-4.

Appendix B

Energy Emission Measurement for the Omnisound 3000 Ultrasound Generator

PREFACE: This appendix describes testing of the energy emission for the TUS generator utilized for treatment of macrophages in all experiments described in previous chapters. Testing of energy emission was completed in an effort to ensure repeatable treatments (based on intensity) throughout experimentation.

TUS Energy Emission Measurement. All ultrasound treatments were completed using an Omnisound 3000 ultrasound generator with a 5 cm^2 transducer containing a lead zirconate titanate crystal (Accelerated Care Plus Corp, Sparks, NV). The Omnisound 3000 maintains a beam non-uniformity ratio (BNR) < 4:1 and an effective eradiating area (ERA) of 5.0 cm^2, while producing a collimated cylindrical beam when applied. This unit is commonly used in clinical applications of TUS and permits a wide variety of intensities, and duty cycles at 1 or 3 MHz.

To insure comparable energy output between experiments, actual TUS energy emission from the ultrasound generator was measured using an UPM-DT10 ultrasound power meter (Ohmic Instruments Co., Easton, MD). This instrument uses the radiant force method to measure the ultrasound power output of diagnostic and therapeutic ultrasound transducers. Ultrasonic energy is passed through de-gassed water to a submerged conical

target. The radiant power transmitted to the target during ultrasound exposure is proportional to the total downward force (weight). An electro-mechanical load cell of the UPM-DT10 measures this force and converts force measures into power measures using the following equation: $\boldsymbol{p = Wgc}$ where;

p = power in watts

W = measured force in grams

g = acceleration in dynes

c = velocity of ultrasound in centimeters/second

Ultrasound watt density (mW/cm^2) was calculated manually by converting the watt values into milliwatts and then dividing the milliwatts values by the cross sectional area of the transducer (Ohmic Instruments, UPM-DT10 operators manual).

Pre-experiment and post-experiment measurements were completed for each TUS experiment. TUS exposures from the Omnisound 3000 ultrasound generator at various intensity and frequency levels (Table B1) were applied to the UPM-DT10 and power measurements recorded. This process was completed immediately prior and immediately after each sonication experiment to insure intra and inter experiment consistency of ultrasonic exposure. Testing for $100mW/cm^2$ was completed only for 24-hour experimentation as this level of intensity was not utilized in the short-duration experiments.

Table B1

TUS Treatment Intensity **Omnisound 3000 settings**

	1 MHz	**3 MHz**
40mW/cm^2 SATA	200 mW/cm^2 at 20%	200 mW/cm^2 at 20%
100W/ cm^2 SATA	500 mW/cm^2 at 20%	500 mW/cm^2 at 20%
400mW/ cm^2 SATA	2000 mW/cm^2 at 20%	2000 mW/cm^2 at 20%

Table B1. *Ultrasound Power (Intensity) Analysis Testing Parameters*. Ultrasound intensity and parameter settings for the Omnisound 3000 TUS generator utilized prior to and immediately after each ultrasound experiment. Analysis consisted of three different intensities (40, 100, 400 mW/cm^2 SATA) delivered using 1 or 3 MHz wavelength frequency immediately before and immediately following each experimental block of sonications.

Data Analysis/Statistics.

Differences between pre-experiment and post experiment measurements were analyzed for each TUS parameter set (Table A5.1). For 24-hour post-TUS incubation period, values represent mean ± SEM for n = 6 experiments. For short duration experimentation (10-minute and 1-hour) values represent mean ± SEM for n = 5 experiments.

Results

Omnisound 3000 Energy Measurements. TUS energy emittance was assessed immediately prior to and immediately following each experiment to insure consistent ultrasound delivery. TUS delivered with 3 MHz at 40, 100 and 400 mW/cm^2 and with 1 MHz at 400mW/cm^2 showed consistent ultrasound energy emittance throughout the 10-minute and 1-hour incubation experiments (Tables B2 and B3). No significant differences were found among pre and post testing for 24-hour experiment at any level of TUS. For the short duration experiments, TUS delivered with 1MHz at 40mW/cm^2 showed a statistically significant variation ($p = 0.040$) when pre and post values were compared using a t-test (Table B3). Actual energy variation was approximately 4mW/cm^2 from pre to post testing.

Table B2

	40mW/cm^2	**100mW/cm^2**	**400mW/cm^2**
1 MHz Pre-TUS	44.64 ± 1.23	105.33 ± 2.23	374.67 ± 6.25
1 MHz Post-TUS	44.00 ± 1.03	105.33 ± 1.69	372.67 ± 4.43
p-value (*pre to post*)	*0.687*	*1.00*	*0.799*
3 MHz Pre-TUS	44.00 ± 1.03	88.67 ± 1.91	324.67 ± 5.60
3 MHz Post-TUS	46.00 ± 1.71	90.00 ± 1.71	336.00 ± 3.43
p-value (*pre to post*)	*0.341*	*0.615*	*0.115*

Table B2. *Omnisound 3000 Ultrasound Generator Energy Emission* at 1 MHz and 3 MHz for 24hr post-TUS incubation experiments. Data reported as mean ± SEM of n = 6 replicates for pre-TUS and post-TUS values. Comparison between pre and post experimental values was completed using a t-test for each pre/post pair. Analysis revealed no significant differences among any pre-post pair indicating consistent energy emittance of the Omnisound 3000.

Table B3

	40mW/cm^2	**400mW/cm^2**
1 MHz Pre-TUS	36 ± 1.265	378.4 ± 11.496
1 MHz Post-TUS	40.8 ± 1.497	380 ± 3.347
p-value (*pre to post*)	*0.040*	*0.897*
3 MHz Pre-TUS	41 ± 0.980	344 ± 5.215
3 MHz Post-TUS	39.2 ± 1.497	338.4 ± 3.250
p-value (*pre to post*)	*0.217*	*0.389*

Table B3. *Omnisound 3000 Ultrasound Generator Energy Emission at 1 MHz and 3 MHz for revised experiments with 10-minute and 1-hour incubations*. Data was collected using the UPM DT10 power meter and is reported as mean ± SEM of n = 5 replicates for pre-TUS and post-TUS energy emittance values. Comparison between pre and post experimental values was completed using a t-test for each pre/post pair. Analysis revealed a significant difference between pre and post energy levels when applied using 1MHz at 40 mW/cm^2. All other tested parameters were not significantly different from pre to post experimentation.

Discussion

Omnisound 3000 Ultrasound Generator: Measurement of Exposure Intensities. Ultrasound energy emission at the experimental TUS parameters was measured before and after each sonication experiment. Over the entire course of experimentation, TUS energy emission remained nearly constant at each intensity level. Student's t-test comparisons among intensity levels demonstrated no significant difference between any pre/post measurements indicating the TUS generator emitted consistent doses throughout the completion of all ultrasound exposure experiment sets outlined in Table B2. Although TUS energy delivery remained essentially constant throughout the experimental sets, differences were recorded when comparing actual TUS energy and the Omnisound 3000 intensity display.

For 1 MHz treatment frequency, intensity settings closely matched with actual energy emission measured. However, for 3 MHz wavelength, intensity settings at 400 mW/cm^2 produced only 324 to 336 mW/cm^2. The possibility exists that this decreased overall energy, compared to 1 MHz, 400mW/cm^2 muted the cellular response to this parameter set of TUS. As such, 3 MHz exposure at 400mW/cm^2 could have induce macrophage release with an intensity comparable to that at 1 MHz. Additional experimentation using 3 MHz wavelength and fully comparable output intensities should be performed to clarify this issue.

In addition to the intensity difference noted at 1 and 3 MHz, pre to post testing for 1 MHz, 40 mW/cm^2 SATA was found to be significantly greater at post-testing (Table

B3). The measured difference in intensity before and after experimentation indicates a slight increase (4.0 ± 1.497 mW/cm^2) in TUS intensity from beginning to end of a daily experiment set for the short duration (10-minute and 1-hour) experiments. To prevent any bias in treatment parameter set usage, delivery of specific parameters sets were randomized for each daily experiment such that the order of parameter exposures were varied among the experiments. This treatment randomization should have reduced any effect of increasing TUS intensity from beginning to end of each experiment. In addition, no effects occurred with TUS exposure at 40 mW/cm^2 regardless of wavelength frequency, or treatment duration assessed. Thus, the difference noted in those pre-post intensity testing do not appear to have influenced the findings described in this investigation.

VITA

Thomas Todd Turner was born on November 29, 1965 in Stuttgart, Germany. He graduated from Prince George County High School in Prince George, Virginia in 1984. Thomas began his collegiate career at Old Dominion University, Norfolk, Virginia where he earned a Bachelor Degree in Biology in 1988. After graduation, he worked for several years as a laboratory technician at Virginia Commonwealth University, Department of OB/GYN. Thomas moved on to matriculate in the Physical Therapy Program at Virginia Commonwealth University, where he graduated with a Master's of Science in Physical Therapy in 1997 and received his state licensure to practice physical therapy later that year. In 2001, Thomas was accepted into the Combined Physical Therapy and Anatomy & Neurobiology Doctoral Program at Virginia Commonwealth University, Medical College Campus. Thomas is currently an Assistant Professor at Shenandoah University's Doctorate in Physical Therapy Program, Winchester, VA.